GT-SUITE SIMULATION OF A POWER SPLIT HYBRID ELECTRIC VEHICLE

by

ANDREW ROGER OGILVIE

MARCUS ASHFORD, COMMITTEE CHAIR
KEVIN CHOU, COMMITTEE CO-CHAIR
CLARK MIDKIFF
TIM HASKEW

A THESIS

Submitted in partial fulfillment of the requirements
for the degree of Master of Science in the
Department of Mechanical Engineering
in the Graduate School of
The University of Alabama

TUSCALOOSA, ALABAMA

2011

ABSTRACT

In the recent decades, hybrid electric vehicles (HEVs) have gained popularity within the automotive industry for several reasons. Most notably, this is because of their fuel efficiency advantage over traditionally powered vehicles due to their ability to combine more than one energy storage medium within their drivetrains. Of interest in this project is an HEV that combines a gasoline engine with a high voltage battery capable of powering a motor that is coupled with the engine to propel the vehicle. The greatest area for efficiency improvement is within the control strategy employed by this vehicle.

To minimize the costs associated with research and development of HEV control strategies, vehicle simulations are becoming very popular. The goal of this project is to develop a model for a Ford Escape HEV by comparing the simulation results to actual vehicle data. When completed, the control scheme for this vehicle can be modified and used to research the effects of various control scheme modifications.

To validate the model created for this project, data from previous research performed on the Escape will be used. The testing was performed using a chassis dynamometer at Argonne National Laboratory (ANL) and their Powertrain Systems Analysis Toolkit (PSAT). Although the PSAT model was successfully built, an improvement on the simulation results was expected by using GT Suite to model the vehicle.

After the model was built and tested the simulation results were used to prove that the simulated components maintained operation within their actual limits and the simulation results were compared to the previous vehicle test results in regard to the motor, engine and battery

operation. By comparing these various results, a clear trend was present between the actual and simulated vehicle data and the model was assumed to be a valid representation of the actual Ford Escape Hybrid. The model developed for this research also showed improvement on the results of the previous PSAT testing. Thus, this research produced a reasonable model of the Ford Escape Hybrid that can be further improved upon in future work.

DEDICATION

I dedicate this work to my mother and father, Luisa and Roger Ogilvie, and all of my siblings, Jessica, Daniel and David. Thank you for all you have done for me through the years, not the least of which is providing your unwavering love and encouragement. The ability and opportunity to perform this research and write this thesis would not have been possible without you.

LIST OF ABBREVIATIONS AND SYMBOLS

ABS	Anti-Lock Brake System
AC	Alternating Current
ANL	Argonne National Laboratory
APRF	Advanced Powertrain Research Facility
BMEP	Brake Mean Effective Pressure
CAE	Computer Aided Engineering
CAN	Controller Area Network
CAVT	Center for Advanced Vehicle Technologies
cm^3	Cubic Centimeters
cFP	Compact FieldPoint
cRIO	Compact Reconfigurable Input/Output
CVS	Constant Volume Sampling
CVT	Continuously Variable Transmission
DAQ	Data Acquisition
DC	Direct Current
DOE	Department of Energy
eCVT	Electronic Continuously Variable Transmission
EGR	Exhaust Gas Recirculation
EPA	Environmental Protection Agency
GTI	Gamma Technologies, Inc.

GUI	Graphical User Interface
HEV	Hybrid Electric Vehicle
hp	Horsepower
HV	Hybrid Vehicle
HWY	EPA Highway Drive Cycle
ICE	Internal Combustion Engine
IP	Internet Protocol
kg	Kilograms
kPa	Kilopascals
kW	Kilowatts
L	Liter
mph	Miles per Hour
NI	National Instruments
NiMH	Nickel Metal hydride
Nm	Newton-meters
OEM	Original Equipment Manufacturer
PM	Permanent Magnet Motor
PSAT	Powertrain System Analysis Toolkit
rpm	Revolutions per Minute
SOC	State of Charge
SUV	Sport Utility Vehicle

UDDS	Urban Dynamometer Driving Schedule
V	Volt
VI	Virtual Instrument
W	Watt
^{o}C	Degrees Celsius
^{o}F	Degrees Fahrenheit
%	Percent

ACKNOWLEDGEMENTS

First, I would like to acknowledge Dr. Robert Taylor for allowing me the opportunity to study, teach and perform research towards my Master's of Science in Mechanical Engineering at the University of Alabama. To receive the support from the Mechanical Engineering department that I have for the past couple of years is a blessing.

I would like to thank Dr. Marcus Ashford for supporting my decision to pursue this research and providing guidance and knowledge concerning the project. Also, Dr. Clark Midkiff and Ms. Sherry Barrow in the Center for Advanced Vehicle Technologies deserve a special thanks for their help in providing the vehicle used for this research and ensuring that it was in great condition throughout the project.

For getting me started and interested in research as well as assisting me in publishing two prior research papers, I would like to acknowledge Dr. Kevin Chou for his encouragement and support. Also, I would like to thank Dr. Tim Haskew for graciously accepting an invitation to serve on my thesis committee with Dr. Marcus Ashford, Dr. Kevin Chou, and Dr. Clark Midkiff.

For their assistance with GT Suite I would like to thank Jon Zeman for his help with debugging issues encountered during this research and Tara Petrusha for her administrative help in enabling licenses for the software.

Last, but certainly not least, I would like to acknowledge all my family and friends that supported me throughout this research with their encouragement, kind words and insights. Although I am sure to neglect some of these, I would like to personally thank my mother and father, Mebougna Drabo, Timothy Pyles, and Daniel Leverton.

CONTENTS

LIST OF TABLES

LIST OF FIGURES

CHAPTER 1

INTRODUCTION

Background

In the transportation industry recent developments concerning the world supply of petroleum, as well as the adverse environmental effects associated with the use of petroleum, have caused an increased demand for vehicles with increased efficiency. According to the Environmental Protection Agency's (EPA) report on sources of greenhouse gas emissions in the United States (U.S. EPA, 2010) personal vehicles are the largest contributor of greenhouse gas emissions in the transportation section of the report, and thus have received a great amount of attention from efforts to increase vehicle efficiency. The ultimate goal for maximizing the efficiency of personal vehicles is the complete electrification of the vehicle powertrain and accessory systems (Thomas, 2009). Thus, the most obvious solution to this problem is the development of fully electric vehicles. However, in addition to the significantly greater cost associated with electric vehicles, current limitations of practical energy storage technology, such as batteries, limit the range of today's electric vehicles such that the range is not sufficient enough to meet the demands of everyday drivers (Heywood, 2007) and thus they are not a practical solution. Other solutions for the electrification of vehicles, such as hydrogen fuel cell vehicles, have not gained acceptance due to concerns over their safety and the fact that the costs of installing the proper infrastructure (most significantly, hydrogen fueling stations) would

more than offset the foreseeable potential benefits of these vehicles thus creating an, overall, negative effect (Heywood, 2007).

A practical compromise between completely electric and conventional petroleum fueled vehicles is the hybrid vehicle. The powertrains for this class of vehicle are composed of two energy storage components such as batteries, petroleum fuel, ultra-capacitors, hydrogen fuel cells, or mechanical flywheels (Bossche, 2003). Although a hybrid powertrain can be composed of any combination of such energy storage components, the type of hybrid that is most documented is the hybrid electric vehicle (HEV) consisting of an internal combustion engine (ICE) and an electric motor. Thus, for energy storage, these vehicles carry a petroleum fuel tank and a battery, although research in the area of flywheels is increasing.

Types of Hybrid Electric Vehicles

Several architectures for HEVs have been conceived and developed. These include series, parallel and series-parallel (specifically, the power-split arrangement). Since these are the three most prevalent architectures, they will be briefly explained.

(i) The series architecture is the simplest from a control point of view. In this architecture, the engine is mechanically coupled to a generator, typically through a gear train. The type of generator is flexible, both alternating current (AC) and direct current (DC) generators have been used successfully when paired with the proper power electronics. The generator provides an electric input to the battery stack and from the battery stack, electric power is sent to the motor which is used to generate the tractive power for the vehicle. The greatest benefit of this configuration is that the engine speed is decoupled from the vehicle speed which allows the engine to be operated as close as possible to its most efficient operating point(s). The limitations of

this arrangement include decreased total efficiency (because of the additional energy conversions as compared to the other architectures) and the limits placed on the vehicle performance related to the fact that the motor is the only component providing tractive force. A generic schematic for this configuration is shown in Figure 1 (Miller, 2004).

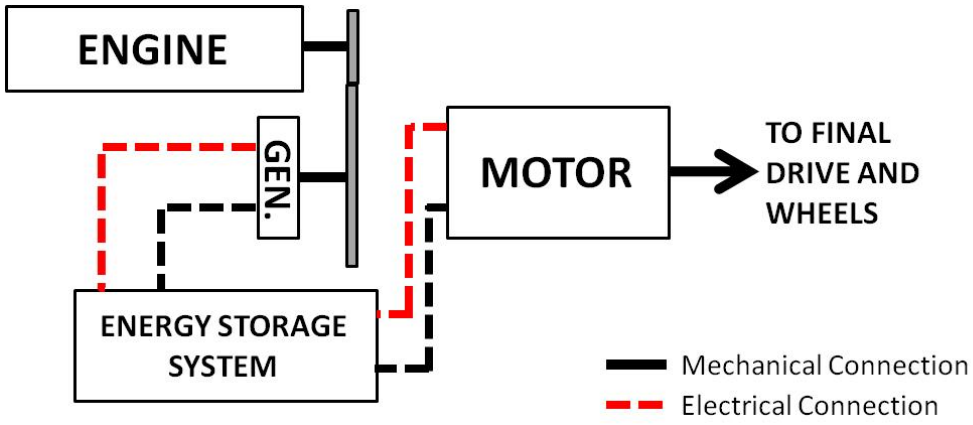

Figure 1. Series Hybrid Architecture Schematic.

(ii) The parallel architecture allows tractive force to be provided by a combination of the engine and motor. This is done by either coupling the speed or torque of the engine and motor; whichever one is not coupled is summed by the transmission to define the performance of the vehicle, which is typically better than series HEVs. Due to the engine having to operate at various points though, this configuration exhibits lower engine efficiency compared to the series configuration. Also, the control for this arrangement is more complex than that of the series architecture. Parallel architectures do, however, allow power to flow backwards through the motor under braking to recharge the electrical energy storage system; this is known as regenerative

braking and works to boost the overall efficiency. Figure 2 shows a general schematic for the parallel hybrid configuration that utilizes a speed coupling device (in this case a gear train) (Miller, 2004).

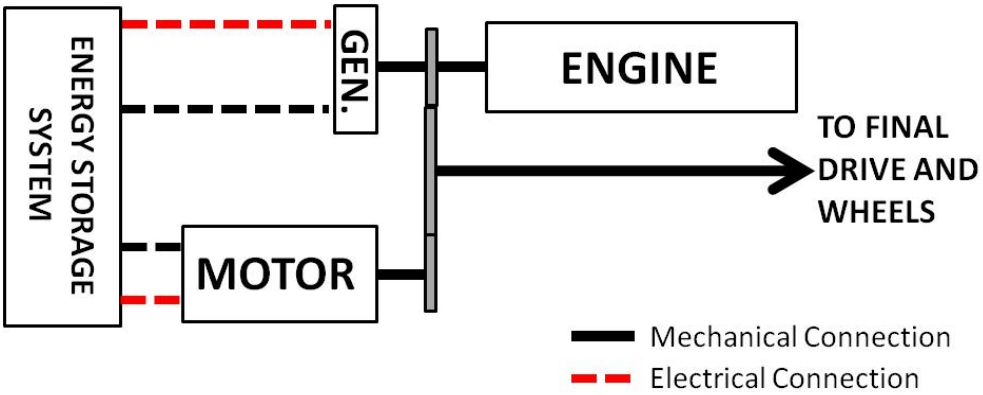

Figure 2. Parallel Hybrid Architecture Schematic.

(iii) Finally, the power-split architecture was developed in order to combine the benefits of each of the above architectures. In this configuration, a power-split device, such as the planetary gear set in Ford's Hybrid System, is used to combine the torques of the engine and motor. The planetary gear set allows for a continuously variable transmission between the drivetrain components - engine, motor, generator and final drive allowing the components to operate in, or near, their most efficient speed bands. This architecture allows for various operating modes: engine only propulsion, motor only propulsion, hybrid propulsion, motor propulsion with engine charging, and regenerative braking. The control law that governs the transitions through and between these modes defines the overall efficiency of the vehicle. An example of this architecture is displayed in Figure 3(Miller, 2004).

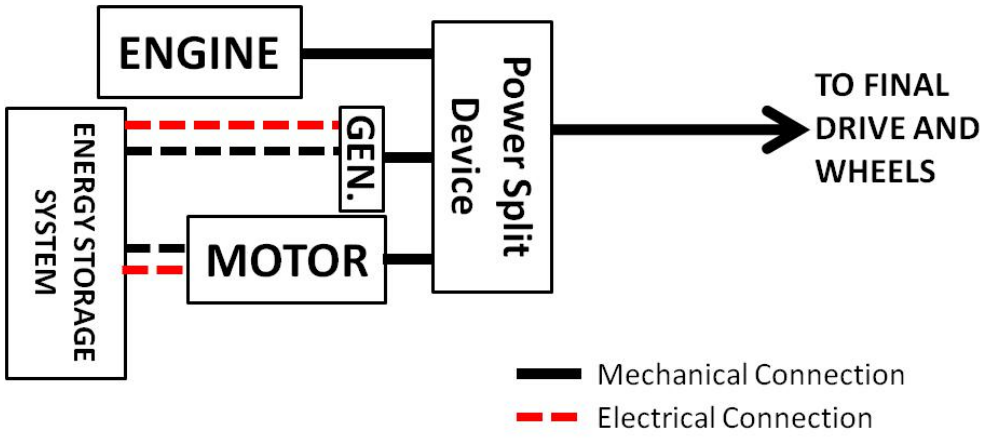

Figure 3. Power-Split Hybrid Architecture Schematic.

The results of a study performed at Argonne National Laboratory (ANL) where the final performance characteristics (power at the wheels, for example) of each vehicle were comparable show that for short range travel the series configuration is more efficient than the other two, but for longer range driving, the parallel configuration is more efficient (Karbowski, 2009). Due to the variation of drive cycles, the power-split configuration represents a compromise between the other two configurations. The vehicle used for this research project is a power-split vehicle, thus, the power-split architecture is the most pertinent to this research.

Hybrid Optimization

The various possible architectures of hybrid electric vehicles have been well researched and documented and the probability of the emergence of a better architecture seems unlikely. Therefore, for further improvements to hybrid vehicle technology, the researcher must look within the system itself. Areas for improvements in efficiency can be found within the properties of the various components (engine, motor, etc.) or the improvements can be realized by altering the way each of the components interacts with the other components. Improved performance due to better interaction between the components can be achieved by optimizing the control scheme.

As an example of component optimization, an area that has the potential to create a significant increase in system efficiency deals with the ICE and its relatively low efficiency (typically 28% for gasoline engines (Atkins, 2009)). Although the use of Atkinson cycle engines can boost the efficiency of HEVs approximately 10%, the regions of highest engine efficiency occur at high engine loads (Miller, 2004). In real world driving though, the vehicle is rarely used at high loads, with these loads only occurring during acceleration. Therefore, to increase the system efficiency the engine should only be operated at high loads, when possible. The decision of when to operate the engine at high loads, as well as the realization of the maximum load the engine should be subjected to, are complicated but can be dealt with via the implementation of an effective control technique.

Optimization of hybrid vehicles is usually defined in one of two ways, both of which are discussed in papers by Chen and Aswani, et al (Chen, 2009; Aswani, 2008). The first definition, as described by Chen is the minimization of fuel consumption and the second, elaborated on by Aswani, is the maximization of performance while maintaining better efficiency than a conventional powertrain. These different optimization goals, which may not necessarily be conflicting, further complicate the HEV control strategy.

Hybrid Control

The control systems of hybrid vehicles are more complex than those for their counterparts in conventional vehicles due to the additional components and the complicated interactions between the components. In addition to the accessory systems hybrid vehicles share with conventional vehicles (lights, air conditioning, horn, etc.), the hybrid control system must also deal with a traction motor, generator, high voltage (HV) battery, regenerative braking system and the power electronics required of each of these additional systems.

In the power-split HEV, a planetary gear set is used as an effective continuously variable transmission (CVT) that is electronically controlled through the generator speed. This type of device is referred to as an electronic continuously variable transmission (eCVT) and is discussed in more detail later in this paper.

For each of the possible hybrid states, the control system must effectively control the speeds and torques of the engine, motor and generator, maintain a desired battery state of charge (SOC) and safely distribute the braking power between the electrical (regenerative) and mechanical brake systems when braking. For a power-split HEV, the possible hybrid states include, engine only propulsion, motor only propulsion, hybrid propulsion, engine-battery charging, and regenerative braking, all of which are discussed below.

(i) As its name implies, the engine only propulsion state uses only the ICE to provide the requested road load. The vehicle will run in this state if the battery SOC is below a desired minimum threshold or for high speed acceleration where the efficiency of the motor is such that it would hurt the vehicle's overall efficiency.

(ii) For motor only propulsion the traction motor is the only component that is used to provide the requested road load. This state is utilized when the battery SOC is within its acceptable limits and the vehicle speed is low, approximately 25mph or less (Grabainowski, 2005). At this speed, the motor can operate in its most efficient regime while the engine would have to run in its least efficient regime.

(iii) In hybrid propulsion, all three components – engine, motor and generator – are used in some combination that provides the requested road load as well as charge the battery, if needed. This is the state that allows the HEV to display its greatest benefits in regard to efficiency. The engine and motor can be coupled to provide

the road load while any excess power generated by the tandem is used to charge the battery via the generator. If the battery SOC is acceptable, all three components may be used to provide the tractive power requested. Although the combined output torque of the three components is coupled to the vehicle speed the component speeds are not coupled to the vehicle speed and therefore all components can be controlled to run at their most efficient operating speeds.

(iv) Engine-battery charging is employed when the battery SOC has fallen below a desired minimum threshold. Therefore, in this mode no electric power is consumed (motor is not used) and additional load demands are placed on the engine so that power is transmitted through the generator and into the battery. Since the engine is more efficient at higher loads, this state allows the engine to operate more efficiently than it would under solely the road load demand. This mode is also used to provide charging power to the battery when the vehicle is stopped if the SOC is less than desired.

(v) When the HEV is braking, some of the energy that would be lost to the braking activity can be recaptured by the motor and/or generator. HEV regenerative braking systems consist of the electrical (regenerative) brakes and mechanical brakes. The control strategy must balance the battery SOC, charging limits and required braking force in order to determine the amount of braking force applied by each type of brake that will safely slow the vehicle at the deceleration demanded. While in this state, the engine may be on or off, depending on how low the battery SOC is. If additional charging power is desired, the engine will provide power to the battery via the generator.

As evidenced by the above sections, the design of an HEV control strategy is not a simple task and care must be taken during the development of the strategy to ensure consumer safety and efficient operation of the HEV. In order to understand the abilities and shortcomings of the HEV control strategy, computer simulations of these vehicles are becoming widely used.

Objective of Research

The objective of this research is to create a detailed, accurate computer aided engineering (CAE) model of an actual Ford Escape Hybrid Sport Utility Vehicle (SUV). For this project, a research Escape belonging to the Center for Advanced Vehicle Technologies (CAVT) at the University of Alabama will be used. This vehicle has been previously modeled using the Powertrain Systems Analysis Toolkit (PSAT) that is available from ANL (Jenkins, 2006). However, for this research GT Suite, a modeling and simulation package produced by Gamma Technologies Incorporated (GTI), will be used. The advantages of GT Suite over PSAT will be discussed later in the paper. Since this vehicle has previously had instrumentation installed, real world data will be obtained and compared with the GT Suite model. In addition, some of the results of the previous research done on this vehicle will be compared to the GT Suite model to validate the decision to use GT Suite. The final model will provide for an increased understanding of the interaction between the various components of the HEV as well as serve as a test model for control strategy modifications aimed at improving the performance and efficiency of HEVs.

Organization of Thesis

In the next chapter, an elaboration on the components of the HEV will be provided. Most importantly, the engine, motor, generator, high voltage battery, eCVT and regenerative braking systems will be discussed. Chapter 3 will discuss the instrumentation of the vehicle and what

changes were made to the instrumentation that was in the vehicle at the advent of this project. The testing procedures employed in this research will be discussed in Chapter 4. Chapter 5 will provide an overview and process for creating the model in GT Suite as well as discussing the reasons GT Suite was chosen. The results and comparison to previous research will be provided in Chapter 6 and the thesis will conclude in Chapter 7 with conclusions and recommendations for future work.

CHAPTER 2

HEV COMPONENTS

Since the vehicle being used for this research is a power-split HEV, the major components of this type of HEV will be elaborated on, specifically as they are designed for use in the Ford Escape Hybrid vehicle. Only the components that vary significantly from conventional vehicle components will be discussed. Accessory systems such as the radio, air conditioning and headlights do not need to be covered within the scope of this research as they are not critical components to an HEV control system.

Engine

For a hybrid vehicle the engine can be downsized with regard to the engine of a conventional vehicle with similar size and weight. This is due to the fact that the engine alone is not required to provide all of the tractive force needed to propel the vehicle; this duty is shared with the motor and generator. To illustrate this point, Table 1 provides a comparison of the hybrid and conventional Escapes, according to MSN Autos (MSN Autos, 2005), offered by Ford for the 2005 model year.

The most noticeable difference in the engines described above is the fact that the Escape Hybrid engine runs on an Atkinson cycle as opposed to an Otto cycle. The Atkinson cycle utilizes a higher compression ratio that allows for more efficient combustion and provides a higher power output, but at the cost of torque output, which is what is of importance when considering vehicle dynamics. Although, for the same displacement, the Atkinson engine

Table 1. Comparison of Various Engine Parameters for all 2005 Escape Models Offered.

Vehicle Trim	Hybrid 4WD	XLS 4WD	XLT 4WD
Engine Displacement (cm^3)	2261	2261	3000
Engine Power (hp)	155 @ 5000 rpm	153 @ 5800 rpm	200 @ 6000 rpm
Engine Torque (lb-ft)	124 @ 4250 rpm	193 @ 4850 rpm	152 @ 4250 rpm
Compression Ratio	12.3:1	10.0:1	9.7:1
Engine Cycle	Atkinson	Otto	Otto

produces more power than the Otto engine, it produces significantly less torque. By inspecting a pressure-volume (P-v) diagram for both cycles, shown in Figure 4, the reason for the increased efficiency of the Atkinson cycle is apparent. It can be assumed that for geometrically identical engines, with an equal amount of fuel combusted, the cylinder pressure will reach equal magnitude. Thus the only difference in the two cycles is present on the right side of the plot where the Atkinson cycle displays increased area inside the cycle curve. This extra area allows for additional work to be extracted from the cycle and thus, for equal power demands, less fuel is required and the efficiency of the engine is improved, but at a cost to torque (Heywood, 1988). Figure 5 shows a comparison of the torque output from both the Atkinson cycle engine and the Otto cycle engine (Rairigh, 2007).

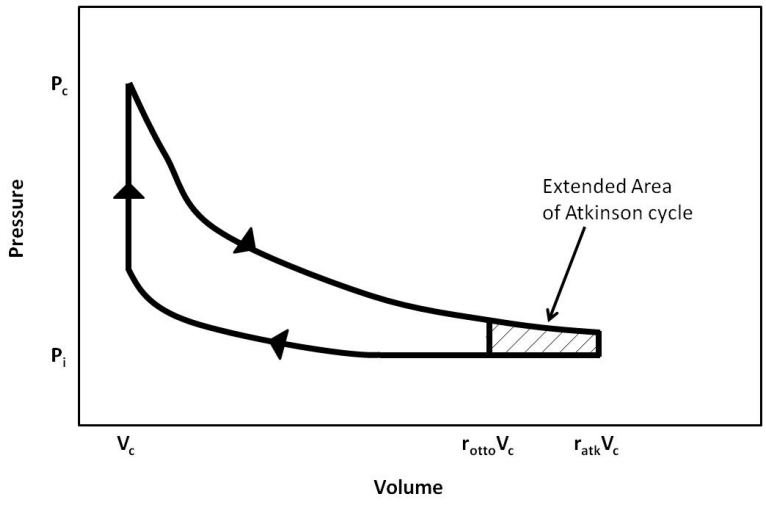

Figure 4. Thermodynamic Comparison of Otto and Atkinson Cycles.

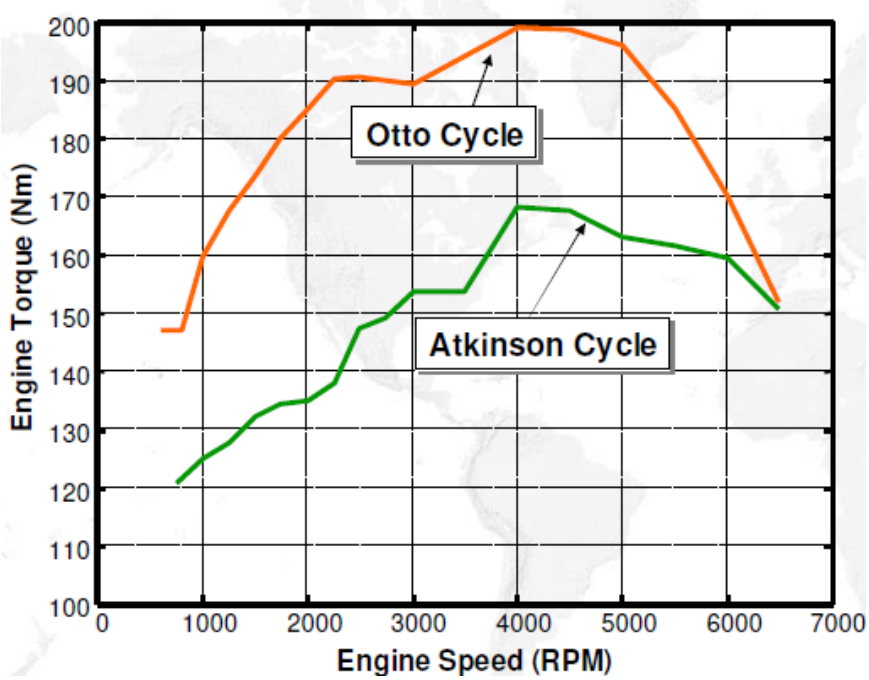

Figure 5. Comparison of Output Torques for Ford Atkinson and Otto Cycle Engines.

Traction Motor

Unique to the HEV drivetrain, compared to the conventional drivetrain, is the traction motor. This motor is employed to provide additional torque in order to meet the road load demanded by the driver. The coupling of the engine and motor to provide the tractive force requested by the driver results in an advantage over using one or the other because, while the engine can provide greater torque at high speeds, the traction motor produces more torque at lower speeds.

In the hybrid Escape the traction motor is manufactured by Aisin AW (Hisada, 2005). The motor is a permanent magnet (PM) synchronous electric machine capable of running at speeds up to 13,500rpm and producing up to 210Nm of torque. The traction motor is sized based on the load request it is expected to be asked to handle and the regenerative power expected to be produced by typical vehicle braking events. Figure 6 displays the efficiency map for the traction

motor and from the figure, as mentioned above, it is evident that it is capable to generating more torque in lower speed regimes.

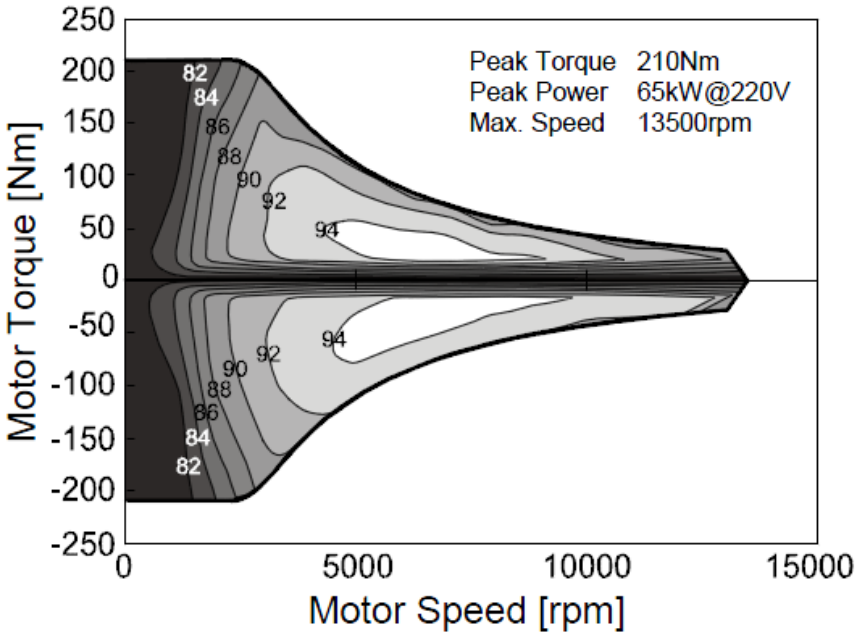

Figure 6. Efficiency Map for Ford Escape Hybrid Traction Motor.

Generator

For an HEV, a generator is required primarily to maintain a sufficient battery SOC. This SOC is determined when the control scheme is designed and tested. If the present SOC is lower than the desired minimum value, the generator, and possibly the motor, is used to provide charging power to the battery. The power limits of the generator are designed to be compatible with the charge limits of the battery system.

Aisin also manufactures the generator for the Ford Escape Hybrid and packages it in with the motor and eCVT within the transmission system. Like the traction motor, the generator is a PM alternating current (AC) machine. However, the generator has a larger region of operating points at a cost to the maximum speed and torque, with these limits being restricted to 11,000rpm and 75Nm, respectively. This reduction in maximum speed and torque is permissible due to the

fact that, although it sometimes does, the generator is not expected to provide any tractive power. The generator's power output is constrained by the speed and torque of the generator and the maximum output power is constrained by the charge limit of the battery system. Hence, the "cost" of a larger efficient operating regime is not considered a "cost" as much as a positive tradeoff. In fact, the generator is designed to meet, and not exceed, the charging limitations of the HV battery (McGee, 2005).

For the generator of the Ford Escape Hybrid, the efficiency map is shown in Figure 7. By comparing this curve to the performance curve of the traction motor, it is clear that the operating area is larger, but the maximum speed and torque are lower.

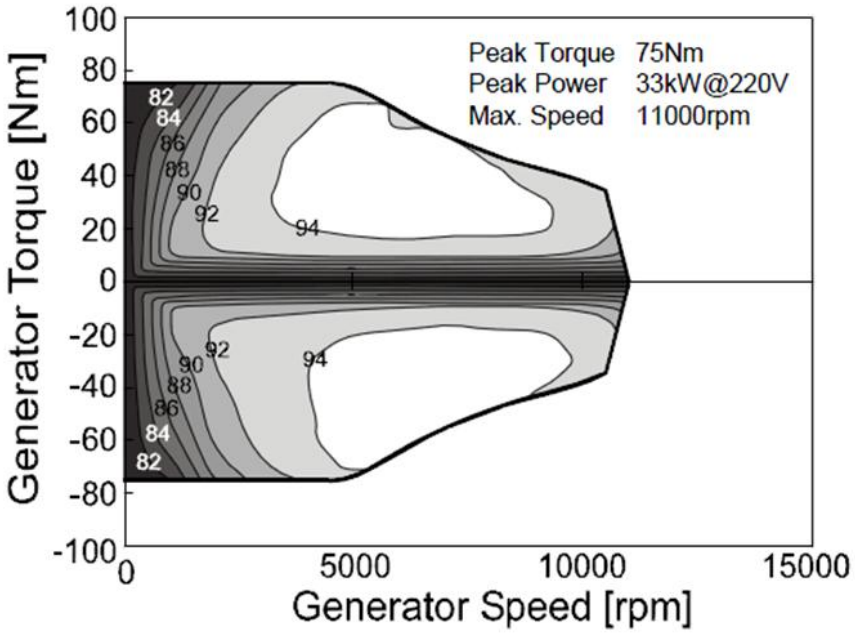

Figure7. Efficiency Map for the Ford Escape Hybrid Generator.

Electronic Continuously Variable Transmission

One of the greatest achievements in the design of the Escape Hybrid is the design and packaging of the electronic continuously variable transmission (eCVT). The eCVT is also manufactured by Aisin and is packaged with the traction motor and generator in the transmission

system, which is similar in size to a standard 4-speed automatic transmission (Hisada, 2005). The packaging is beneficial in that it requires only one coolant system for the planetary gear set, traction motor, generator and associated power electronics.

A schematic of the transmission packaging is shown in Figure 8 (Hisada, 2005), while Figure 9 shows tractive force curves of the components within the transmission at various vehicle speeds (Hisada, 2005). Figure 10 shows a cut away view of a fully assembled transmission system (Rairigh, 2007). The gear ratios of the planetary gear set and reduction gears of the traction motor and engine define the performance abilities of the transmission and the calculated ratios are given in Figure 11 (Hisada, 2005).

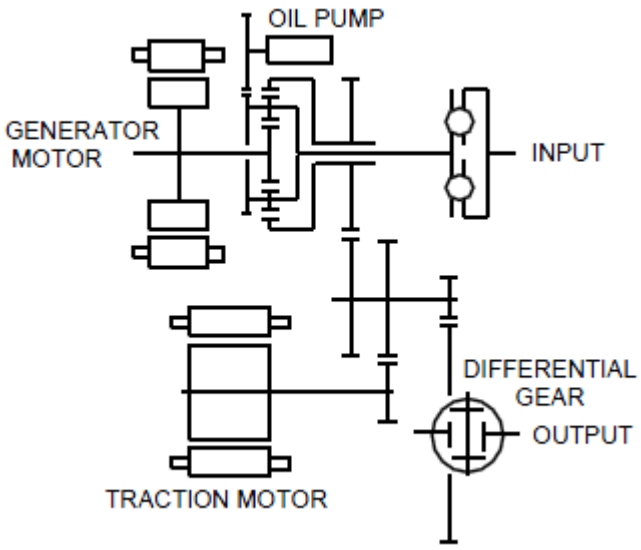

Figure 8. Transmission System Schematic.

High Voltage Battery

The high voltage battery in an HEV is responsible for providing electric power to the traction motor and generator, when these components are providing tractive power, as well as receiving power from these components when they are being used to charge the battery. The battery is also one of the main constraining factors of an HEV. Countless types of batteries have

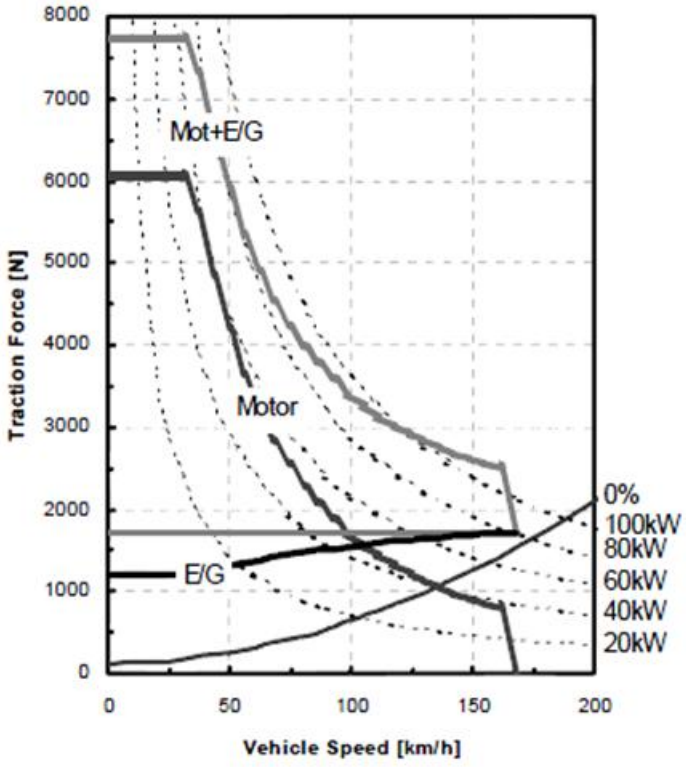

Figure 9. Tractive Force as a Function of Vehicle Speed for Transmission Components.

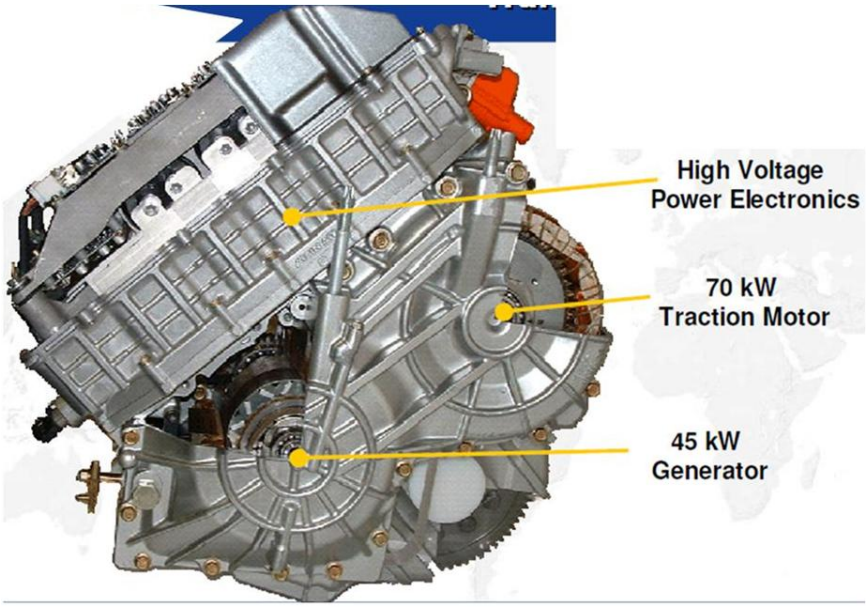

Figure 10. Cutaway View of Assembled Transmission System.

Planetary Gear Set	0.705 (79,23,33)
Engine Total	3.781
Traction Motor Total	10.706

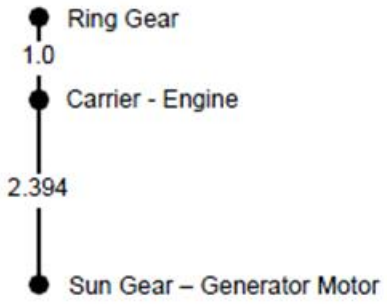

Figure 11. Calculated Gear Ratios and Visualization for eCVT.

been designed, built and tested for use in HEVs, but current battery technology still severely restricts the amount of electric energy that can be carried by a battery.

For the Escape Hybrid, the battery is manufactured by Sanyo, Inc. and is composed of 250 Nickel Metal-Hydride (NiMH) battery cells. Each cell is capable of providing 1.35VDC when fully charged. This gives the battery assembly in the Escape a theoretical maximum voltage of 337.5VDC with a capacity of 5.5Ah, but the control scheme of the Escape maintains the SOC lower than 100% to ensure long and consistent battery life (McGee, 2007). Ford claims a maximum voltage of 300VDC from their HV battery. According to McGee, the Ford Escape control scheme aims to maintain an SOC of 40-70%

Another key factor for the life and quality of the HV battery is the charge/discharge limit which is capped at 100/-100A for the Escape's HV battery (Ford, 2005). This means that the battery control will not allow more than 100A of current flow into the battery for charging or more than 100A of current flow from the battery to meet the electrical demands of the vehicle. This ensures that the battery is not subjected to harmful stresses that result from charge/discharge currents outside of its maximum capability.

Power Electronics

In order to handle the various power demands of the multitude of electronics present in HEVs, several forms of power electronics must be incorporated into the design. Mainly, these electronics are inverters and converters that convert various forms (AC or DC) and magnitudes of voltages (for instance, 12VDC or 240VAC) into the form and magnitude of that requested by the power receiving system.

In the Ford Escape Hybrid, most of the power electronics are incorporated into the systems they are designed to control power flow for. For example, as previously mentioned, the power electronics for the traction motor and generator and packaged in with them as part of the vehicle transmission system. The proximity of the power electronics to their systems reduces the probability of encountering a major problem between the power conversion step and the usage of that power.

Power electronics are incorporated into the hybrid vehicle mainly to convert between AC and DC voltages. Due to their construction, batteries can only store energy as a DC voltage. However the traction motor and generator run on AC voltages. Additionally, the motors and battery operate at different levels of voltage. To illustrate, consider the generator being turned to provide a charging power to the battery. The power electronics of the battery system are receiving a variable AC voltage. In order to charge the battery, the voltage must first be converted into a DC voltage and then stepped up (via a boost converter) to the desired battery input voltage. Conversely, when the battery is providing power to the traction motor a DC voltage must be converted into an AC voltage (inverted) in order to be used by the traction motor. The magnitude of the AC voltage must be controlled (via switches within the power electronics) to the level requested by the motor.

Without the advanced power electronics employed by HEVs, the ability to combine a DC HV battery with AC motors would be impossible. Even the use of less efficient DC motors would be difficult and their performance would be critically limited by the voltage of the battery at that instant.

Control System

When designing the control system for an HEV several decisions must be made, the most important of which is the definition of optimization for the vehicle being designed. Based on what the ultimate design criteria is for a particular system, the relationships between the various components will differ. The inputs to the control system are typically the same for any HEV control scheme with minor, if any, variations. These inputs include the accelerator pedal position, brake pedal position, battery SOC, maximum battery current, and vehicle speed (McGee, 2007).

The Ford Escape Hybrid's control system is made up a supervisory controller and sub-system controllers as shown in Figure 12. Each of these controllers contains a micro-processor that is coded with an algorithm built to handle the inputs to that particular system and bring the outputs to a desired state as determined by the supervisory controller. The controller of most significance is obviously the supervisory controller as it controls the actions taken by all the other controllers in the vehicle. The supervisory controller for the Escape is based on a torque control technique meaning that it outputs a desired torque to the engine, traction motor and generator. Then (given input data on the requested torque, battery SOC, and battery current availability, etc.) the controllers for each of these components calculates an "optimal" speed for that component and requests the required electric power from the battery (in the case of the traction motor and generator) or required throttle position and fueling rate (in the case of the

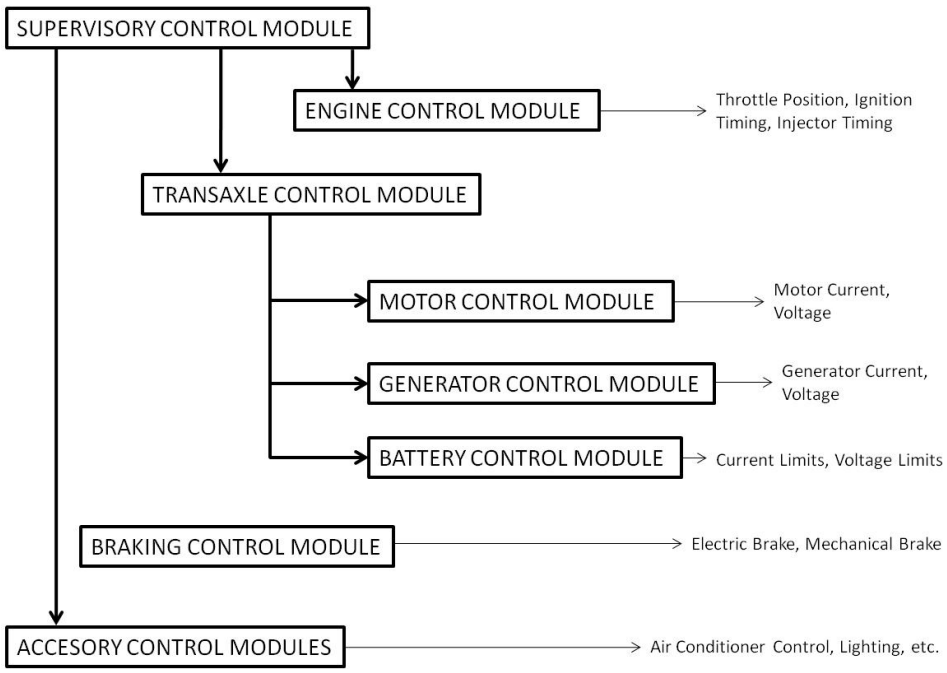

Figure 12. Simplified Control Diagram for Ford Escape Hybrid.

engine). For the engine outputs (throttle position and fueling rate) a simple analog signal from the engine controller is sufficient. For the motors, their controllers must first determine the proper control of the power electronics for each motor and then their power requests must go through the HV battery control module which ensures that the traction motor or generator do not draw more current from the battery than it can safely and reliably deliver. It then routes the requested electrical power to the proper destination.

When choosing a control scheme, the designers must also decide whether to use a linear or nonlinear controller within the control systems. While the nonlinear controller more accurately represents the actual system to be controlled, the linear system provides a good approximation of the nonlinear dynamics within reasonable bounds and is significantly less complex than its nonlinear counterpart. For this reason, linear control is the control design chosen by most control designers (Bradley, 2009). Another downfall of current hybrid control strategies is the fact that the models built into the controller are time-invariant – that is, their

characteristics do not change in time. However, for an actual system this is not the case. Any system will change as it wears and is pushed to its limits, sometimes past its limits. Thus, the models for any particular system will change in time unlike the models built into the control scheme and the control scheme will become inaccurate in time. Unfortunately, the control strategies of commercially manufactured vehicles are highly proprietary which will produce the greatest obstacle to the development of the model in this research. An initial control strategy will be derived from the paper by McGee, et al. The strategy will then have to be modified until it can achieve a simulated performance similar to that of the actual vehicle while still reflecting the system set forth by McGee, et al.

CHAPTER 3

VEHICLE INSTRUMENTATION

The Ford Escape Hybrid used for this research has been used for research projects twice before. As a result, the vehicle previously had instrumentation installed on it that was used to provide actual data from the vehicle over the course of this research. However, at the onset of this project, some of the instrumentation was not working properly or missing and some of the instrumentation and devices used to record operating data were not compatible with each other. Additionally, the DAQ device in the vehicle had to be erased and reformatted; thus, a new LabVIEW virtual instrument (VI) had to be written in order to utilize the data acquisition (DAQ) system that was installed in the vehicle.

Data Acquisition System

In order to sample the signals from the various sensors installed in the Escape, a data acquisition (DAQ) system was used. The DAQ system consists of a real time control module on a chassis along with various modules that work to filter, amplify and buffer the signals coming into the control chassis. A virtual instrument (VI) was created to handle the input to the controller as well as record the signals for future analysis.

Originally, a National Instruments (NI) Compact FieldPoint (cFP) control chassis was installed (Jenkins, 2006). The cFP model chosen was the cFP-2020 which came equipped with an Ethernet interface and removable storage capability (via a compact flash card). The VI

originally created to receive and save the incoming signals was loaded into the controller's permanent storage drive. In order to receive these signals, four modules were installed into the chassis including two AI-118 modules used to receive voltage signals, an AI-100 module to record voltage or current and an AI-120 module to receive thermocouple signals. The VI written for the controller was capable of receiving the signals and recording them in a Microsoft Excel format for further processing; the block diagram of the original VI is shown in Figure 13. All the hardware for the controller and its modules were installed inside a box, herein referred to as the DAQ box, which was placed in the cargo area of the vehicle where the audio amplifier was originally installed.

Also included in the DAQ box that housed the control chassis and modules was a Dataforth 8B back panel and Dataforth 5B back panel. The 8B back panel required 12VDC and was wired with thermocouple modules that filtered and amplified the thermocouple signals to a level that could be read by the AI-118 modules of the cFP chassis. The 5B back panel required 5VDC to operate and was used to collect data on the Anti-lock Brake System (ABS) wheel frequency by converting the frequency signal to a voltage that could be read by the AI-118 modules. The configuration of the original DAQ box is shown in Figure 14.

After collecting data, the compact flash card was removed and the signals were loaded in Excel and then converted from raw voltages into appropriate units for the signal (for example, a thermocouple voltage was converted into a temperature using the calibration curve for the proper type of thermocouple). Plots of relevant data were then created in order to make a comparison between the varying drive cycles and test setups used during the testing procedure.

Shortly after the original testing was completed, Argonne National Laboratory (ANL) was lent the Escape for further research into the drive system. As part of their work with the

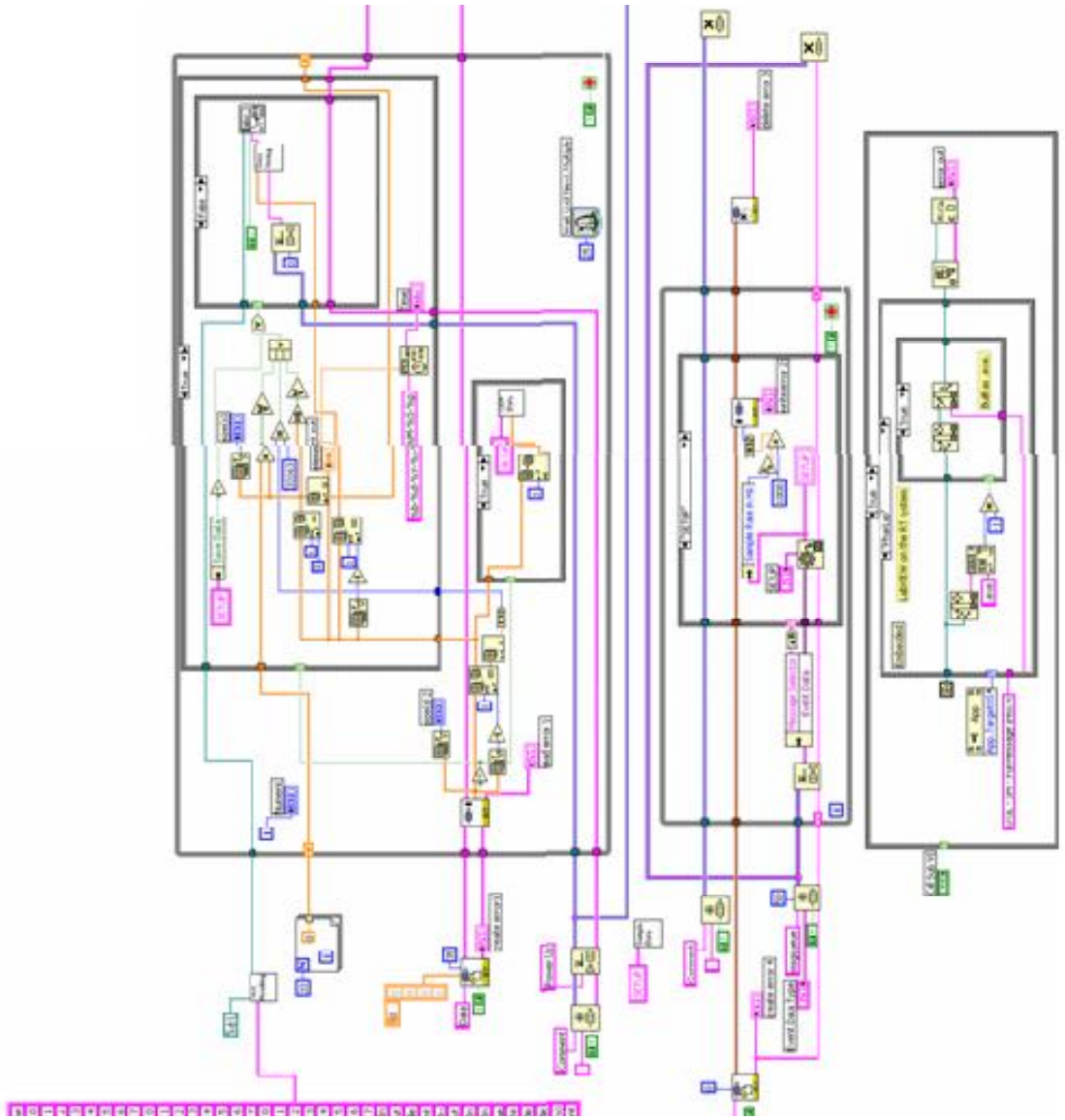

Figure 13. Block Diagram of Original DAQ Code (Jenkins, 2006).

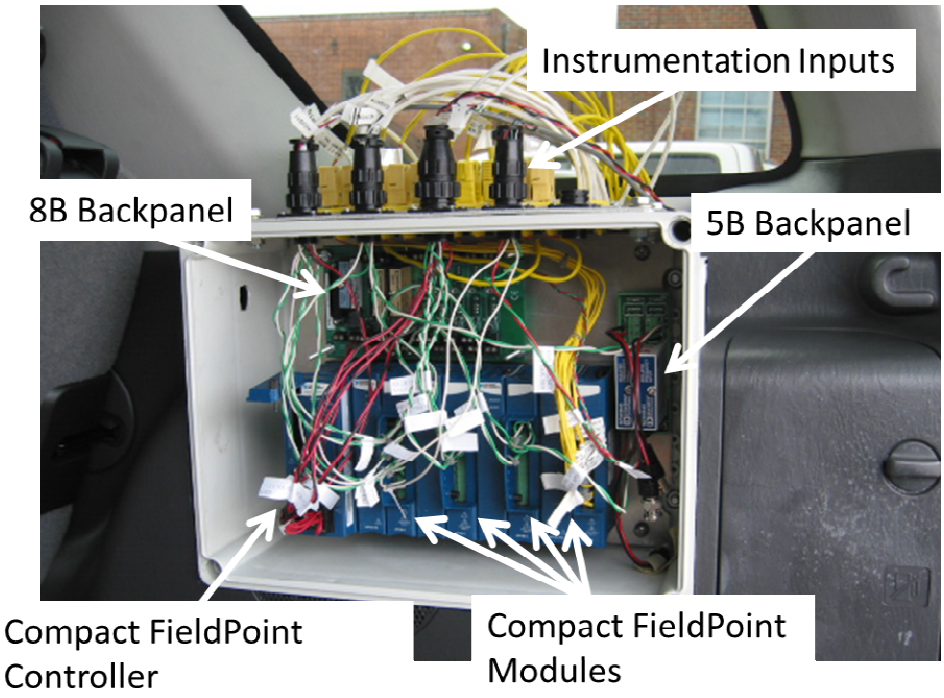

Figure 14. Original Configuration of DAQ Box.

vehicle, the cFP chassis and 5B back panel were removed, but the 8B back panel and its modules were retained. The DAQ controller was replaced with an NI Compact Reconfigurable Input/Output (cRIO) cRIO-9011 chassis. The modules installed in the chassis consisted of two NI-9211 modules used to receive thermocouple signals, an NI-9205 module that receives voltages and an NI-9853 that reads controller area network (CAN) signals. The 8B back panel was equipped to read, in addition to the previous two thermocouple signals, the brake pedal position sensor and accelerator position sensor as well as provide conditioned power to the ANL installed battery current probes. Although the DAQ box retained its original location, the components within the box changed. The current configuration of the DAQ box is shown in Figure 15.

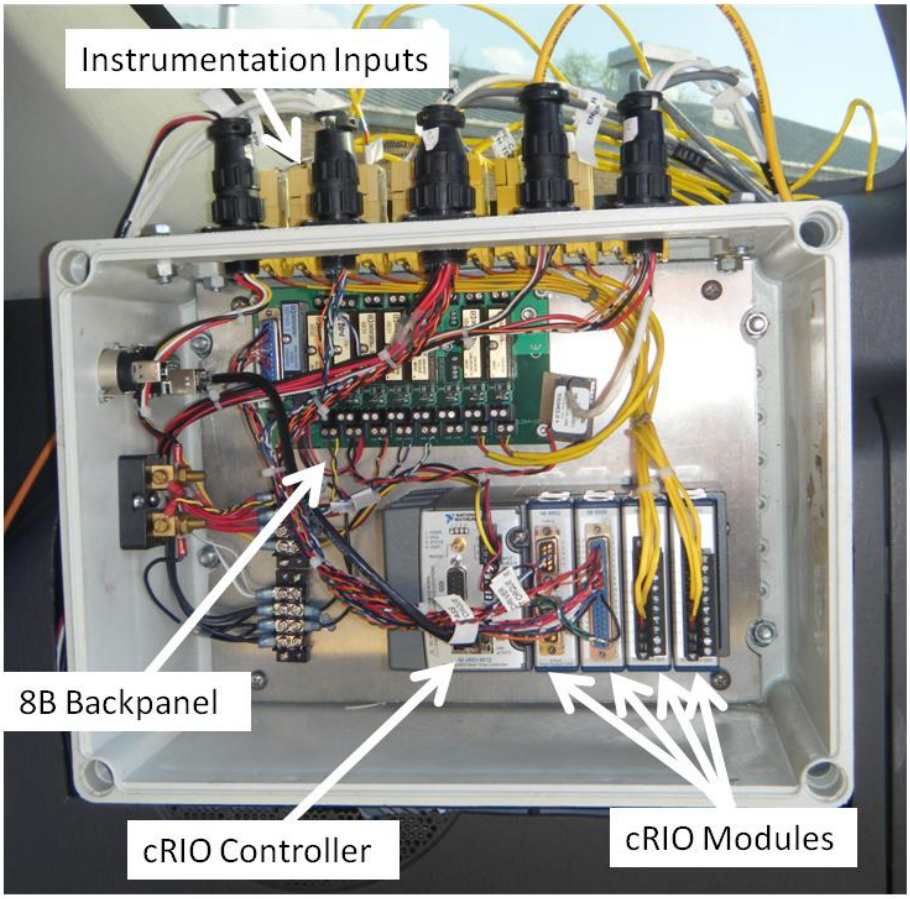

Figure 15. Current Configuration of DAQ Box.

LabVIEW was chosen for the data acquisition due to its relative ease of programming and deployment. Unlike traditional programming languages, LabVIEW VIs are programmed via graphical tools that allow code to be developed by placing icons in the workspace and connecting them with wires. These icons represent sub-VIs that replace lines of code to execute a command and thus is more compact and easier to follow than other programming languages.

Although the ANL engineers would have been required to have a VI installed on the cRIO controller to capture and save the input signals, when this research began the cRIO hard drive had been corrupted. In order to use the controller again an NI employee had to completely erase the hard drive and reinstall the operating system and drivers for the controller. Which,

unfortunately, meant losing the VI and a different copy could not be located. Therefore, a new VI was written for this research.

Rather than using one VI, an NI project directory was created that allowed for easy implementation of VIs into the cRIO. The model, modules and IP address of the chassis were defined first, then a host VI and embedded VI were created and placed into the project directory. The embedded VI was responsible for the actual collection of data while the host VI provided the user interface (if real time acquisition was being performed) and was responsible for writing the data into a text file. An example screenshot of the LabVIEW project and host VI are shown in Figure 16; the remaining VIs are shown in the Appendix. Although the CAN module would have produced invaluable data, only the thermocouple and analog module signals could be utilized for each test due to the highly proprietary nature of the CAN which prohibited it from being used in this research. The VI was coupled with a MATLAB algorithm that was capable of loading the DAQ information from the saved .txt file, converting the signals into properly scaled measurements and creating plots of the data. An example plot of catalytic converter temperature measurements, after MATLAB processing, is given below in Figure 17.

Acquired Signals

The instrumentation originally installed in the Escape is listed in Table 2 (Jenkins, 2006) and the location of each piece of this instrumentation is shown in Figure 18. Additionally, a comparison of documented instrumentation installed in the first research done with the vehicle and what was in the vehicle at the beginning of this research led to a list of ANL installed instrumentation which is given in Table 3.Four important pieces of instrumentation were installed while the vehicle was at Argonne. The first two listed in Table 3 are current probes, one of which monitors the current flow into and out of the 12V low voltage battery that is used for

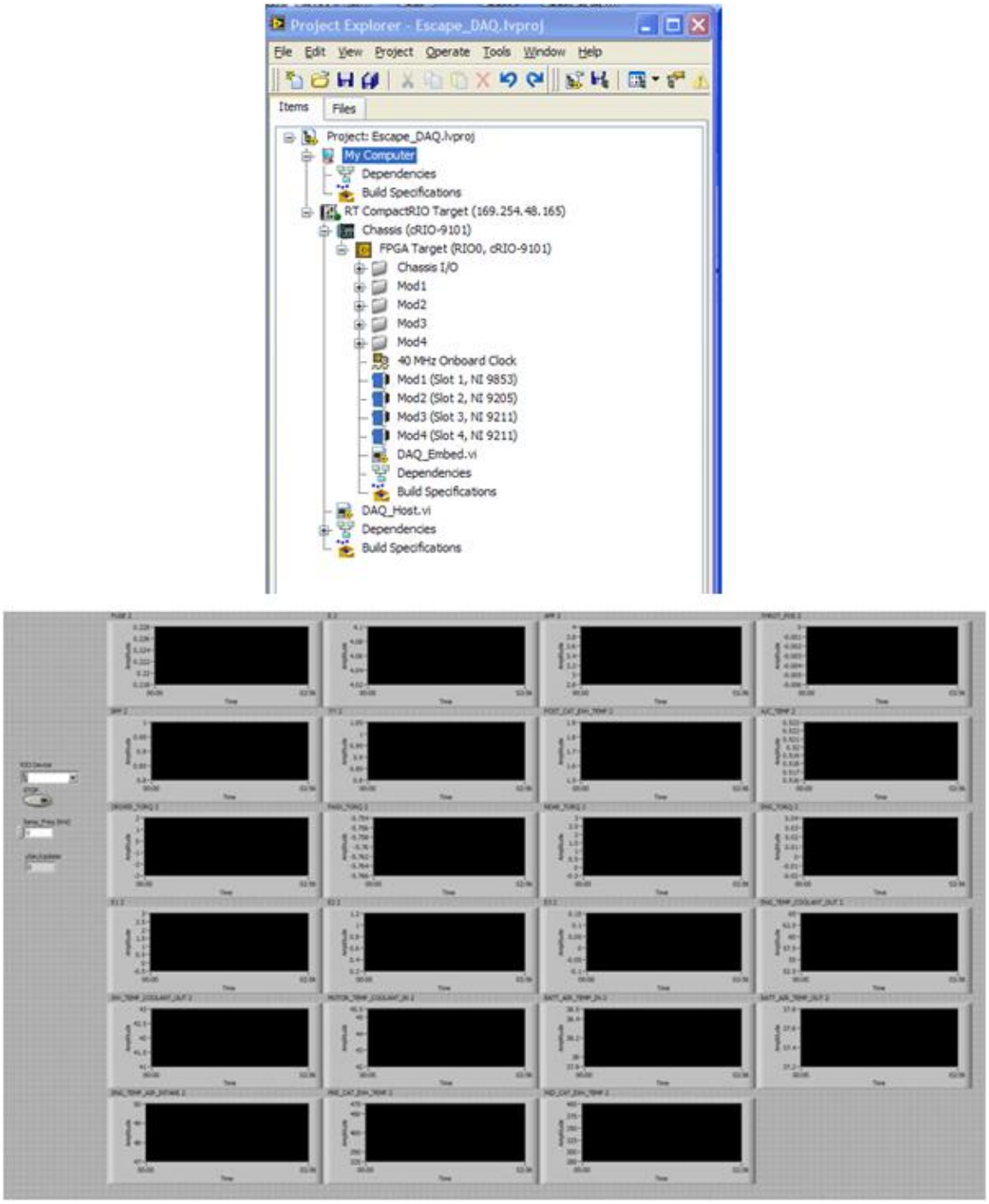

Figure 16. LabVIEW Project and Host VI.

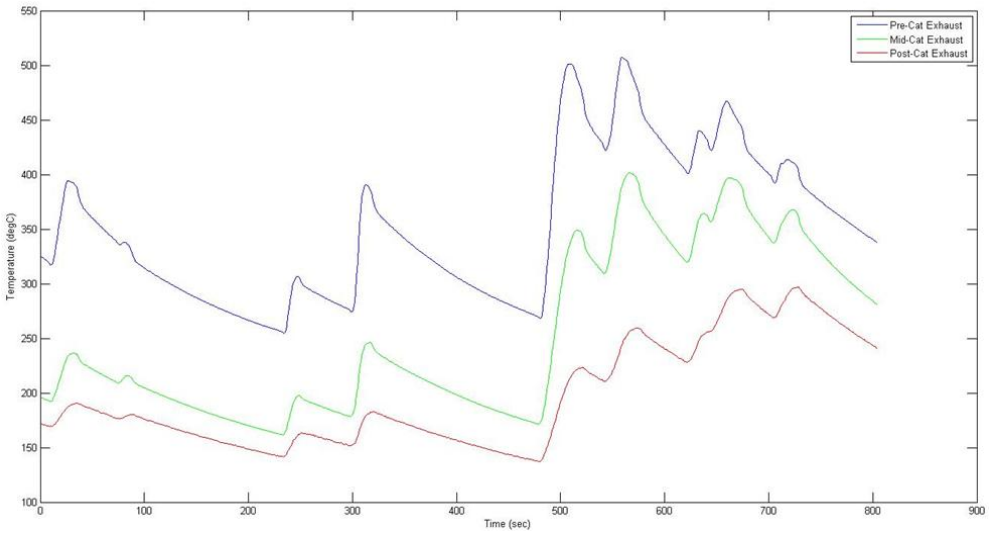

Figure 17. Example plot of Catalytic Converter Temperatures.

Table 2. Original Escape DAQ Signals.

Thermocouples	**Units**	**Data Name**
Battery Air Temperature In	°C	Batt Air Temp In
Battery Air Temperature Out	°C	Batt Air Temp Out
Motor Coolant Temperature In	°C	Motor Temp Coolant In
Inverter Coolant Temperature Out	°C	Inv Temp Coolant Out
Engine Temperature Coolant Out	°C	Eng Temp Coolant Out
Exhaust Pre-Catalyst Temperature	°C	Pre-Cat Exh Temp
Exhaust Mid-Catalyst Temperature	°C	Mid-Cat Exh Temp
Exhaust Post-Catalyst Temperature	°C	Post-Cat Exh Temp
Engine Air Temperature In	°C	Eng Temp Air Intake
Air Conditioning Temperature	°C	AC Temp
Vehicle Sensors	**Units**	**Data Name**
Engine Speed	Hz	Engine Speed
Motor Torque	Hz	Motor Torque
Accelerator Pedal Position	V	APP
Brake Pedal Position	V	BPP
Electronic Throttle Position	V	TPS
Heated Oxygen Sensor Pre-Catalyst	V	HO2SII Pre-Cat
Manifold Absolute Pressure	V	MAP
Intake Air Temperature	V	IAT
Other Signals	**Units**	**Data Name**
Axle Torque Left	N-m	Axle Torque Left
Axle Torque Right	N-m	Axle Torque Right
Axle Torque Rear	N-m	Axle Torque Rear
Accelerometer X-Direction	g	Accel X

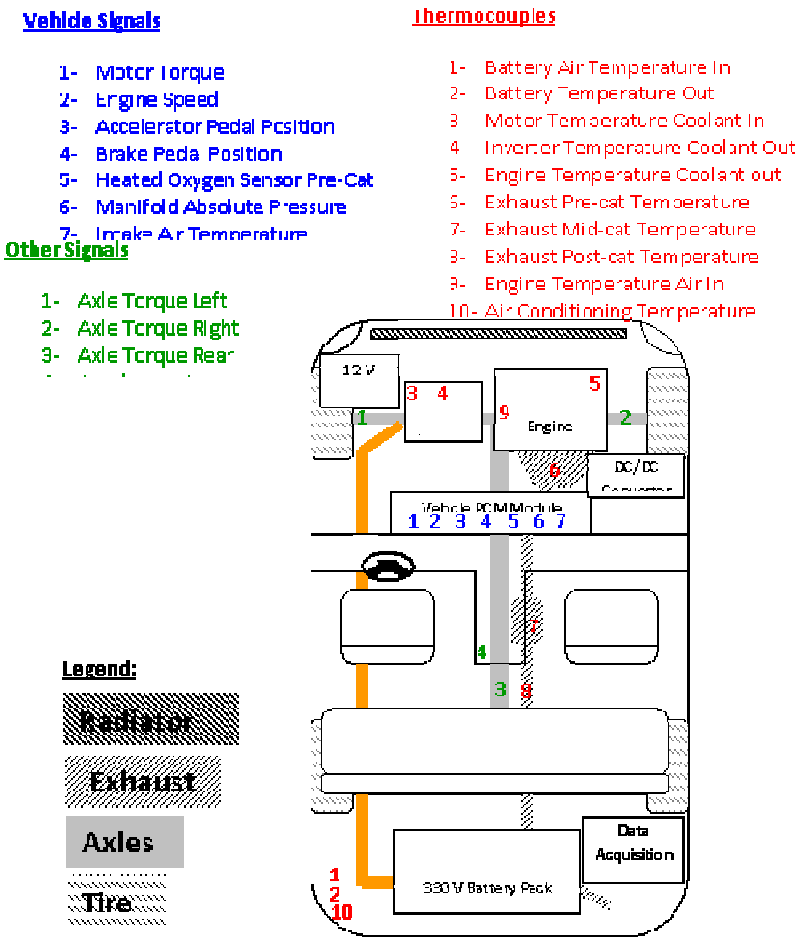

Figure 18. Original Escape DAQ Signal Locations.

Table 3. ANL Installed Instrumentation.

Current Probes	**Units**	**Data Name**
High Voltage Battery Current	A	HV_Bat_Cur
12V Battery Current	A	LV_Bat_Cur
Fuel Flow	**Units**	**Data Name**
Gasoline Flow Rate	gpm	Qfuel
Torque	**Units**	**Data Name**
Engine Torque	Nm	Eng Torq

auxiliary systems while the other probe monitors the current flow into and out of the DC/DC converter that is used to provide high voltage DC power to the traction battery. Another key

piece of instrumentation installed by ANL is a fuel flowmeter that was placed under the floor board approximately half way between the fuel tank and injector rail.

When research began for this project some of the previously installed instrumentation was either no longer installed or not functioning. Table 4 provides information on which signals were not functioning properly along with a description of the issue(s) and the action(s) taken to rectify those issues.

Table 4. Malfunctioning Signals with Description and Fixes Described.

Signal	**Description/Action Taken**
BPP	Testing confirmed a non-linear sensor; signal not used.
Post-Cat Exh Temp	Improper thermocouple type installed. Replaced with proper type.
AC Temp	Thermocouple was not reading proper temperature. Tested and confirmed to not be working. AC Temperature not used in research.
Axle Torque Right	Fuse was blown in amplifier. Replaced fuse to obtain readings.
Acceleration	Accelerometer had been removed.

CHAPTER 4

VEHICLE TESTING

In order to perform a comparison between the actual Escape and the model built for this project, testing had to be undertaken. In an attempt to achieve consistent results across the various tests a common drive cycle had to first be chosen for all tests. Since previous dynamometer testing had been performed using the vehicle used in this study, the driving cycle used for this research was matched to the drive cycle employed in the previous work. This drive cycle, nicknamed AL-University, uses roads in and around the University of Alabama campus and is roughly derived from the EPA's Urban Dynamometer Driving Schedule (UDDS) (Jenkins, 2006). Since this is the drive cycle that was used for the previous testing of this vehicle, it will be used in the GT Suite simulations of this project. For this cycle, the route followed is shown in Figure 19 and the vehicle speed as a function of time for this cycle is shown in Figure 20.

Tuscaloosa Drive Cycles

As part of the prior research performed on the Escape, two Tuscaloosa drive cycles were created and used for the testing procedure. These cycles were constructed to match, as closely as possible, the EPA Highway (HWY) cycle and the UDDS while driving in real world traffic. The Tuscaloosa drive cycle (AL-University) is chosen for this project and the results from the previous iterations of these tests will be used for comparison of data that was obtained at ANL. A comparison of the AL-University drive cycle and the actual UDDS is given in Figure 21 (Jenkins, 2006). The signals recorded during these tests were described in Chapter 3.

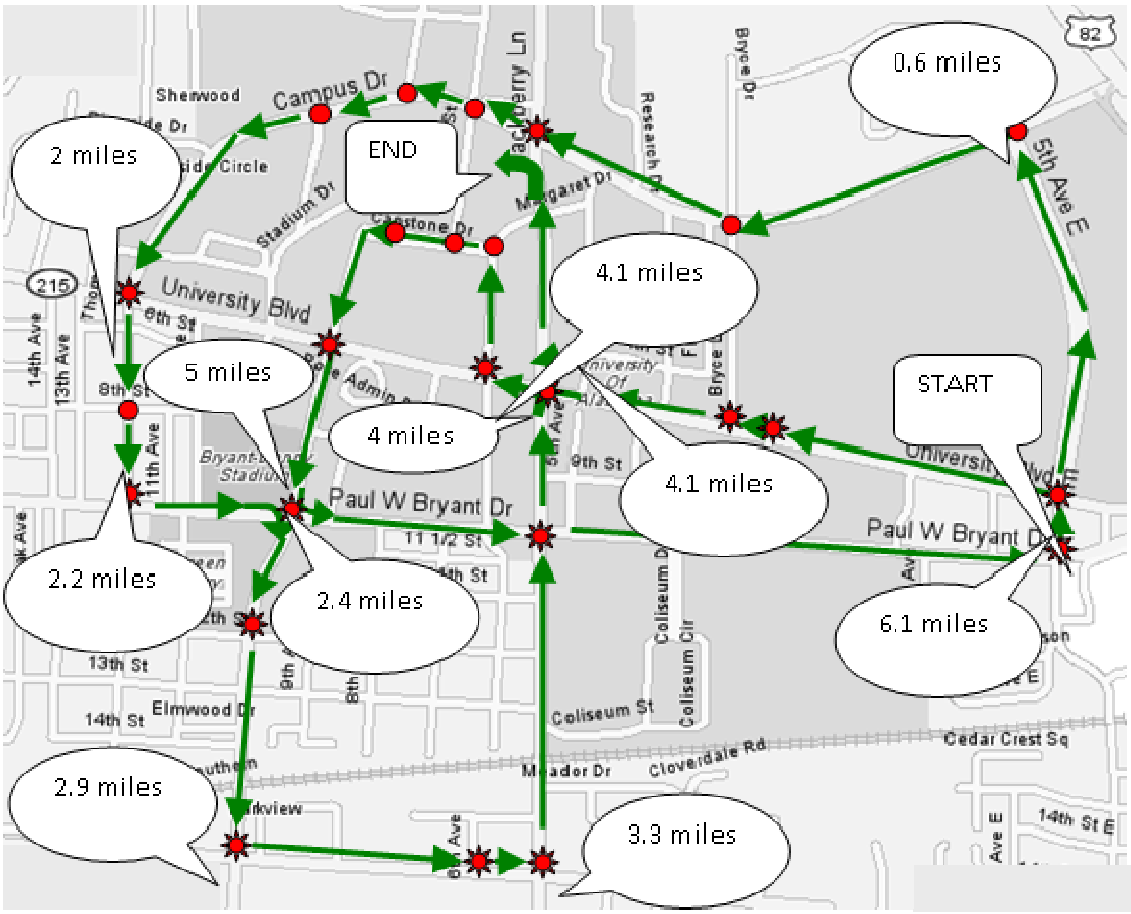

AL- University cycle

1) Start at University Blvd. and 5th Ave. E.

2) Take 5th Ave. E. for 0.6 miles

3) Turn left onto Campus Dr.

4) Take Campus Dr. for 1.4 miles

5) Go straight on 12th Ave. for 0.2 miles

6) Turn left on Paul Bryant Dr.

7) Take Paul Bryant Dr. for 0.2 miles

8) Turn right on 10th Ave.

9) Take 10th Ave for 0.5 miles

10) Turn left on 15th St. E.

16) Turn right on 6th Ave

17) Take 6th Ave. for 0.2 miles

18) Turn left on Capstone Dr

19) Take Capstone Dr. for 0.2 miles

20) Turn left on Colonial Dr.

21) Take Colonial Dr. for 0.5 miles

22) Turn left on Paul Bryant Dr.

23) Take Paul Bryant Dr. for 1.1 miles

24) Turn left on 5th Ave. E.

25) Take 5th Ave E. for 0.1 miles

Figure 19. AL-University Drive Cycle Route.

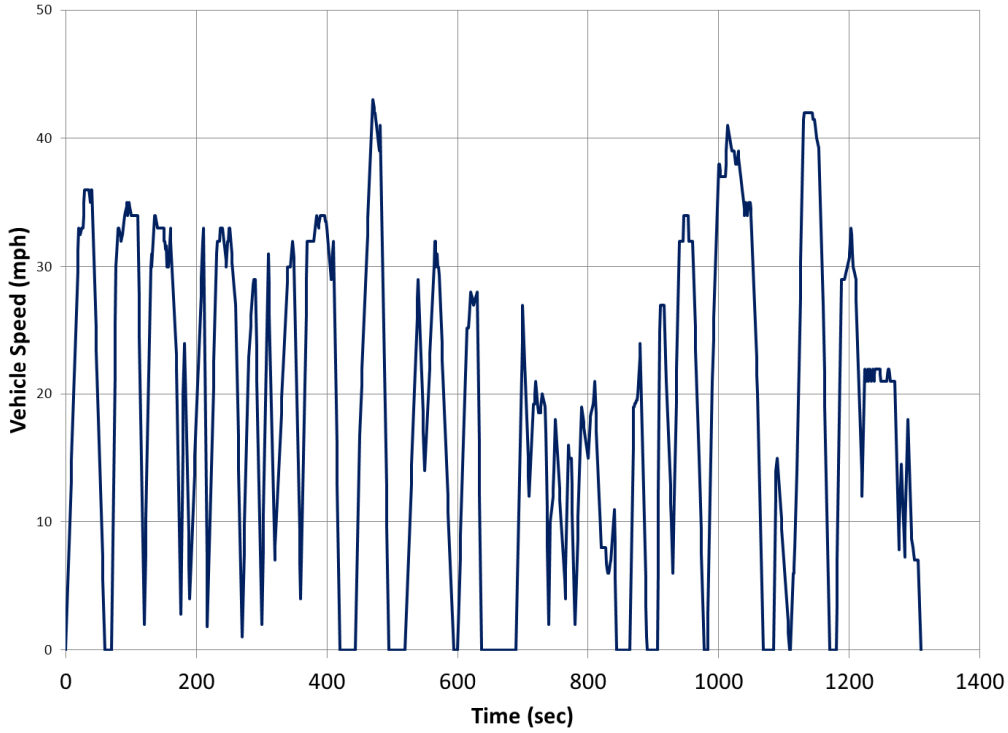

Figure 20. Vehicle Speed as a Function of Time for AL-University.

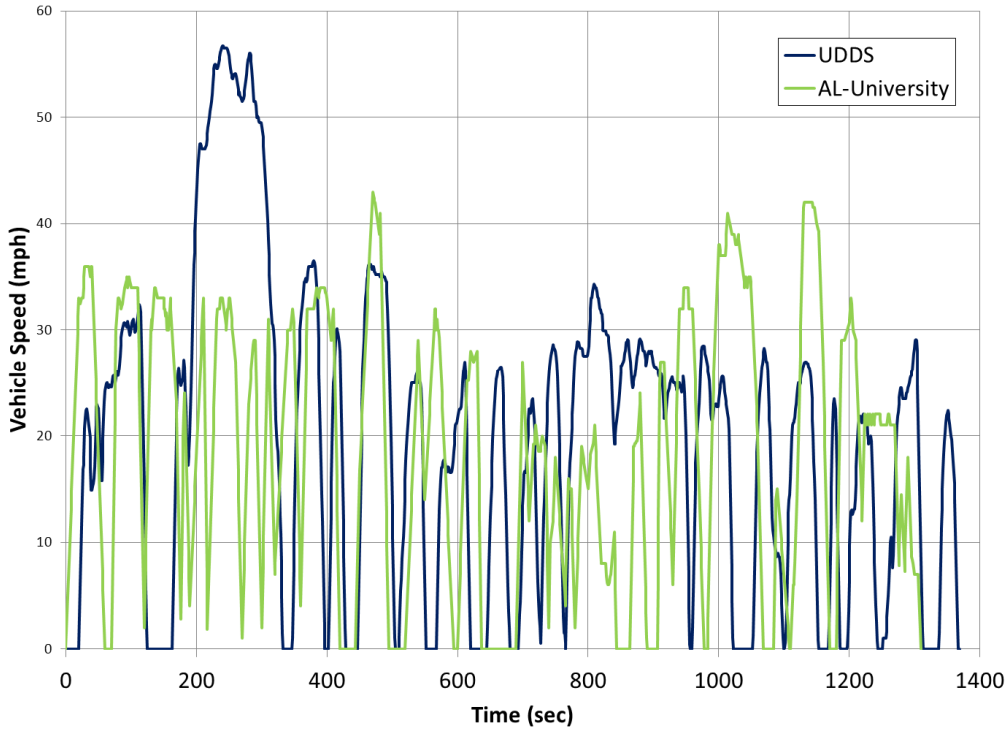

Figure 21. Comparison of AL-University and UDDS Drive Cycles.

Chassis Dynamometer

Previously, nine drive cycles were performed at ANL on their chassis dynamometer. These cycles included two steady state cycles, a US06, UDDS and five custom cycles based on the on-road testing described above. For this research, the chassis dynamometer results for the AL-University cycle were of greatest significance due to the fact that the GT Suite simulations were performed on this cycle. For all of the tests undertaken at ANL, emissions data, vehicle speed and various vehicle operating data were recorded to be used for comparison to the actual tests and the simulation results. A list of the recorded data for the dynamometer testing is provided in Table 5.

Table 5. Dynamometer Recorded Signals.

Signal	Units
Vehicle Speed	mph
Battery Current	A
Battery Voltage	V
Battery Power	kW
Exhaust Temperature	°F
Coolant Temperature	°F
Battery Air Temperature	°F
Wheel Torque	Nm

The dynamometer testing was performed at ANL's Advanced Powertrain Research Facility (APRF) and the procedure for dynamometer testing laid out by the EPA was followed. As part of this procedure, the vehicle was placed in a soak room for 24 hours prior to the testing where the vehicle temperature was brought to between 73 and 77°F, which is the temperature of the test cell, per EPA guidelines. After 24 hours, the vehicle is driven, at idle speed, onto the dynamometer and strapped in the front and rear of the vehicle to minimize lateral motion of the vehicle – limited to 4 inches in the rear and 2 inches in the front. The exhaust system was connected to a Constant Volume Sampling (CVS) unit to analyze vehicle emissions and the

vehicle hood was opened to allow a cooling fan to push air across the engine compartment for cooling. All the accessory systems in the vehicle were turned off and the vehicle driver's aid computer screen was positioned in front of the windshield. Figure 22 shows the Escape ready for chassis testing. After the cycle has been completed, the vehicle is driven off the chassis dynamometer, again at idle speed, to complete the testing procedure.

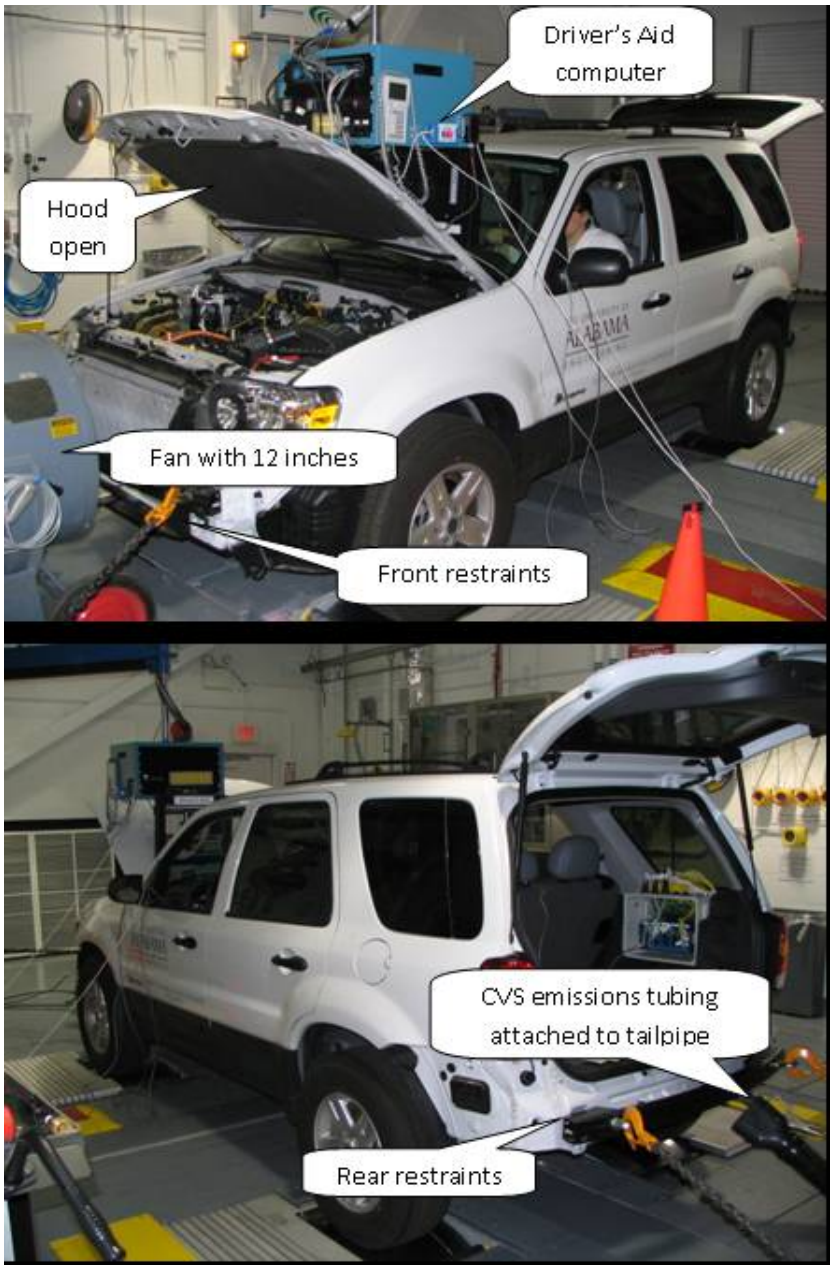

Figure 22. Photographs of Escape on Chassis Dynamometer.

GT Suite

In GT Suite, the controller for the vehicle will work to maintain a minimal error between the model's actual speed and the target speed set by the AL-University drive cycle. This is done by calculating the error in actual and target speed then calculating the anticipated acceleration, and thus powertrain torque, required to meet the target speed for the future timestep. An in depth discussion of this process will be reserved for the following chapter.

CHAPTER 5

GT SUITE

In contrast to the previous research performed with the Escape, GT Suite was chosen for this project over PSAT. This choice was made due to various advantages GT Suite holds over PSAT, the most important of which will be discussed in the next section. The interface of GT Suite and a simple example assembly will be demonstrated in order to give an introduction to the software and show its ease of use. At the conclusion of this chapter a thorough description of the model will be given; however, an understanding of the complete model would be impossible to convey in the scope of this paper.

Background

Gamma Technologies, Inc. (GTI) was founded as a computer aided engineering (CAE) software firm in 1994 by Dr. Thomas Morel. Originally, the principle clients for the company were Original Equipment Manufacturers (OEMs) in the automotive and engine industries who were interested in reducing the costs to their companies by utilizing simulation tools. GTI began with software designed to model flow systems (such as automotive air intakes) and basic engine cycles. Throughout its development, GT Suite has been focused on providing an integrated engineering solution to automotive simulations whereby each vehicle subsystem can partake in the simulation rather than each subsystem requiring its own simulation.

Over the course of the past few years GTI's software has expanded to include the ability to model much more complex systems, such as Exhaust Gas Recirculation (EGR) and complete vehicle models, including control systems (which can utilize Simulink if required). Most important to this research project, the ability to model HEVs has been implemented and improved upon in GT Suite within the last couple of years. This includes pre-built models for HV batteries, planetary gear sets and power electronics.

The greatest advantage of GT Suite is its graphical user interface (GUI) that allows for the visual assembly of components and customization of their parameters. The main workspace for GT Suite is shown in Figure 23.

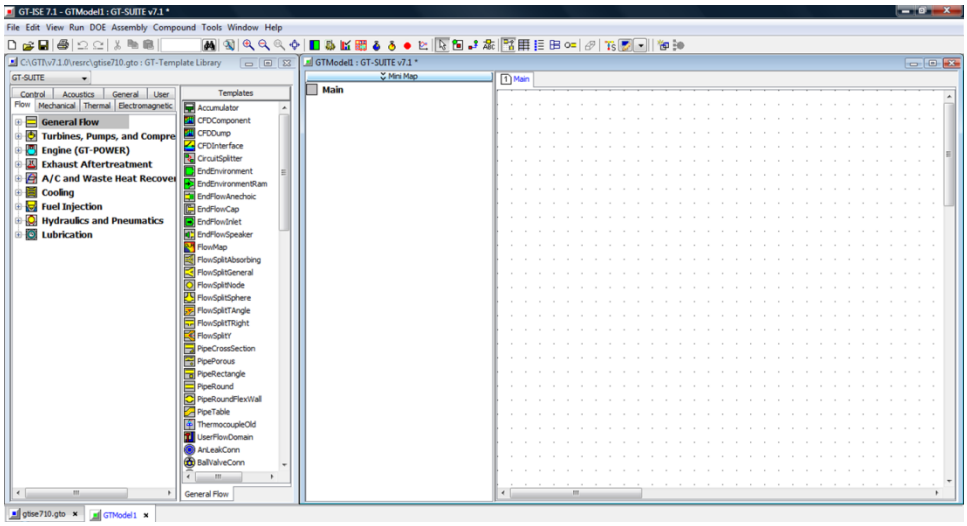

Figure 23. GT Suite Main Workspace with Component Library on Left.

In addition to the ease of component placement and connection, a multitude of component models are pre-built within the software. This means that instead of constructing, for example, a battery model from the individual resistances, voltages, capacities, etc. of each cell and then connecting the cells, a prebuilt battery model can be loaded and the total resistance, voltage, capacities, etc. can be customized. These pre-built models are divided into several

component libraries that include, among others, Engine, Thermal Management, Electric and Control libraries.

Once a model is built, the user has several options for outputs and monitors that can be employed during and after the simulation. Virtually any vehicle or subsystem operating characteristics can be monitored during the simulation granted the user provides sufficient information to GT Suite for these characteristics to be calculated during the simulation. Once the simulation has ended, all of the desired characteristics can be viewed and saved within GT Post which is a post-processing software program that is bundled within GT Suite. GT Post can provide these results via a plot or table. All table values can be exported into other software programs for further analysis or comparison.

Overview

To build a model in GT Suite the user must import parts from the object libraries or build their own parts from their respective elements. For this research, only pre-existing objects were used so the process used to build custom objects will not be detailed. Figure 24 below shows a screen shot of GT Suite with the object library opened to the left. To add an object, the user simply clicks and drags the object from the library to the design tree. In the figure, an 'EngineState' object has been added to the model.

Once the user has imported all desired objects from their respective libraries, each object can be customized with its properties to create a part that can be placed in the assembly. In Figure 25 an 'EngineState' part is being created and it parameters input. Once it is created it is drug into the assembly space as seen in Figure 26.

The part placement procedure continues until all desired parts are placed in the assembly space. After this is completed, the user must connect the various parts in the way that is desired

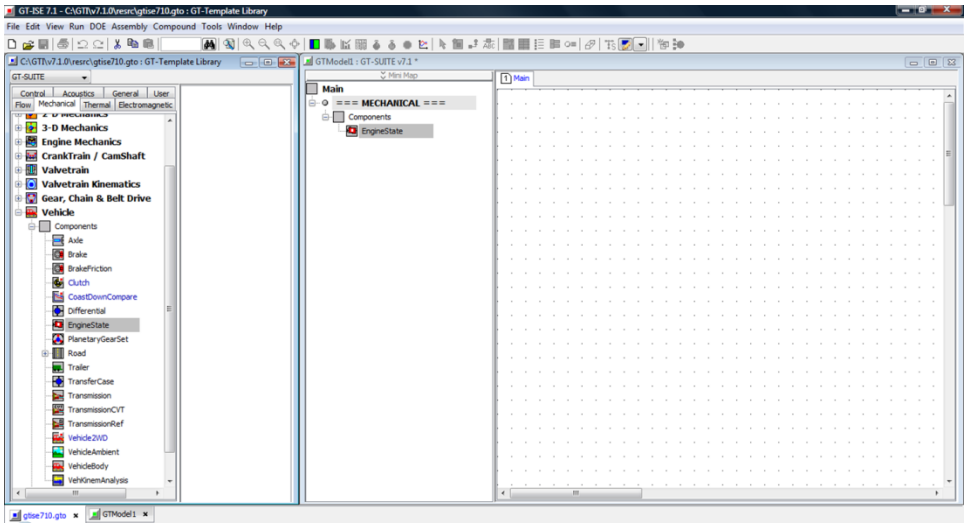

Figure 24. GT Suite Project Window with Added EngineState Object.

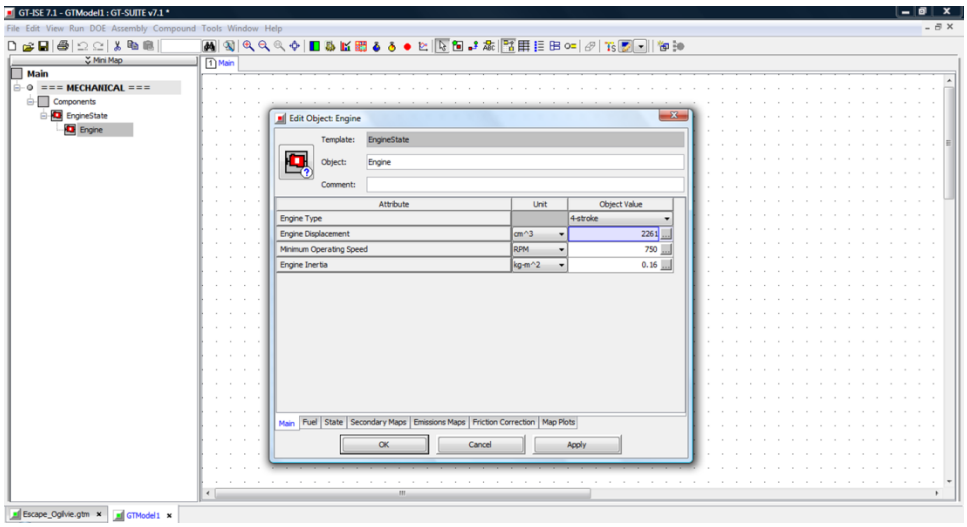

Figure 25. Editing Parameters for an EngineState Object.

or most closely matches the configurations of the parts in the actual system. Between all parts some type of connection constraint is imposed, the ‘RigidConn’ part is the most common and represents a rigid connection in which there is no slipping, damping or spring forces present. Figure 27 shows the main assembly space of a vehicle model from a GT Suite example model. In this picture, all parts of the main assembly and their connections are visible.

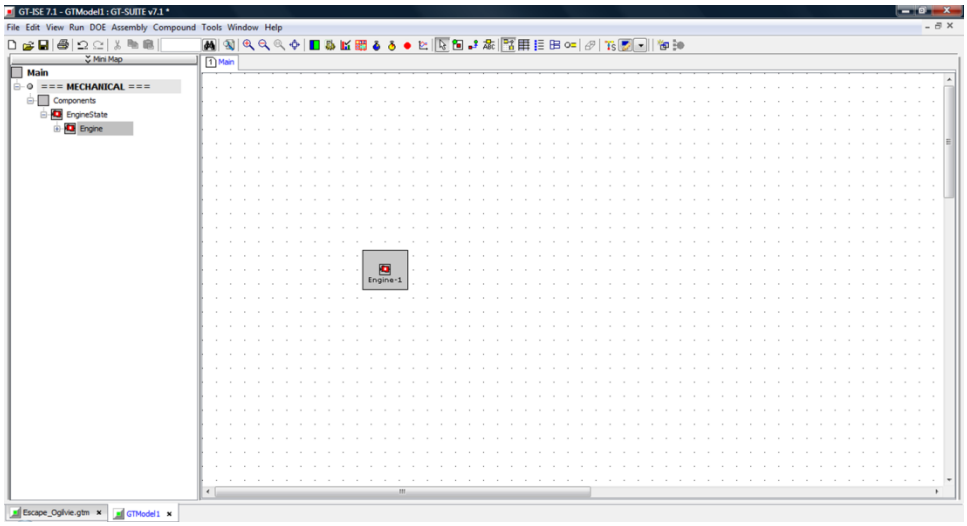

Figure 26. EngineState Object Added to Assembly.

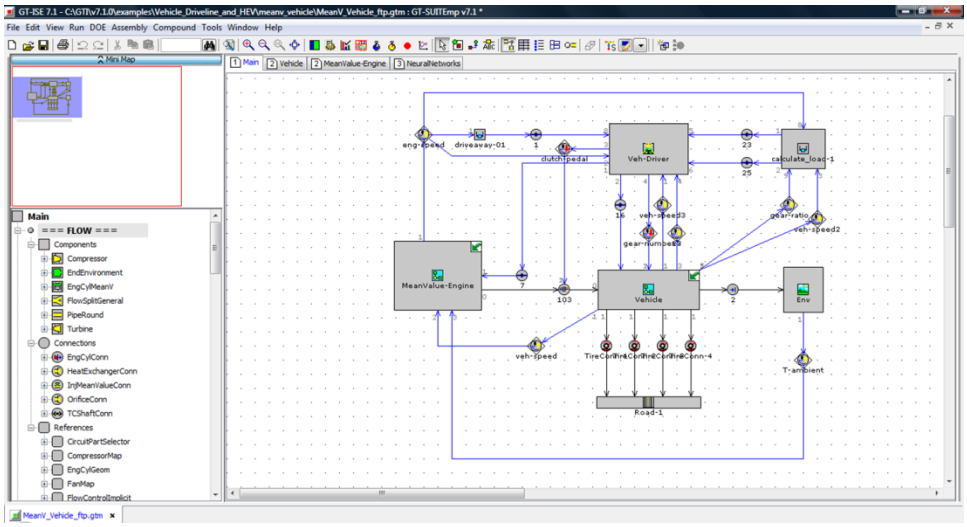

Figure 27. Example GT Suite Vehicle Model.

In Figure 27 the vehicle is represented as a subassembly – note the tab at the top of the assembly space that is labeled ‘Vehicle’. The use of subassemblies greatly reduces the number of components in the main assembly space and allows the user to clearly see the interactions of the parts within the model. By clicking on the subassembly tab, the subassembly is visible as displayed in Figure 28.

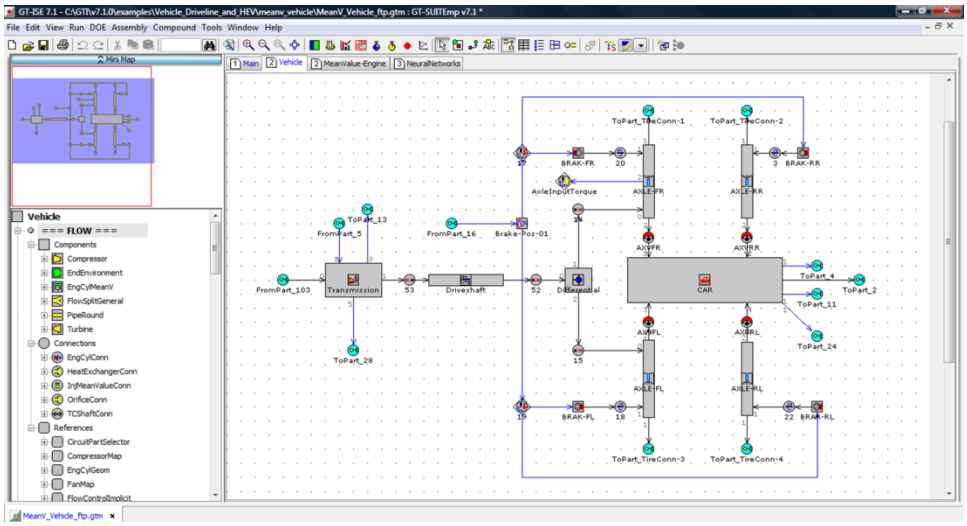

Figure 28. Vehicle Subassembly of Example Vehicle Model.

Once the model is built, the desired plots can be set to be acquired within the ‘Edit Part’ window. For the same example used above, the ‘Car’ object parameter window is shown in Figure 29 with the option boxes that represent the desired output plots and data enabled.

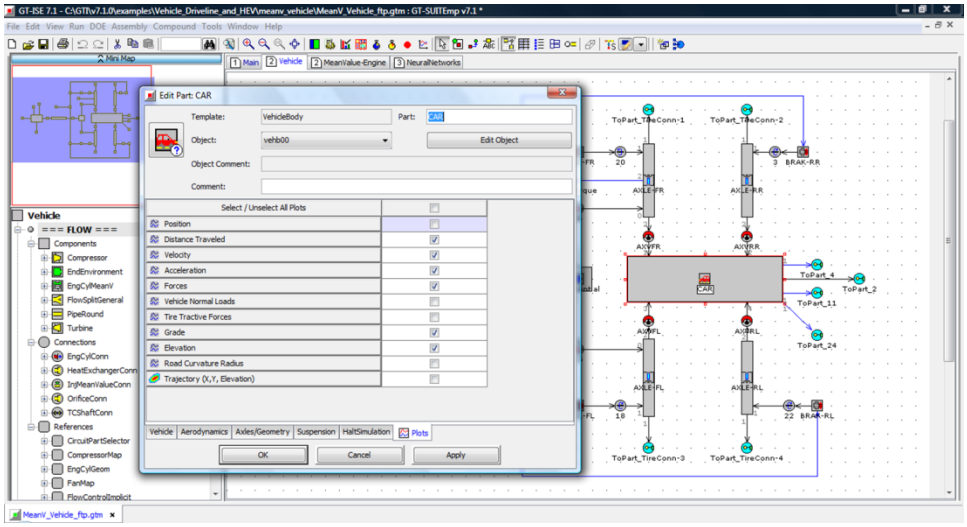

Figure 29. Output Plot Selection for Vehicle Body.

After running the vehicle simulation the model and results can be opened in GT Post. When first loaded, the screen looks similar to the GT Suite main window, but it is greyed out due to the fact that it is not editable. Plots that have been requested prior to running the simulation

can be viewed by either finding the object of interest in the parts tree to the left or by right clicking on the object in the model space. A screen shot of GT Post with a plot of vehicle speed as a function of simulation time is shown in Figure 30.

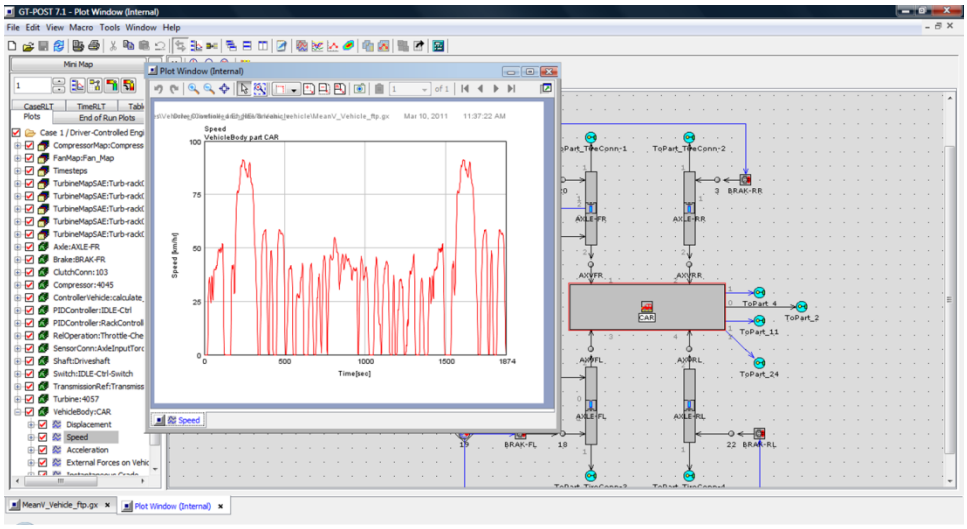

Figure 30. GT Post Output Plot of Vehicle Speed for Example Vehicle Model.

For this project, the GT Suite model consisted of the main assembly and seven subassemblies. The subassemblies include vehicle, power demand, engine control, motor control, generator control, battery control and braking control. A section below is dedicated to each of these and will begin with a screen shot of that particular assembly followed by a brief discussion of the assembly.

Model: Main

The main assembly of the Escape model melds together the various components that make up the vehicle system model. These include the battery, battery power electronics, motor, generator, eCVT, vehicle chassis and body, and engine. Also visible in the main assembly, since all subassemblies must be present in the main assembly are the power demand and braking control. The separate controllers for the battery, motor, generator, and engine make up subassemblies within the main assembly as seen in Figure 31.

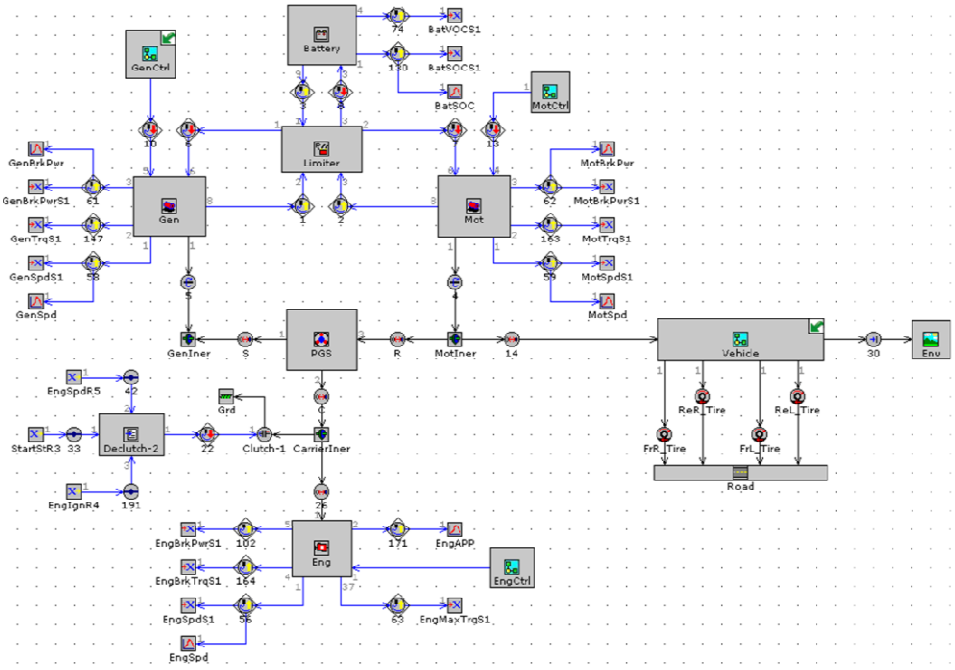

Figure 31. Main Assembly of Escape Model.

The quickest parts to mention in the main assembly are the power demand and braking control subassemblies. Both of these will be described within their own section and they are only present in this assembly because the subassemblies must originate from the main assembly and by creating a subassembly for these parts the main assembly page can be kept neat.

Starting with the battery at the top of the assembly, it receives a power demand from the battery control subassembly placed near the battery part. Using electrical actuator and sensor connections it is capable of sending or receiving electrical power to the battery system power electronics that is modeled as a ‘PowerLimiter’ part and ensures that the charge or discharge demand of the vehicle electronics does not exceed the entered maximum fraction of battery power. To the left and right of the battery part are sensor connections that instruct GT Suite to send signals for the battery open circuit voltage (VOC) and state of charge (SOC) throughout the simulation to be used by other parts. Additionally, the SOC is monitored while the simulation is

running via the ‘MonitorSignal’ part that is paired to the same sensor connection and the SOC ‘SendSignal’ part. For the battery and limiter parts, the parameters given in Table 6 were calculated using two studies performed by the U.S. Department of Energy Advanced Vehicle Testing Activity (DOE, 2005).

Table 6. Battery and Limiter Parameters.

Parameter	Units	Value
Initial SOC	-	0.6
Battery Temperature	K	300
Battery Capacity	Ah	5.5
Open Circuit Voltage Map	V	Appendix D
Internal Resistance Map	Ohm	Appendix D
Coulombic Efficiency	-	0.95
Maximum Battery Power Fraction	-	0.95

To the right of the battery power electronics is the motor part. This part is built from a ‘MotorGeneratorMap’ object that uses a map based technique to match a requested input power to a speed and torque when an efficiency map is provided. Its inputs are a brake power request (through the motor control subassembly) and an electrical power from the limiter. In order to maintain a desirable state of charge, the motor is also capable of sending power into the battery through an electrical connection that points into the limiter. The power limits of the motor are calculated in the motor control subassembly and ensure that the motor does not request more electrical power than it is capable of receiving. The mechanical output from the motor is connected to the vehicle driveline by first going from the motor part output to a torque connection to a motor inertia part and then into the eCVT and driveline. The eCVT connection is made through a rigid connection to the ring gear of the planetary gear set and the driveline connection is made through another rigid connection to the output shaft of the eCVT. In order for the simulation to execute real time control, several signals are sent from the motor. These are the

brake torque, brake power and motor speed, with the last two also set to monitor in real time during the simulation. For the motor and its inertia, the values given in Table 7 were used.

Table 7. Motor Parameters.

Parameter	Units	Value
Electromechanical Conversion Efficiency	-	Appendix D
Load Control Option	-	Power-Brake
Static Brake Torque Limit	Nm	10000
Maximum Brake Torque	Nm	Appendix D
Minimum Brake Torque	Nm	Appendix D

To the left of the limiter part is the generator part, which is also built using the 'MotorGeneratorMap' model and uses an input brake torque signal to operate. Similarly to the motor part, the generator is capable of both sending and receiving power from the battery via electrical connections through the battery power electronics. Its mechanical output is connected to the eCVT through a torque connection part to a generator inertia part and then through a rigid connection into the sun gear of the planetary gear set. The signals sent by the generator are the brake torque, brake power and speed with the last two monitored in real time using 'SignalMonitor' parts. Table 8 lists the generator parameters used for the model.

Table 8. Generator Parameters.

Parameters	Units	Value
Electromechanical Conversion Efficiency	-	Appendix D
Load Control Option	-	Torque-Brake
Static Brake Torque Limit	Nm	80
Maximum Brake Torque	Nm	Appendix D
Minimum Brake Torque	Nm	Appendix D

At the bottom of the main assembly tab is the engine part. The engine model was created using an 'EngineState' part that is a map based approximation, similar to the motors. Inputs to the engine include an accelerator pedal position, from the engine control subassembly, and the

carrier speed from the eCVT. The carrier speed is an input to the engine due to the presence of the clutch at the carrier and its directional requirements. Signals sent by the engine part include the brake power, brake torque, speed and maximum torque at that particular speed. Both the engine speed and accelerator pedal position signals are displayed during the simulation via 'MonitorSignal' parts and the parameters set for the engine are given in Table 9.

Table 9. Engine Parameters.

Parameter	**Units**	**Value**
Engine Type	Stroke	4
Engine Displacement	cm^3	2261
Minimum Operating Speed	rpm	750
Fuel Density	kg/m^3	719.7
Fuel Heating Value	MJ/kg	44.4
Mechanical Output Map	Nm	Appendix D

From the carrier inertia part of the model, the clutch and clutch control parts are connected. These parts work to engage or disengage a clutch between the engine and carrier of the planet gears in the planetary gear set. This allows the planets to rotate about the sun gear and maintain the CVT behavior of the planetary gear set even when the engine is not running. Without the clutch, the carrier would be locked and the eCVT would no longer be able to operate with infinite effective gear ratios. The clutch control parts work by receiving the starter state, engine ignition and engine speed signals and determining if the engine is providing power and, if so, engages the clutch so the engine output power is sent to the eCVT. If the clutch 'EventManager' object detects that the engine is not being used to provide power, the clutch disengages so that power does not try to go from the eCVT into the engine.

For the hybrid Escape vehicle, the eCVT is the most important part because it is responsible for receiving power from the various components and creating a drive power for the vehicle. In GT Suite, a 'PlanetaryGearSet' part is used as the basis for the eCVT with the

generator connected to the sun gear, motor connected to the ring gear (also the output of the eCVT) and the engine connected to the planet gear carrier. In GT Suite the 'PlanetaryGearSet' part is based on the speed and torque relations of a simple epicyclic gear set with no gear lash taken into consideration. Unfortunately for this project not all parameters of the eCVT could be found or determined; for these parameters, values from the GT Suite example Prius model were used. The parameters for the eCVT part are displayed in Table 10 with the Prius values used denoted by an asterisk.

Table 10. eCVT Parameters.

Parameter	Units	Value
Number of Sun Gear Teeth	-	33
Number of Ring Gear Teeth	-	79
Ring Gear Pitch Radius	mm	57.5*
Sun Gear Moment of Inertia	kg-m^2	1.1E-4*
Carrier Moment of Inertia	kg-m^2	1E-9*
Ring Gear Moment of Inertia	kg-m^2	0.003*
Planet Gear Moment of Inertia	kg-m^2	1.6E-5*
Number of Planet Gears	-	4
Sun to Planets Efficiency	-	0.96
Ring to Planets Efficiency	-	0.96

From the eCVT the connections follow from the ring gear through the motor inertia (since these components share a similar connection to the output of the planetary gear set) and a rigid connection to the vehicle subassembly. Although it is not visible in the main assembly, this connection goes through a small shaft that represents the eCVT output and into the transfer case. The vehicle subassembly has five outputs to other objects on the main assembly page. One of these connections is to the ambient air conditions which were taken to match typical atmospheric air properties and the remaining four outputs are the tire connection parts that represent the interaction of the road and vehicle axles. The tire connection parts' parameters were set to match the properties of the actual tires on the Escape which are Continental Contitrac Eco Plus with a

radius of 0.359m at an inflation of 241.3kPa and have a rolling resistance factor of approximately 0.015.

Model: Vehicle

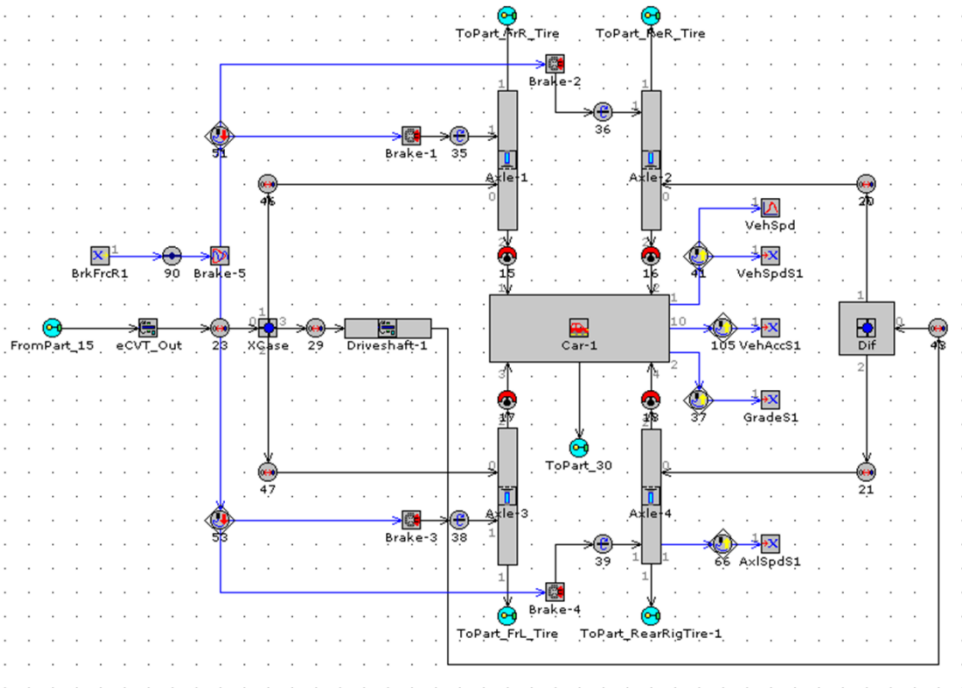

Figure 32. Vehicle Subassembly of Escape Model.

The vehicle subassembly is made up of the vehicle chassis and body components seen in Figure 32, including the axles, differentials and drive shafts. Beginning at the left of the subassembly, the input to the subassembly is the output from the ring gear of the eCVT. This connection is made to a drive shaft, given a small inertia (approximately 0.0001kg-m^2), which is used to connect the ring gear output to the transfer case (since this is an all-wheel drive vehicle). From the transfer case, a rigid connection part sends the rotational energy to the rear drive shaft at one output port and to the front axles at the other two output ports. The power split at the transfer case was modeled to be 25% to each of the front wheels and 50% to the rear wheels.

The output port of the rear drive shaft, whose inertia was estimated to be 0.04kg-m^2, is connected via another rigid connection to the differential in the Escape, whose final drive ratio was found to be 3.77 and the input and output inertias are both 0.05kg-m^2. Two output ports of the differential point to the rear axles of the Escape while the front axles receive energy from the transfer case. For all axles, the lengths and masses were obtained from the replacement Ford Motorcraft parts and the inertias were estimated with this data to be approximately 1.4kg-m^2. Each axle also has a connection between it and the brakes for each wheel via a torque connection. The 'Brake' part receives the braking force signal from the 'ReceiveSignal' part on the left of the screen and actuates a force that opposes vehicle motion at each axle.

In order to propel the vehicle, the axles had to be connected with the vehicle body. This task was accomplished using a 'VehicleAxleConn' part between each axle and the vehicle body. The vehicle body itself contains most of the parameters within the vehicle subassembly; these parameters are detailed in Table 11. Five output signals are generated within the vehicle subassembly and used for various calculations throughout the model, including the vehicle speed, vehicle acceleration, road grade and axle speed.

Table 11. Vehicle Body and Chassis Parameters.

Parameter	**Units**	**Value**
Vehicle Mass	kg	1741.3
Passenger and Cargo Mass	kg	90.7
Vehicle Frontal Area	m^2	2.685
Vehicle Drag Coefficient	-	0.4
Vehicle Wheelbase	M	2.619
Number of Rear Axles	-	1
Horizontal Distance from Last Rear Axle to Mass Center	M	1.321
Vertical Distance From Axles to Mass Center	M	0

Model: Power Demand

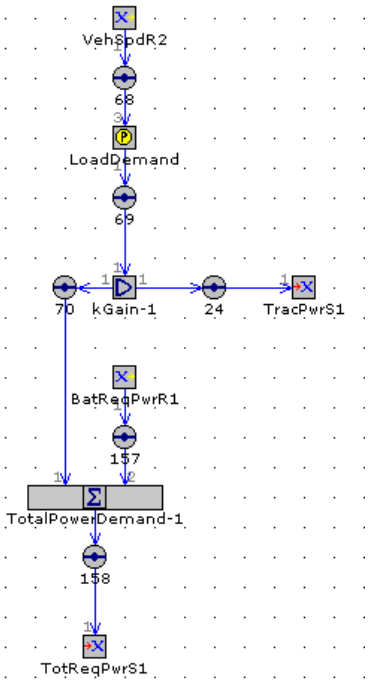

Figure 33. Power Demand Subassembly of Escape Model.

The power demand subassembly is responsible for calculating the tractive power required to propel the vehicle at the target vehicle speed and for summing that power with the battery requested power to determine the total power request of the vehicle for each simulation iteration. The inputs to this subassembly are the current vehicle speed and requested battery power.

Beginning at the top, the vehicle speed is fed into a ‘ControllerHEVehicle’ object (through an control connection) that uses the error between the current vehicle speed and target vehicle speed to determine the tractive power that is required to overcome the error. The controller employs a proportional-integral (PI) control technique in an attempt to minimize the error in speeds at each timestep during the simulation. To determine the required tractive power the controller first compares the actual vehicle speed to the desired vehicle speed and determines the required acceleration to get to the desired speed, then finds the tractive force required to

achieve that acceleration. Using that force, along with the tire radius, the torque at the axle is determined and the required power is found by using the required axle torque and current axle speed.

Once the ‘LoadDemand’ object outputs the required tractive power, it is converted from kilowatts to watts using a ‘Gain’ object with a value of 1000. It is then sent as a signal to be used throughout the model, as well as summed with the requested battery power, through a ‘Sum’ object to provide the model with the total power request at that particular time. All connections within this subassembly are control connections since this subassembly deals solely with control relationships.

Model: Engine Control

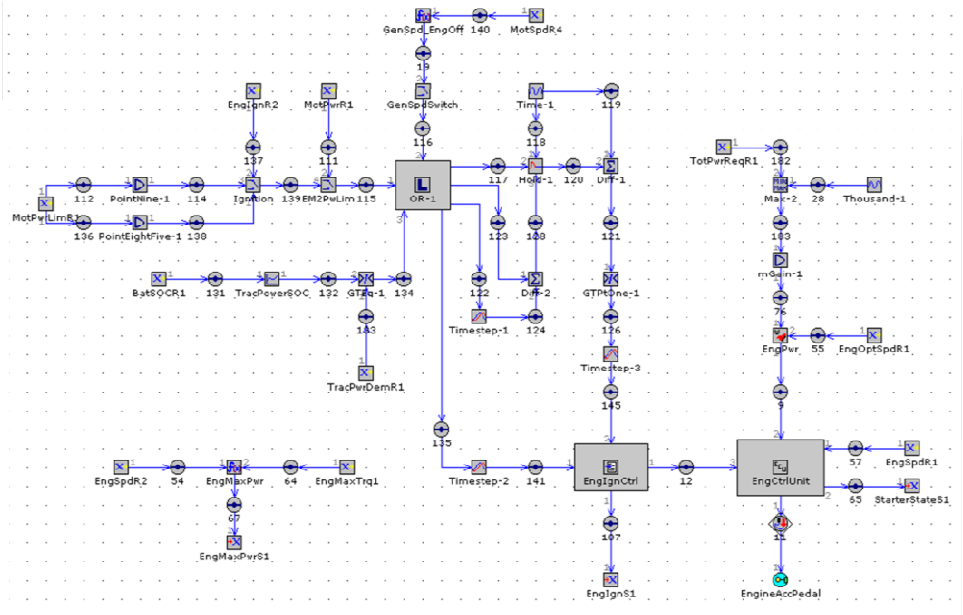

Figure 34. Engine Control Subassembly of Escape Model.

As its name implies, the engine control subassembly is used to control the engine torque and speed outputs. The inputs to this subassembly are the signals sent for the motor power limits, motor speed, motor brake power, engine ignition state, optimum engine speed, current engine

speed, battery SOC, total power request and tractive power demand. The signals generated within this subassembly are the starter state and the engine ignition state. The control strategy actuates the engine accelerator position (in the case of the Escape hybrid, the accelerator pedal position control is analogous to the electronic throttle position) to control the engine. Similar to the Power Demand subassembly, all connections are control connections except for the connection between the engine control unit and the accelerator position actuator. Additionally, the maximum engine power for a current engine speed and torque are calculated within this subassembly and the maximum engine power signal is sent.

Since the procedure for determining the maximum engine power is simple to explain and not too in depth, it will be explained first. The first step in this process is to receive the current engine speed and maximum torque from their respective 'ReceiveSignal' parts. These signals are then sent into a math equation to determine the maximum engine power. This equation is given below:

$$P_{eng,max} = \frac{\pi}{30} N_{eng} \tau_{eng,max}$$

where

$P_{eng,max}$ is the maximum calculated engine power in Watts,

N_{eng} is the current engine speed in rpm, and

$\tau_{eng,max}$ is the maximum engine torque in Nm at the given speed

Finally, the result of the equation is sent as a signal to be used throughout the model during the simulation.

The control strategy for the engine is comprised of three conditions that are fed into a logic 'Or' operator. Depending on the input to the 'Or' part, it outputs a logical '0' or '1' that determines if the control is requesting the engine to be on or off (if any input is a '1', a '1' is

output and results in a request to run the engine). Once the output request is sent, an event manager determines if all the required conditions are satisfied and, if so, initiates the engine ignition system, or does not depending on the current requested engine state. If the engine is on, an engine power calculation takes the total power request and the optimum engine speed signals as inputs to determine an optimum engine power (based on brake mean effective pressure, BMEP) then uses a user provided BMEP map to calculate the required accelerator pedal position. The engine control unit then outputs that desired accelerator pedal position to the engine object in the main assembly.

The first input to the 'Or' operator to look at starts at the motor power limit 'ReceiveSignal' part. The signal is processed through a parallel pair of gains to create hysteresis for the engine on/off event. Depending on the received engine ignition state signal (the control input) a 'Switch' object passes one of the gain outputs to the next switch; if the engine ignition state is true (engine on) the switch outputs the motor power limits from the gain of 0.85, otherwise the motor power limits from the gain of 0.9 are sent ahead. At the next switch, the control input is the current motor brake power. If this signal is greater than the motor power limits, the switch outputs a logical '1' to the 'Or' logic operator at the heart of this subassembly.

Next, using the motor speed 'ReceiveSignal' part, the following equation is used to determine the required generator speed assuming that the engine is off and thus the carrier speed is zero.

$$N_{gen,engoff} = -\frac{n_{ring}}{n_{sun}} N_{mot}$$

where

$N_{gen,engoff}$ is the generator speed, in rpm, when the carrier speed is zero,

n_{ring} is the number of teeth on the ring gear of the eCVT,

n_{sun} is the number of teeth on the sun gear, and

N_{mot} is the current motor speed in rpm

The output from this equation is then passed to a 'Switch' object as the control input. The threshold for the 'Switch' object is set as the generator absolute minimum speed limit (-10,000rpm) and if the calculated generator speed is less than the generator speed limit, the switch passes a logical '1' to the 'Or' operator.

The final input to the 'Or' operator begins with the current battery SOC signal which is then passed through a one-dimensional lookup table that converts the SOC to the total available tractive power at the current battery SOC. A 'Greater-Than' logical operator then compares the available tractive power for the given SOC to the current tractive power demand signal, which is obtained via the 'ReceiveSignal' part below the relation part. If the available power is less than the required power a logical '1' is passed to the 'Or' operator.

Several outputs from the 'Or' operator are visible in the screenshot from the beginning of this section. However, three of the four total outputs are used to create a timer for each engine state change. Starting with the output that feeds into the 'Timestep-1' part (via a control connection) the logical output of the 'Or' part is held from the previous iteration (each iteration in this simulation is 0.1sec) and that previous output is sent from the 'Timestep' to a 'Difference' part. This part calculates the difference between the previous and current 'Or' part outputs and sends the difference to the 'Hold' object. At the 'Hold' object a time is input along with the current 'Or' output and the difference in the current and previous 'Or' output. The initial time input to the 'Hold' part is held until the new input signal becomes a value other than 1. When this happens, the initial time held by the 'Hold' part is passed to the 'Difference' part to its right. This 'Difference' part subtracts the held time from the current time to determine the duration of

the previous engine state. If this duration is greater than 0.1sec a logical '1' is passed to the engine ignition control part. The fourth output from the 'Or' operator is passed into a 'Timestep' part that holds the previous 'Or' output and is then fed into the engine ignition controller. The 'Timestep' parts ensure that the input conditions to the 'Or' operator change state for at least 0.1sec before the engine ignition controller attempts to change the engine ignition state.

The engine ignition controller uses the two inputs (that compare the current engine on/off request to the request from one timestep prior) and an internal timer to control the engine ignition state. Assuming the engine is off, if at the current iteration an engine on state is requested and the duration of that request has been greater than 0.1sec and the internal timer confirms that the engine has been off for at least two seconds, the engine ignition state is changed to the 'on' condition. The criterion for the engine ignition to change states is given in Table 12.

Table 12. Engine On/Off Conditions.

Engine Goes Off to On if: 1) Generator calculated speed (with the engine off) is less than -10,000rpm. 2) Motor torque reaches 90% of its maximum torque available. 3) Calculated tractive power is above given threshold for a given SOC. 4) Engine has been off for at least 2sec.
Engine Goes On to Off if: 1) Generator calculated speed (with the engine off) is above -10,000rpm. 2) Motor torque is less than 85% of it maximum torque available. 3) Calculated tractive power is below given threshold for a given SOC. 4) Engine has been on for at least 2sec.

Looking at the right hand side of the engine control subassembly, the ‘ReceiveSignal’ for the total requested power signal is visible. The signal received for the total power request is compared to a nominal power of 1000W and the maximum value between these two is passed through a ‘Gain’ part that converts the signal from watts to kilowatts (using a gain equal to 0.001). This power request is sent into an engine power controller part that also takes the optimum engine speed (via the ‘ReceiveSignal’ part to its right) as an input. The controller is a map based controller and is responsible for taking these input signals and outputting a requested engine accelerator position to the engine control unit. Within the engine control unit, a desired accelerator pedal position is input and the controller uses this signal to control basic engine functions such as idling and fuel cut off.

Model: Motor Control

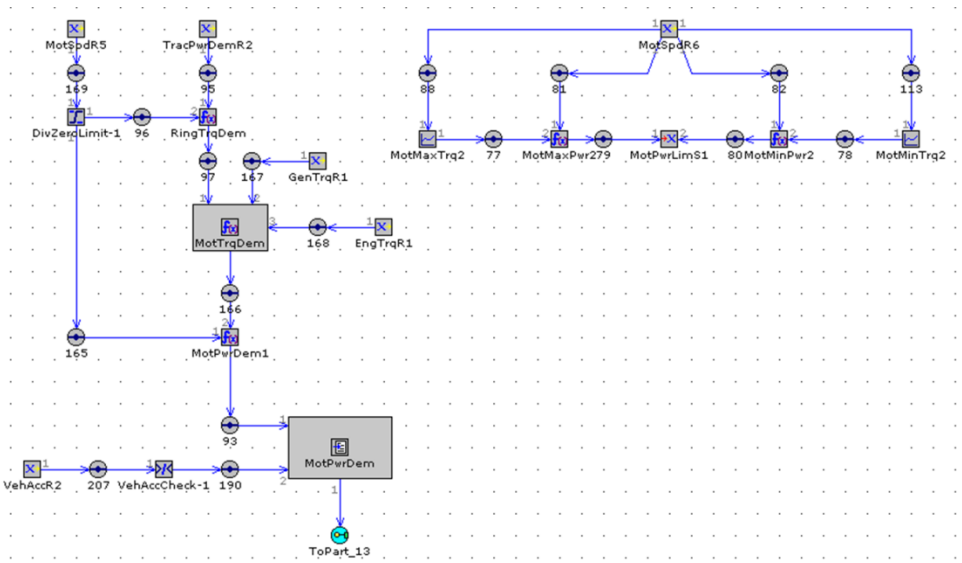

Figure 35. Motor Control Subassembly of Escape Model.

The motor control subassembly is responsible for controlling the requested brake power for the motor part on the main assembly page and also calculates the motor power limits. All the connections used in this subassembly are control connections since no mechanical connections

are needed. As inputs this control strategy uses the current motor speed, motor torque, tractive power demand, generator torque, engine brake torque and vehicle acceleration.

First, the motor power limits portion of this control strategy will be explained since it is straightforward. Two of the outputs from the motor speed 'ReceiveSignal' part are fed into one-dimensional lookup tables that obtain a minimum, or maximum, torque based on the current motor speed. These tables are provided by analyzing the efficiency maps provided in the Aisin AW paper (Hisada, 2005). Once the minimum, or maximum, torque is attained, it is fed into a math equation that, using the motor speed as a second input, calculates the minimum, and maximum, power that can be requested of the motor at that iteration. The results of the equations, given below, are sent as a bundled signal to be used in the control strategy.

$$P_{mot,max} = \frac{\pi}{30} N_{mot} \tau_{mot,max}$$

$$P_{mot,min} = \frac{\pi}{30} N_{mot} \tau_{mot,min}$$

where

$P_{mot,max}$ is the maximum motor power in Watts,

$\tau_{mot,max}$ is the maximum motor torque in Nm,

$P_{mot,min}$ is the minimum motor power in Watts, and

$\tau_{mot,min}$ is the minimum motor torque in Nm

Starting at the top left of the rest of the motor control subassembly, the motor speed is received and input into a 'Limit' part. This part ensures that the motor speed is never passed as a zero through the control scheme since division by the speed is required later in the control scheme; rather, it sets the minimum value it will pass as 0.000001. At the top right side of the scheme, the tractive power demand is received and sent into an equation, along with the motor

speed, that calculates the ring torque required to follow the driving cycle. This equation is displayed below:

$$\tau_{ring,dem} = \frac{30}{\pi}\frac{P_{ring}}{N_{mot}}$$

where

$\tau_{ring,dem}$ is the demanded ring gear torque in Nm, and

P_{ring} is the power at the ring gear in Watts

The output of the ring torque equation is then input into another equation that calculates the motor torque demand to match the given ring torque demand. Other inputs to this equation include the generator torque and engine torque; this equation is given below.

$$\tau_{mot,dem} = \tau_{ring} - \frac{5.17\tau_{eng} - 8.63\tau_{gen}}{10.47}$$

where

$\tau_{mot,dem}$ is the demanded motor torque in Nm,

τ_{ring} is the torque at the ring gear in Nm,

τ_{eng} is the engine torque in Nm, and

τ_{gen} is the generator torque in Nm

From the above equation, the motor torque demand is passed to the motor brake power demand equation, which uses the motor speed previously acquired, shown below:

$$P_{mot,dem} = \frac{\pi}{30{,}000} N_{mot}\tau_{mot}$$

where

$P_{mot,dem}$ is the demanded motor power in kW, and

τ_{mot} is the motor torque in Nm

At the bottom left, the vehicle acceleration is received and sent through a logical relation. If the vehicle acceleration is greater than -4m/sec^2 then the output of the logical operator is a '1' that is sent into the motor power controller. If the deceleration of the vehicle is greater than 4m/sec^2 (corresponding to an acceleration less than -4m/sec^2) then the motor power controller receives a logical '0' as an input. Using this value, along with the motor power demand from above, the motor power controller determines the power to be requested from the motor. If the result of the vehicle acceleration comparison (to -4m/sec2) above returns a 1, then the calculated motor power is passed to the motor. Otherwise, a motor power request of zero is sent to the motor.

Model: Generator Control

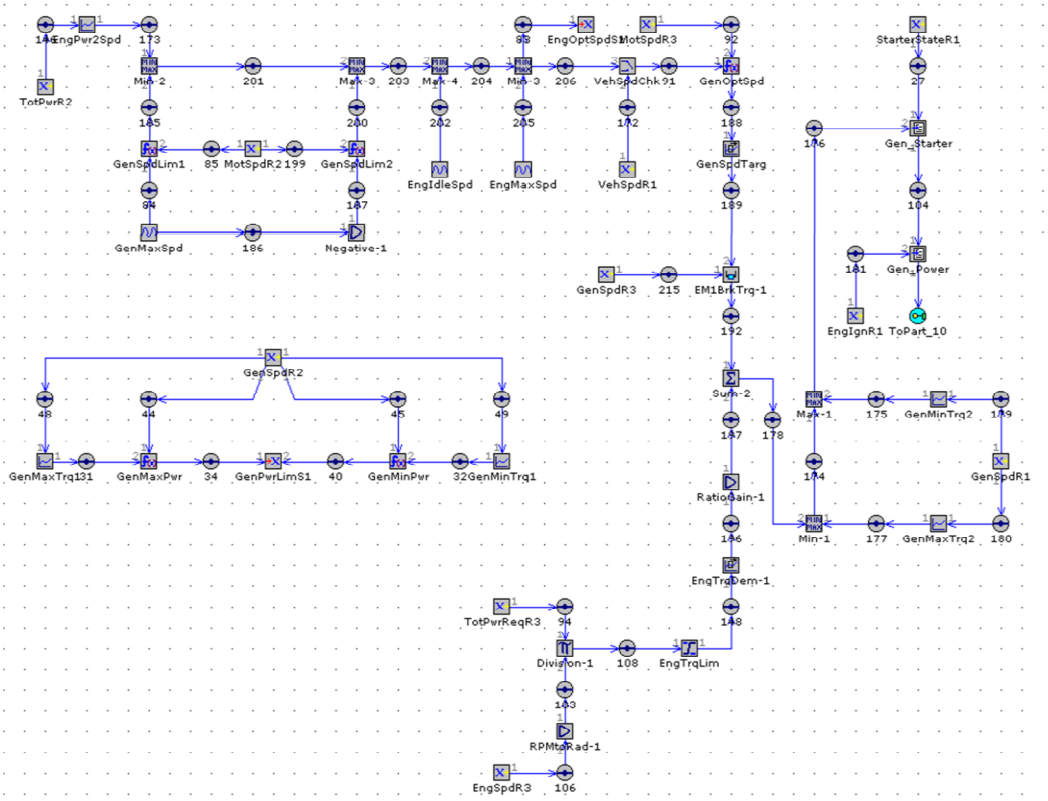

Figure 36. Generator Control Subassembly of Escape Model.

The generator control subassembly is the most complex of the various assemblies created for this model. It must balance the generator and engine torques and speeds since they are connected via the planet carrier and sun gears of the eCVT. All the connections for this subassembly are control connections since they solely pass signals. First the control strategy finds the optimum engine speed, then the optimum generator speed and torque for the desired engine speed. This torque is then summed with the torque at the sun gear that is due to the engine torque (through the planet carrier). Finally, the torque summation is used to determine the generator brake torque, whether it is used to start the engine, assist in vehicle propulsion or charge the battery.

The control strategy begins by receiving the total power request signal and converting it to an optimum engine speed using a one-dimensional lookup table. This value is passed into a 'Minimum' object that compares the optimum engine speed to the minimum generator speed (at the sun gun) for the current motor speed; this speed is calculated by the equation given below, using the current motor speed and the generator's absolute maximum speed.

$$N_{sun,max} = \frac{n_{sun}N_{gen,absmax} + n_{ring}N_{mot}}{n_{sun} + n_{ring}}$$

where

$N_{sun,max}$ is the maximum generator speed at the sun gear in rpm and

$N_{gen,absmax}$ is the absolute maximum generator speed (10,000rpm) in rpm

The generator's minimum speed at the sun gear is also calculated using a similar equation, but using the generator's absolute minimum speed rather than its maximum. The output of the 'Minimum' part is then compared to the generator minimum speed in a 'Maximum' part where the maximum of the two speeds is passed forward. The equation for the generator minimum speed at the sun gear is given below.

$$N_{sun,min} = \frac{n_{sun}N_{gen,absmin} + n_{ring}N_{mot}}{n_{sun} + n_{ring}}$$

where

$N_{sun,min}$ is the minimum generator speed at the sun gear in rpm and

$N_{gen,absmin}$ is the absolute minimum generator speed (-10,000rpm) in rpm

At this point the model has a speed to operate the engine at that will maintain the generator speed within its limits. Although the software attempts to run the engine at the optimum speed given in the lookup table, sometimes this speed is unattainable due to the fact that the speed it would impose on the sun gear would cause the generator to operate at a speed outside of its absolute range. This engine speed is then compared to the engine idle speed through another 'Maximum' part that ensures that the sent engine speed never drops below its idle speed. The final step in the engine speed calculation, before it is sent to the engine control subassembly, is to compare the desired engine speed to the maximum engine speed. For this comparison a 'Minimum' part is used that ensures the minimum speed (out of the maximum engine speed and desired engine speed) is the speed signal that is sent to the engine control strategy. Thus, the engine speed signal that is sent to the engine control unit is calculated such that it is between the engine idle and maximum speeds and will not force the generator to operate outside of its operating speed range.

GT Suite then runs the calculated engine speed through a 'Switch' part that passes a 0 if the vehicle speed is less than, or equal to, 1km/hr; if the vehicle speed is greater than 1km/hr, the switch outputs the calculated engine speed. This switch exists to pass the engine speed forward if the vehicle is stopped (since the engine speed is not being sent through the eCVT). Then the control strategy obtains the current motor speed, via a 'ReceiveSignal' part and uses it, as well as

the speed output from the switch, to determine the optimum generator speed by passing these inputs to the following equation:

$$N_{gen,opt} = \left(1 + \frac{n_{ring}}{n_{sun}}\right) N_{eng} - \frac{n_{ring}}{n_{sun}} N_{mot}$$

where

$N_{gen,opt}$ is the optimum generator speed in rpm and

N_{eng} is the engine speed in rpm

This equation results in the generator speed that is deemed to be ideal by the control scheme and this speed is fed into a first order filter that smoothes the input into the PI controller that is used to determine the target generator speed. The PI controller, which is the next object in the signal flow, determines the generator torque required to match the current generator speed to the desired speed. From the PI controller, the generator torque is input to a 'Sum' part that determines the total requested generator torque at the current operating state of the powertrain.

The other input to the 'Summation' part is the torque at the sun gear that is caused by the torque at the carrier (due to the engine torque). To determine this torque, the control scheme receives the current engine speed and total power request and calculates the engine torque using 'Gain' and 'Division' parts. To save space, the operations carried out by these parts are shown via the equation below.

$$\tau_{eng} = \frac{30 P_{req,tot}}{\pi N_{eng}}$$

where

$P_{req,tot}$ is the total power request for the vehicle in W

This calculated engine torque is then passed through a ‘Limit’ part that ensures that the resultant engine torque is within the torque range of the engine. If it is not, the part passes the maximum torque of the engine forward into the engine torque first order filter object whose operation is straightforward. The smoothed engine torque signal is then sent into a ‘Gain’ part that calculates the torque at the sun gear due to the torque at the carrier provided by the engine. The torque at the sun gear is then sent to the ‘Sum’ part mentioned in the previous paragraph.

Once the control strategy has obtained the total generator torque (provided by the summation of the sun gear and desired generator torques) it is compared to the maximum and minimum generator torques to ensure that the generator torque signal sent to the generator is within the torque range of the generator. The maximum and minimum generator torques are found by receiving the current generator speed and using that value, with a one-dimensional lookup table, to interpolate the current maximum and minimum generator torques. To ensure a permissible output generator torque the total request generator torque is passed through a ‘Minimum’ part that compares the requested torque to the maximum torque and then through a ‘Maximum’ part that compares the requested torque to the minimum torque. If the requested torque is greater than the maximum, the maximum value is passed forward; otherwise the requested torque is passed on. Similarly, the ‘Maximum’ part passes the requested torque forward if it is above the minimum torque and passes forward the minimum torque if not.

The requested generator torque is then sent into an ‘EventManager’ that determines if the requested torque should be used to generate power to charge the battery or if it should be used to start the engine. This distinction is made by using the starter state signal and current generator torque request. If the starter state is ‘0’ the calculated generator torque is sent into the battery

power controller. If the starter state transitions to ‘1’ then a generator torque of 40Nm is sent into the generator power controller to provide the torque necessary to start the engine.

Model: Battery Control

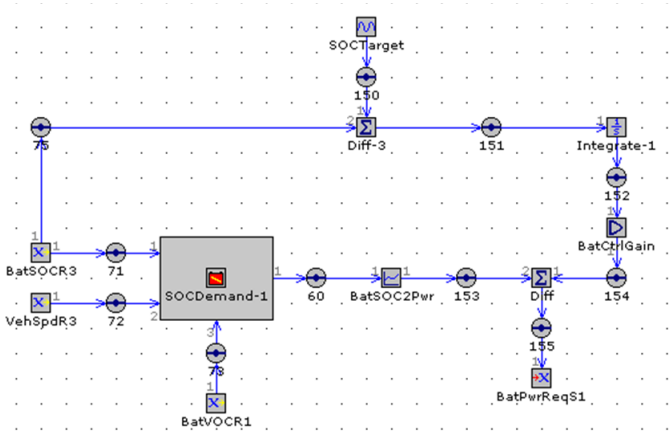

Figure 37. Battery Control Subassembly of Escape Model.

For the battery power control, the goal of the strategy is to maintain a battery SOC between 40% and 70%. To accomplish this task, the strategy receives the current battery SOC and open circuit voltage as well as the current vehicle speed from other parts of the model. It then outputs a battery power request that is required to maintain the SOC within its given ranges.

The target SOC is given via a ‘SignalGenerator’ object that is set to output a constant 0.6 for reference, from which the current battery SOC is subtracted. This difference is then integrated with respect to time and set through an integral gain into another difference object that determines the requested battery power. The other input into the difference object begins with the current battery SOC, open circuit voltage and vehicle speed which are fed into a ‘BatterySOCDemand’ object. This object calculates the battery SOC demand using the equation below.

————————)

where

SOC_{dem} is the battery SOC demand,

SOC_{tar} is the target SOC for the battery,

SOC is the current battery SOC,

K is the regenerative energy factor,

M_{veh} is the vehicle mass in kg,

v_{veh} is the vehicle speed in km/hr,

C_{bat} is the battery capacity in Ah, and

V_{oc} is the battery open circuit voltage in V

The resultant battery SOC demand is passed into a one-dimensional lookup table that outputs the power required (in Watts) to achieve the change in battery SOC that is demanded by the 'BatterySOCDemand' object. This power output is the second input to the previously mentioned difference part and it is subtracted from the integrated difference in target and actual battery SOC. The result of this operation is the requested battery power and it is sent as a signal to the model.

Model: Braking Control

The braking control subassembly is responsible for calculating the braking force necessary to decelerate the vehicle when a reduction in vehicle speed is targeted in the power demand subassembly. From this control subassembly, the mechanical braking force required at each axle is computed by comparing the regenerative braking capacity to the demanded total braking power. All the connections in this subassembly are control connections since there are no physical connections within this control scheme.

First, the tractive power request signal is received and sent into the braking check

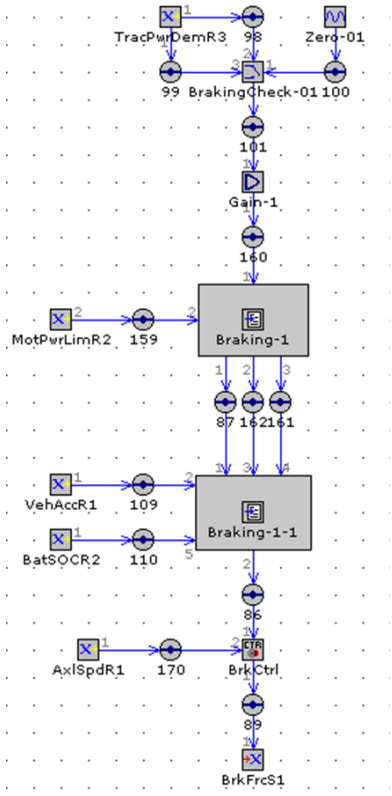

Figure 38. Braking Control Subassembly of Escape Model.

‘Switch’ object as both the control input and a possible output; the other possible output is zero. If the tractive power request is greater than zero (vehicle propulsion) the switch outputs a zero. If it is less than zero (vehicle braking) the switch outputs the tractive power request. Although this seems counterintuitive, the output of this switch is being fed into a braking controller so only negative tractive power requests result in desired braking action. Out of the switch, the signal is sent through a gain part (with a gain of 1) and into the first braking ‘EventManager’ along with the motor power limits signal.

The first braking event manager compares the braking demand (from the switch) to the motor power limits. If the demanded brake power is greater than the regenerative braking limit (defined by the motor power limit) then the three outputs from the manager are, respectively, the braking power demand, the regenerative braking limit and the difference between the braking

power demand and regenerative braking limit. Otherwise, the outputs are the braking power demand (twice) and zero. These three signals are then passed to the second braking event manager.

In addition to the three signals discussed above, the second braking manager also receives the vehicle acceleration and battery SOC signals which are used as event criteria that determine which of the original three signals is output from this controller. If the vehicle acceleration is greater than -5m/sec^2 and the battery SOC is less than 70% then the first output of the manager is the regenerative braking power (the second output from the first manager) and the second output is the mechanical braking power (the third output from the first manager). If the vehicle acceleration is less than -5m/sec^2 or the battery SOC is greater than 70% then the outputs from the second manager are zero and the total braking demand (the first output of the first manager).

The final part of this subassembly is the brake controller the receives the required mechanical braking power signal form the second braking 'EventManager' and the current axle speed of the vehicle to convert the braking torque into a pedal position that is sent as a signal to be used by the brakes in the main assembly.

CHAPTER 6

RESULTS AND COMPARISONS

In this chapter, some results from the GT Suite simulations will be displayed and discussed in order to demonstrate the validity of the model created for this research. Unless otherwise noted, each plot of results will display both the vehicle speed and the performance characteristic of interest versus time. This will allow for a quick reference to vehicle speed and a visual approximation of vehicle acceleration so that the effect of these on the characteristic plotted can be seen. Where comparable previous results (PSAT or dynamometer) are available, they will be provided and a discussion of the differences between the current and previous results will be given. The previous dynamometer results will be used mainly to prove that the model results match the trends of the actual vehicle on the dynamometer. Unfortunately, the numerical results from the dynamometer testing were not available so the comparison are limited to a visual analysis of the plots from the thesis by Jenkins (Jenkins, 2006). However, visual comparisons will be adequate for demonstrating matching trends as they rely mainly on the power delivery throughout the powertrain under acceleration and deceleration.

Engine

The first set of results to be discussed concern the engine of the Escape model. Figure 39 shows the engine speed versus vehicle speed. When on, the engine speed varies between the idle speed, 1150RPM, and approximately 4000RPM which is below the maximum engine speed of 6000RPM. When the requested engine speed is below the idle speed, the control scheme turns

the engine off and the speed goes to zero. For the remaining plots in this section, engine speed is used on the left hand axis rather than vehicle speed since the engine speed is a better indicator of proper results for the brake mean effective pressure (BMEP), power and torque. These performance characteristics are shown in Figures 40, 41 and 42, respectively.

GT Suite uses the torque map provided in the engine model to calculate the given results using the requested engine torque and speed. The maximum BMEP for the engine is about 10bar which is a reasonable value given the operating states of the model. The engine power varies between zero and 72kW which is below the engine maximum power of 99kW so the calculated power for the simulation is valid. For the Escape engine, the maximum torque is 175Nm and the maximum torque during the simulation appears to be limited at that torque so the engine torque produced by GT Suite is in agreement with the actual Escape engine. Therefore, the engine model incorporated into the model can be assumed to be an accurate representation of the actual Escape engine although no previous test results were available for the engine.

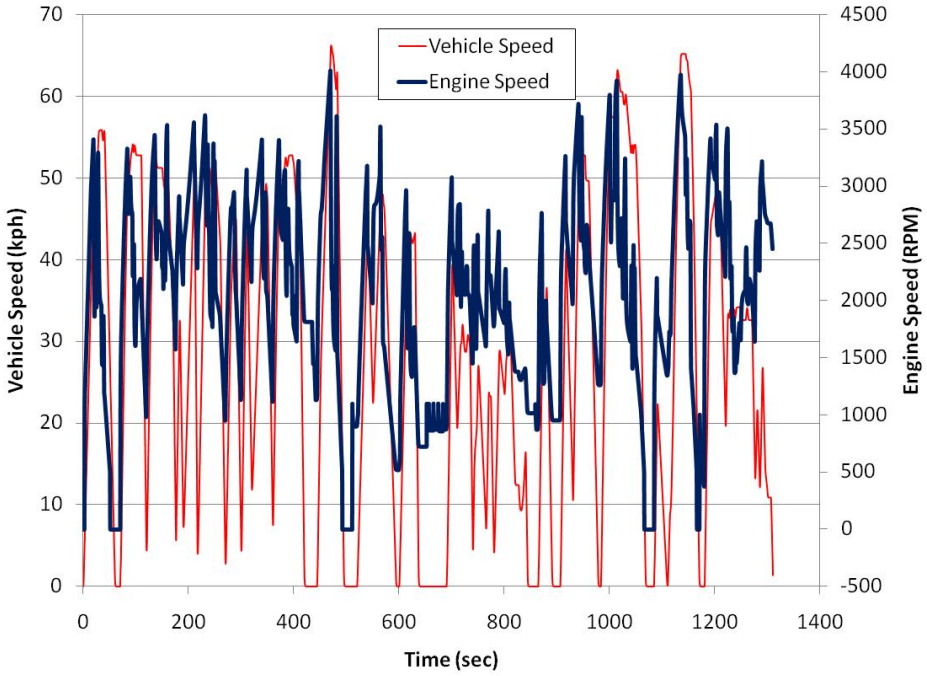

Figure 39. GT Suite Escape Engine Speed.

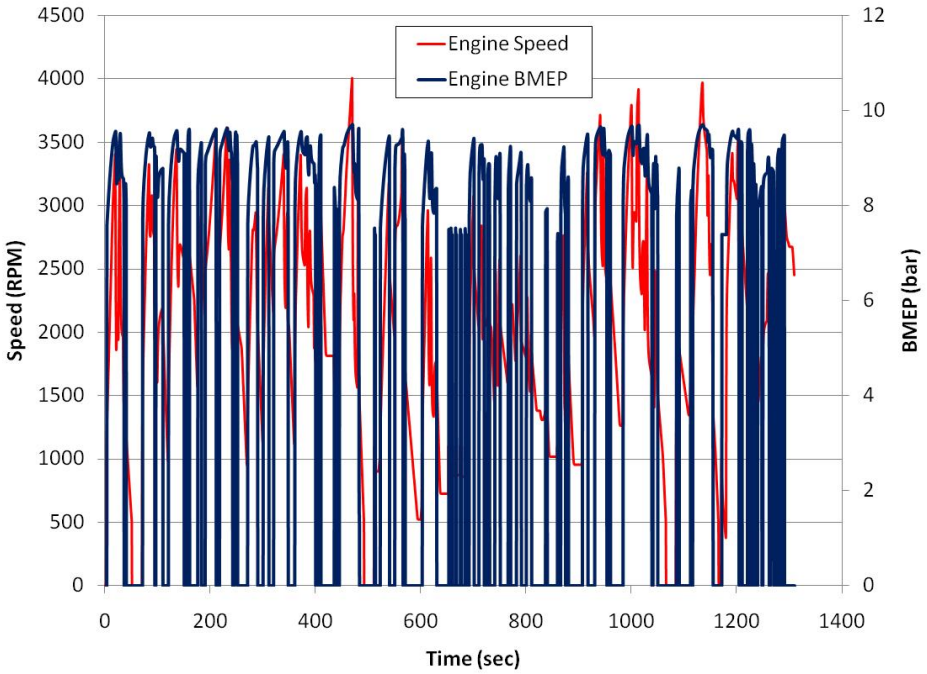

Figure 40. GT Suite Escape Engine BMEP.

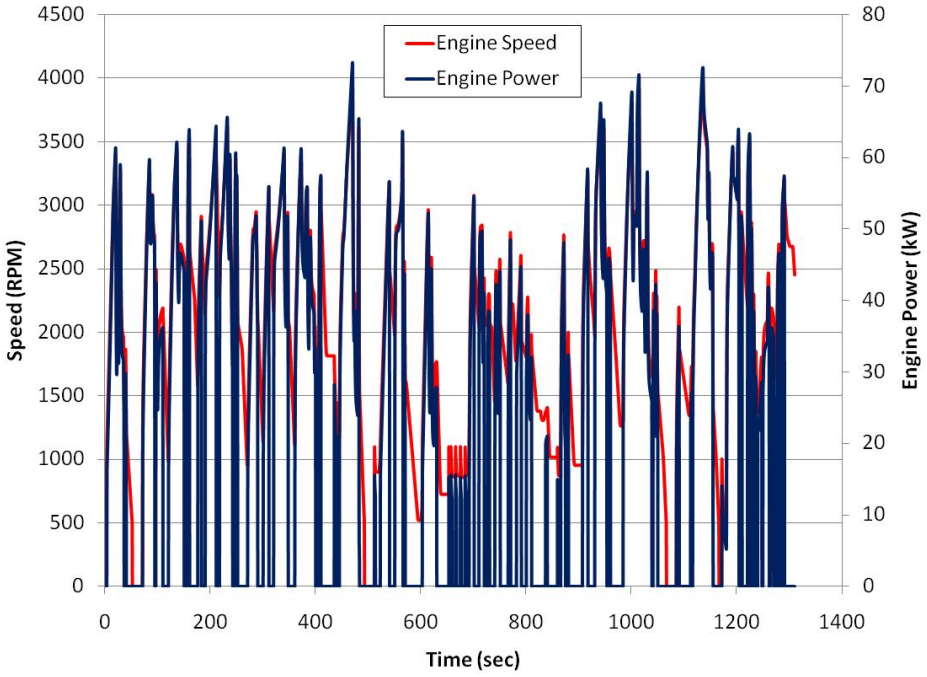

Figure 41. GT Suite Escape Engine Power.

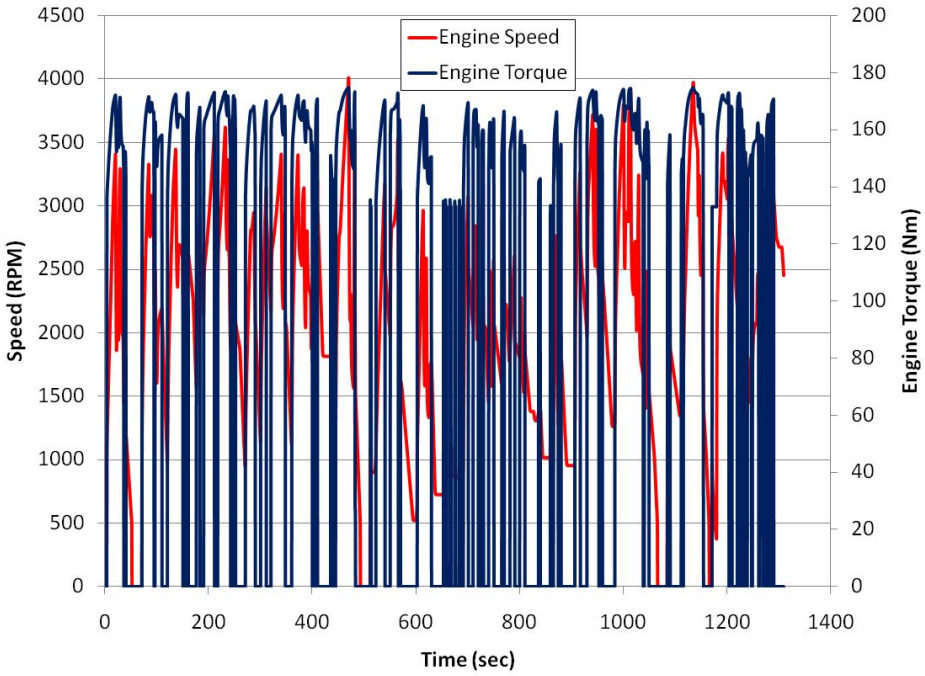

Figure 42. GT Suite Escape Engine Torque.

Traction Motor

For the traction motor, the characteristics to be discussed are the speed, brake torque, brake power and electrical power. Figure 43 shows the GT Suite output for the motor speed during the simulation. Figures 44 and 45 show the GT Suite mechanical motor power and electrical motor power, respectively. The brake torque is shown in Figure 46 with the motor torque from the previous dynamometer testing displayed in Figure 47 and the previous PSAT result shown in Figure 48.

Looking at the GT Suite results, the motor speed tracks the vehicle speed which is reasonable because the motor is connected, through, the eCVT output, to the vehicle driveline so is related to the vehicle speed through the driveline component ratios of the vehicle. For the simulation duration, this speed is well within the motor operating speed range of ±13,500RPM.

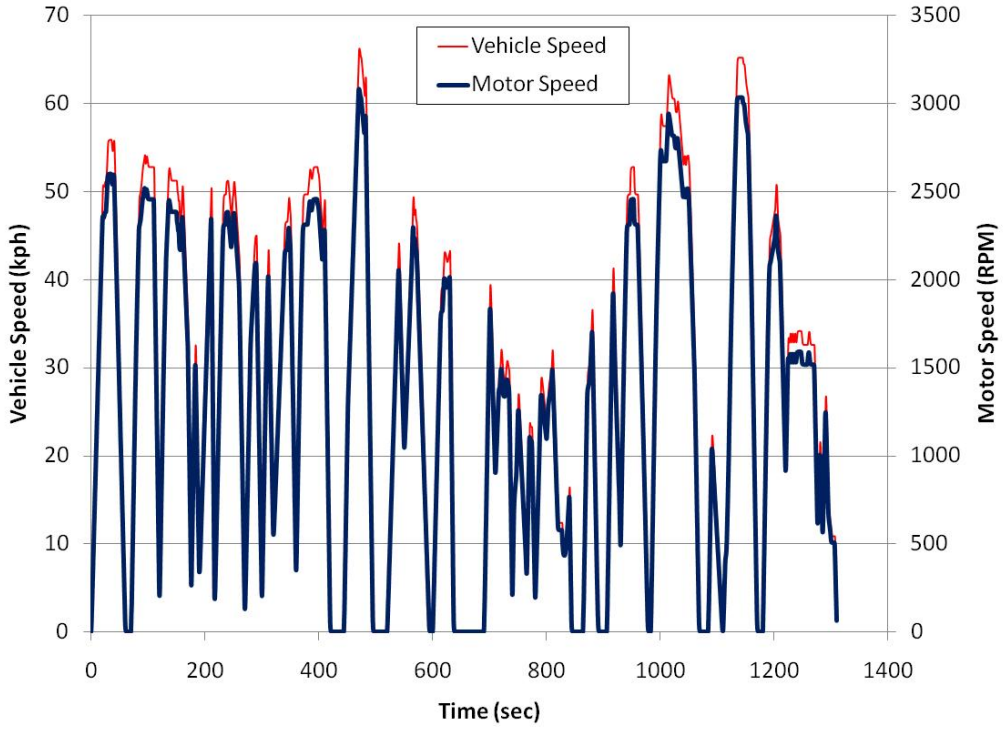

Figure 43. GT Suite Escape Motor Speed.

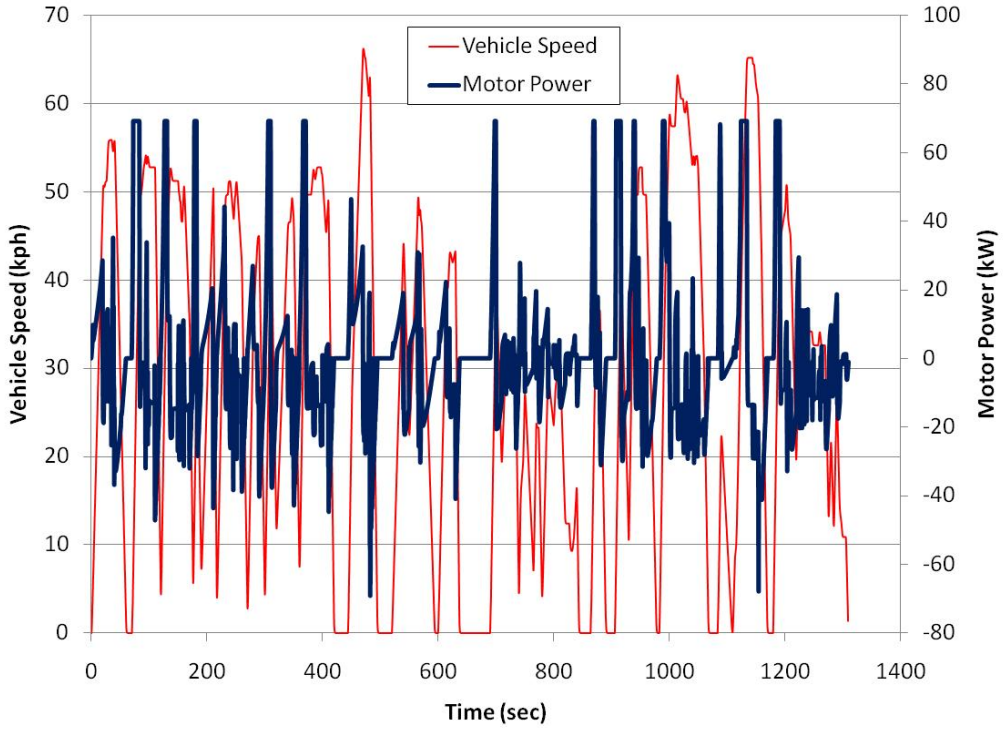

Figure 44. GT Suite Escape Motor Mechanical Power.

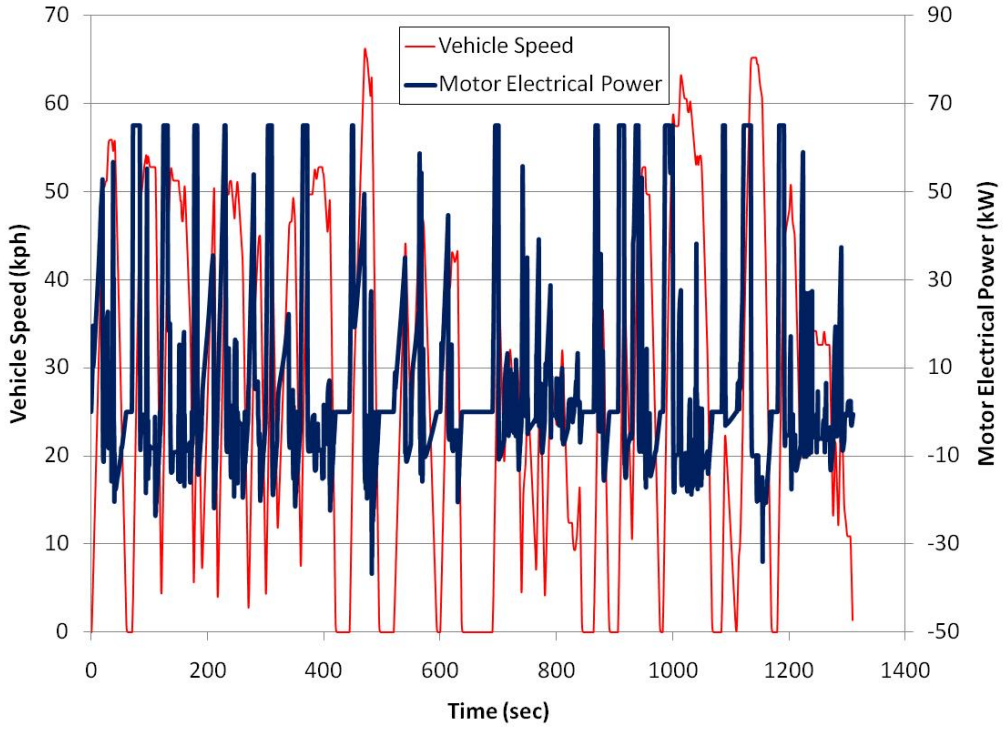

Figure 45. GT Suite Escape Motor Electrical Power.

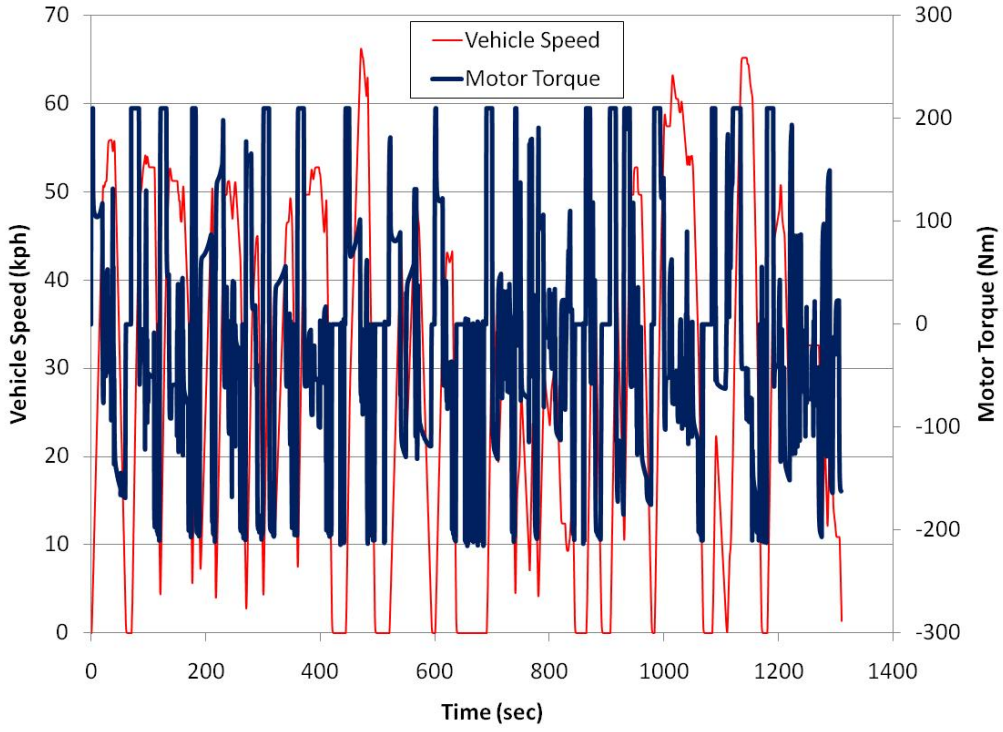

Figure 46. GT Suite Escape Motor Torque.

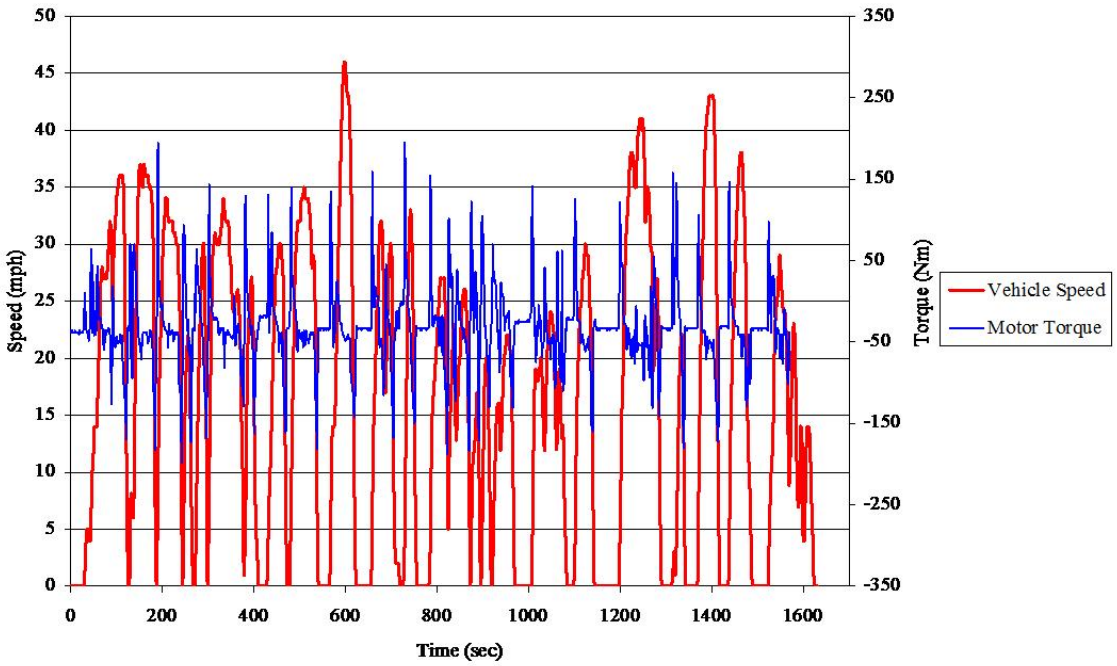

Figure 47. Previous Dynamometer Escape Motor Torque (Jenkins, 2006).

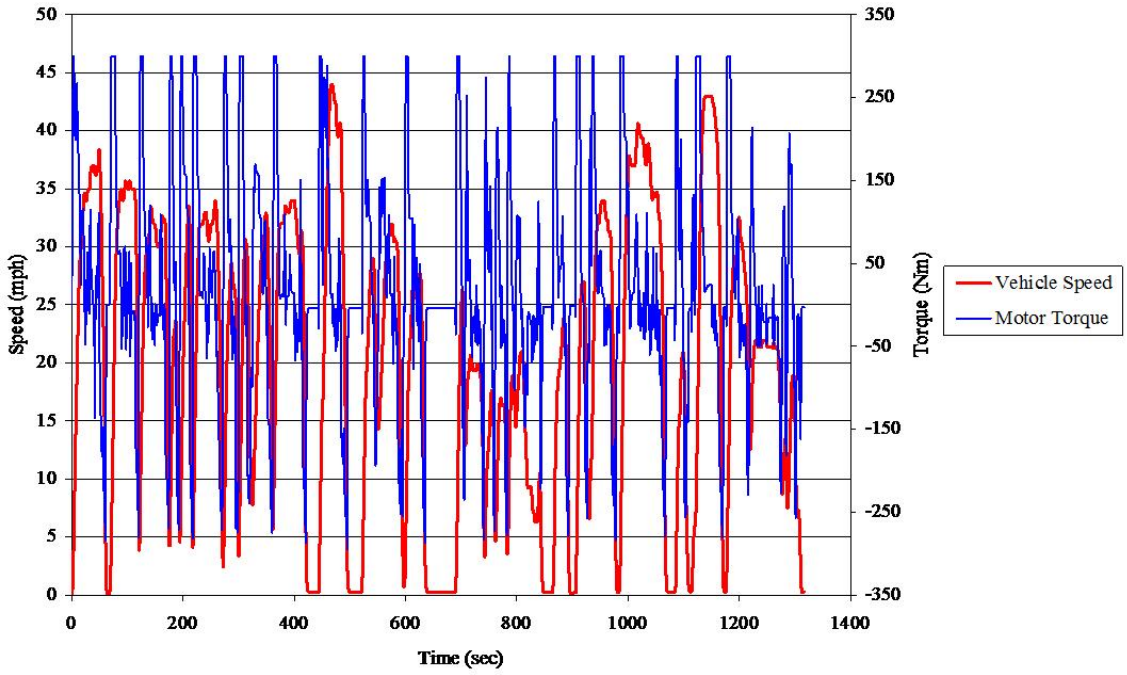

Figure 48. Previous PSAT Escape Motor Torque (Jenkins, 2006).

The electrical motor power also remains within its operating limits of ±65kW and the brake power remains close to those limits. Although the mechanical power of the motor at some points is beyond the limits, no major error is expected because the time spent outside of the limits is small and the losses within the motor constrict the electrical power to below 65kW. The torque of the motor, in some instances, hits the torque limits of the motor, but does not travel outside of the operating range of ±210Nm. GT Suite uses the given maximum torque of the motor to ensure that the motor remains inside of its operating range. However, for the dynamometer results, the motor torque never reaches the maximum torque which can be attributed to the fact that a real driver was used in this testing, so the demanded road load torque transitions are smoother than the calculated transitions of the model. This abrupt change in torque for the model is seen again in the PSAT results. However, in the PSAT model the motor torque is not limited to its maximum as it is in the GT Suite model which shows a shortcoming of the previous PSAT model. Although the motor torque reaches its limit in the GT Suite model, the motor results for the model follow the trends seen in the dynamometer testing and the motor model can be deemed appropriate for this project.

Generator

The generator results to be discussed are identical to the traction motor results discussed in the previous section. These are the speed, brake torque, brake power and electrical power and are shown in Figures 49, 50, 51, and 52, respectively.

Throughout the simulation, the generator speed remains within its operating range of ±11,000RPM with positive speed representing power being generated and sent into the battery (a negative power). Since the generator spends most of the simulation operating with positive speed

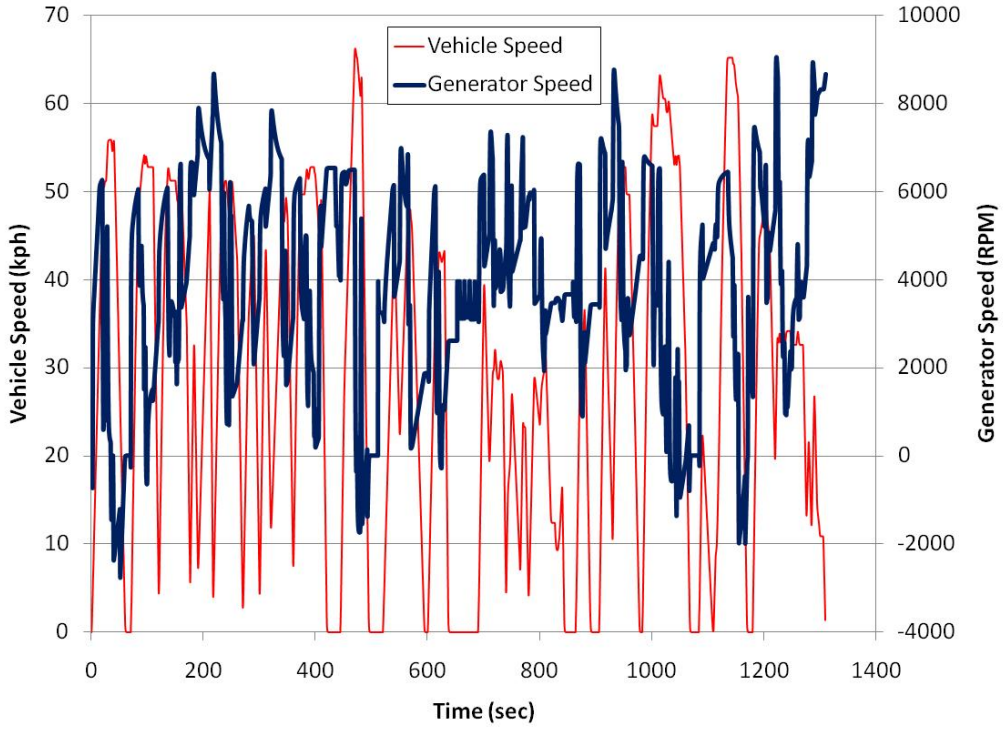

Figure 49. GT Suite Escape Generator Speed.

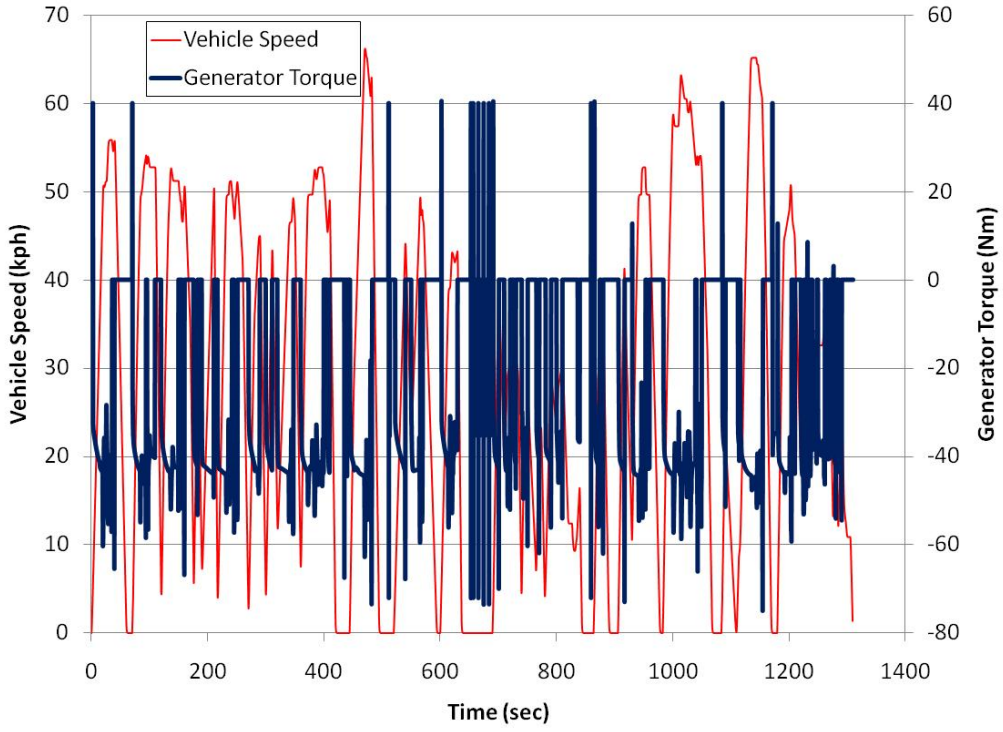

Figure 50. GT Suite Escape Generator Torque.

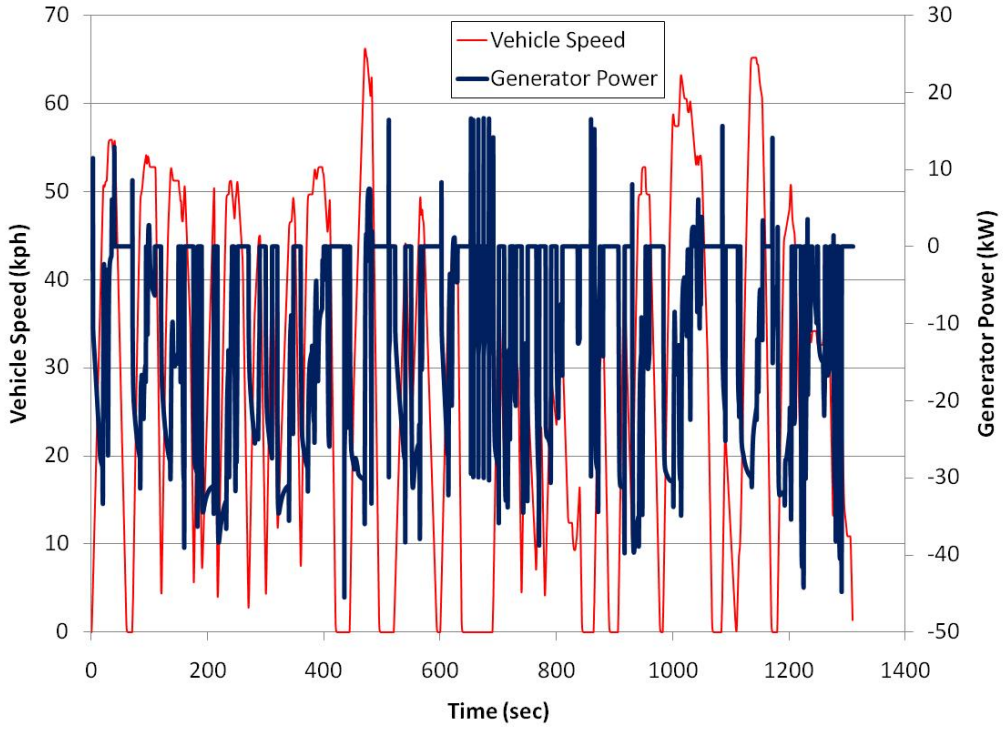

Figure 51. GT Suite Escape Generator Mechanical Power.

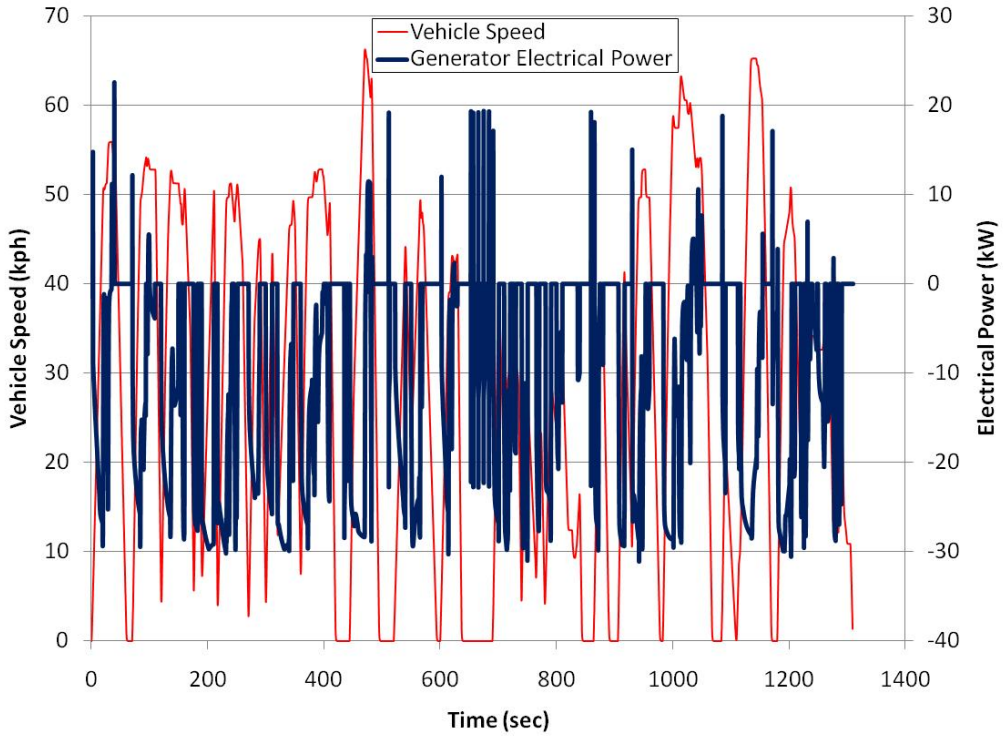

Figure 52. GT Suite Escape Generator Electrical Power.

it works mainly to provide charging power to the battery, as it should, while it is used at some times to provide tractive power (when its speed goes negative). The speeds used to operate the generator throughout the model are thus reasonable. The generator torque reaches its limits at several instances during the simulation which corresponds to maximum power generation, but torque remains bounded by the operating range of ±75Nm. The electrical power for the generator never goes beyond the given electrical power range of ±35kW and although the mechanical power does violate this power limit for short durations, the power electronics should be capable of handling those surges. For the generator, no dynamometer or PSAT results are available. By looking at the GT Suite outputs for the generator, the model can be deemed appropriate although improvements could be made with further experimentation.

Battery

The results selected for the HV battery system are the battery voltage, power and state of charge. For the first two of these, previous test results are available and will be given. Figure 53 shows the GT Suite battery voltage data while Figures 54 and 55 show the dynamometer and PSAT battery voltage data. The GT Suite battery power data is displayed in Figure 56 with Figure 57 showing the dynamometer battery power and Figure 58 showing the PSAT battery power. The battery state of charge for GT Suite testing is given in Figure 59.

For the battery voltage, the dynamometer and PSAT results are more in line with the Ford provided voltage of 330V with expected deviations based upon power draw from the battery. The GT Suite voltage is lower, but still reasonable with the voltage varying between about 314V and 324V. This can be attributed to the difference in model parameters and actual battery parameters as the GT Suite battery model was built using data from the two DOE Escape battery

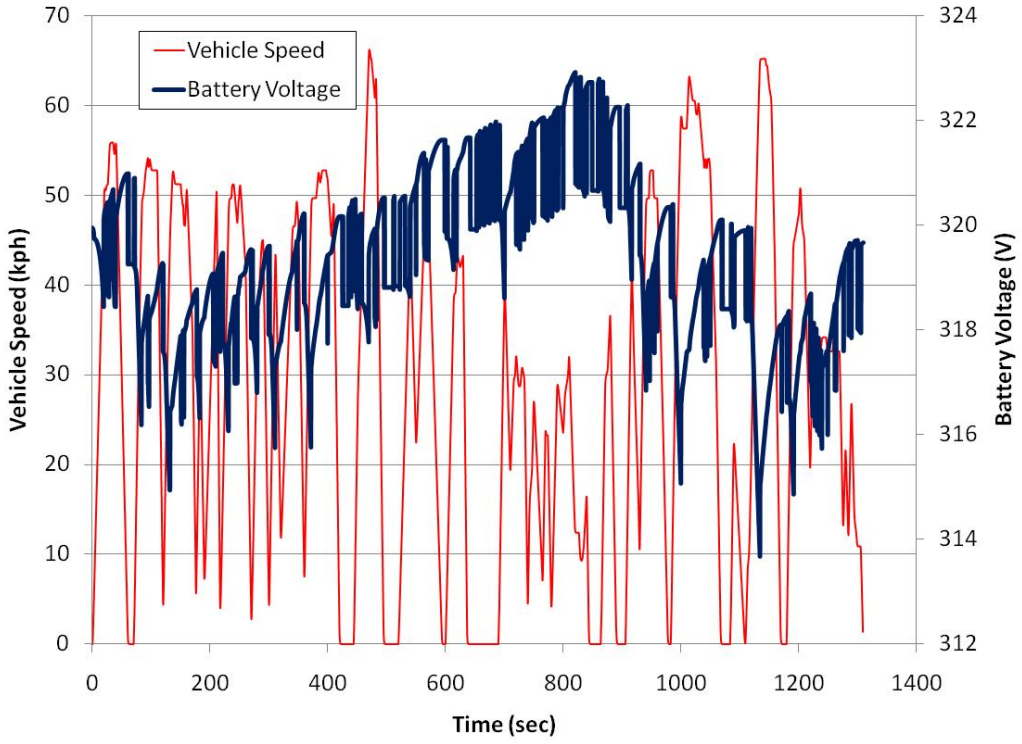

Figure 53. GT Suite Escape Battery Voltage.

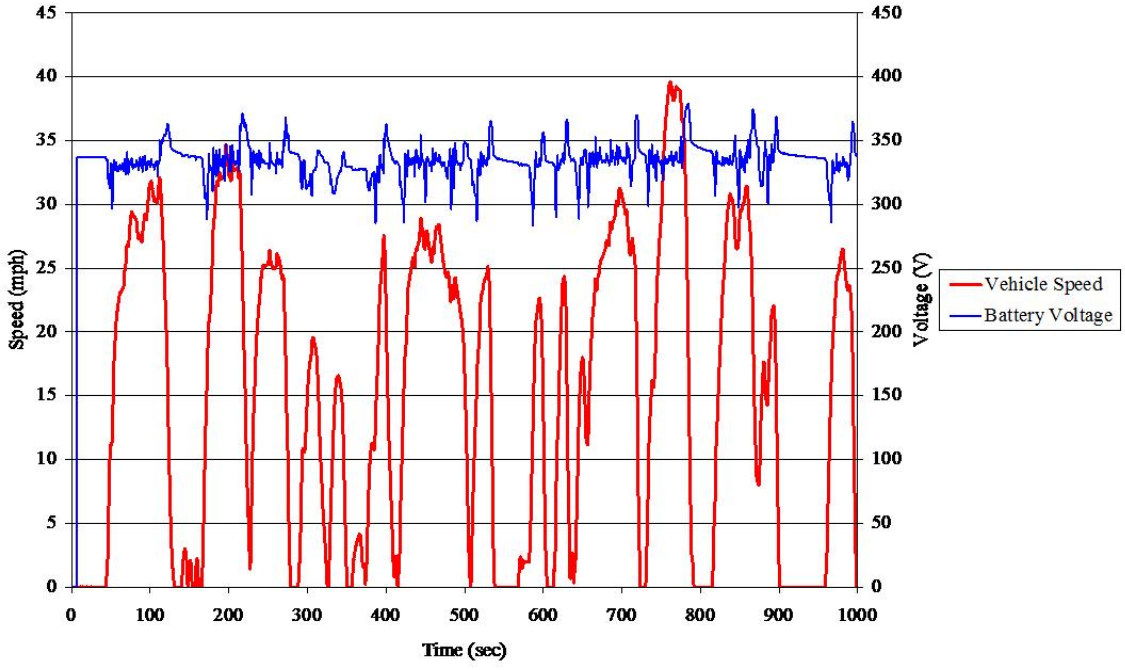

Figure 54. Dynamometer Escape Battery Voltage (Jenkins, 2006).

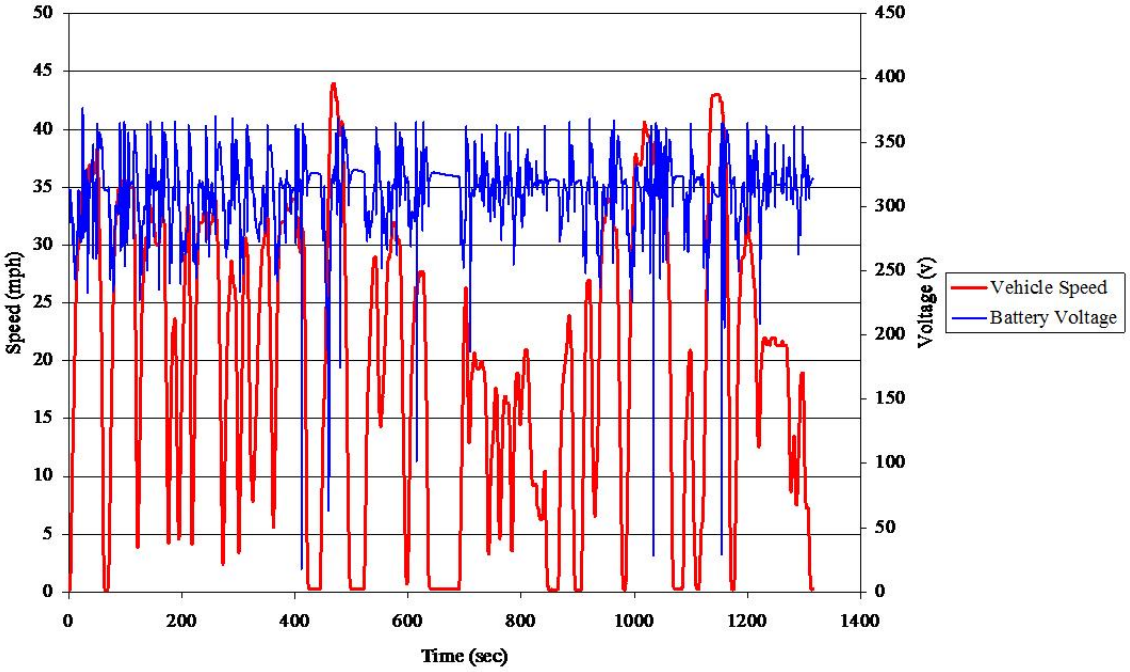

Figure 55. PSAT Escape Battery Voltage (Jenkins, 2006).

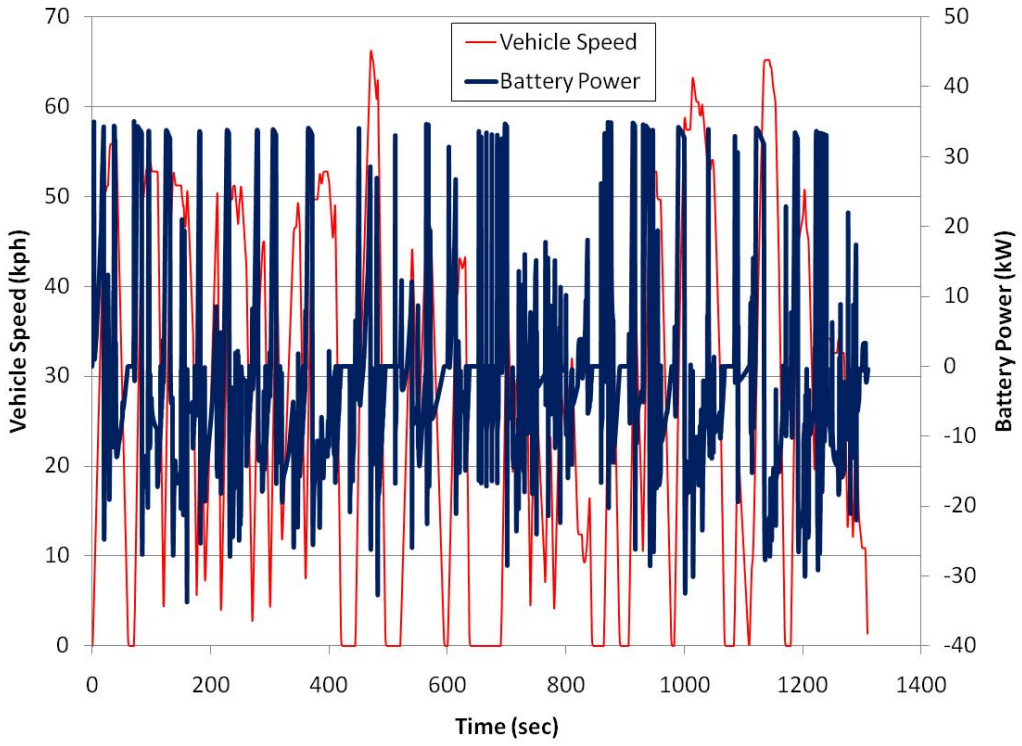

Figure 56. GT Suite Escape Battery Power.

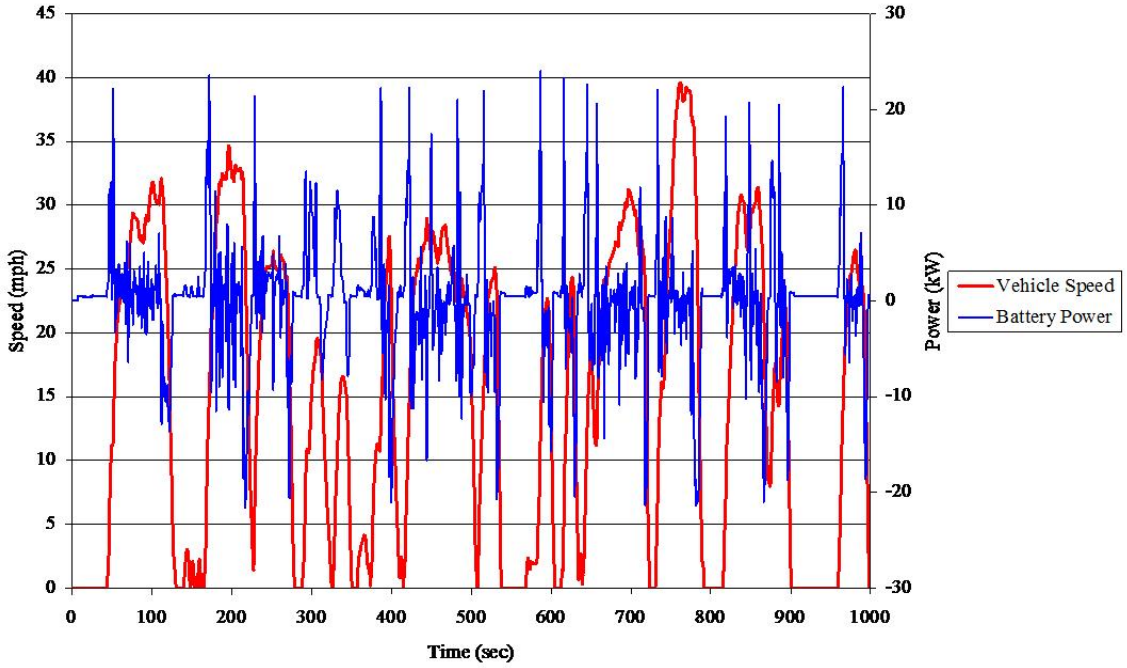

Figure 57. Dynamometer Escape Battery Power (Jenkins, 2006).

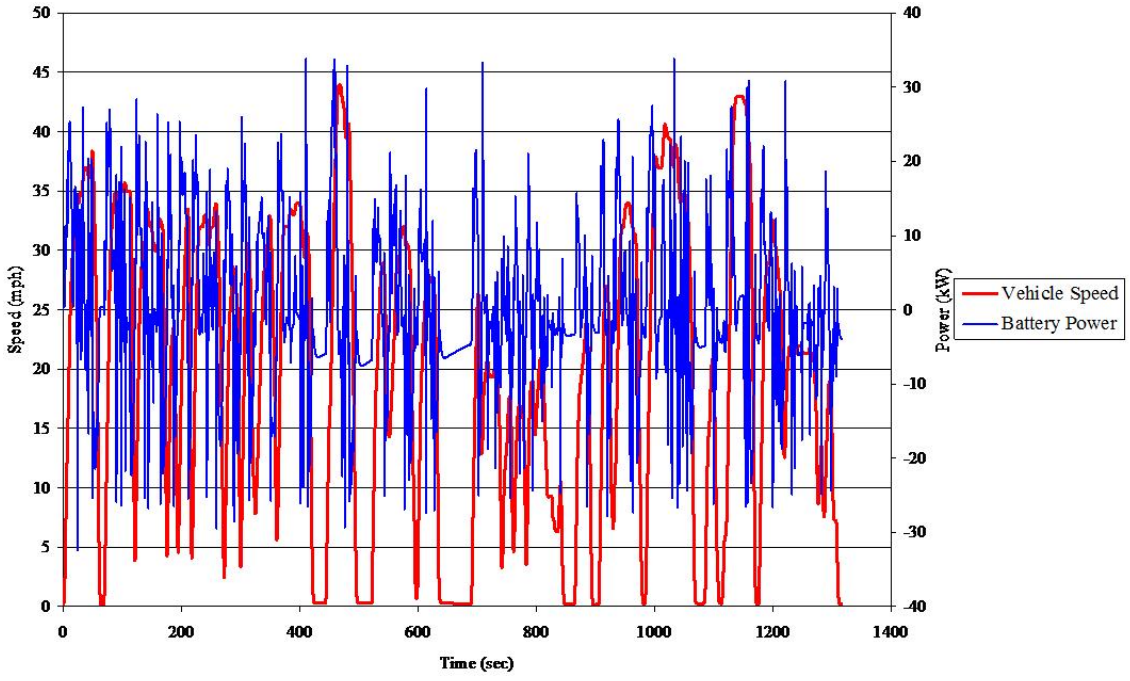

Figure 58. PSAT Escape Battery Power (Jenkins, 2006).

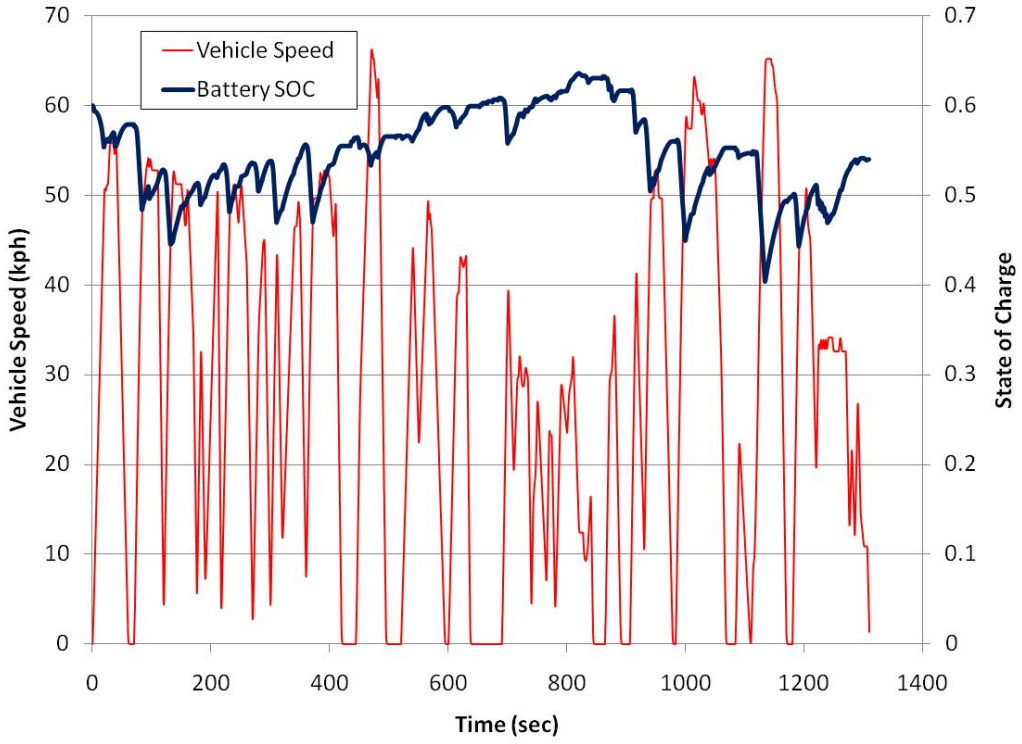

Figure 59. GT Suite Escape Battery State of Charge.

tests (DOE, 2005). These batteries were used so the voltage was degraded somewhat from the Ford provided numbers. The battery power data for the GT Suite and PSAT simulations are similar however both are higher than the dynamometer results. Similarly to the motor and generator powers, this lower power can be attributed to the real driver requesting smoother torque transitions between acceleration events in the drive cycle and thus the motor requested power is lower. Improvements could be made in the GT Suite model that would being the battery voltage and power more in line with the actual vehicle results with further experimentation. Despite the discrepancies in the GT Suite battery voltage and power data, the GT Suite battery SOC remains within the set limits of 0.4 to 0.7 for the entire simulation. For the GT Suite simulation, the battery data appears to be reasonable and, although the model could be improved upon, the battery model is assumed to be reasonable since the voltage swings are kept low and

the direction of power flow from the battery matches that of the dynamometer testing and is within a reasonable range of the power consumption during the dynamometer testing.

System Interaction

Although the individual system components of the model operated as they should in the actual vehicle that does not guarantee proper interaction of the individual components. To show that the simulation appropriately predicted the interactions between the major components a few plots of results that show this are displayed. Figure 60 shows the vehicle acceleration along with the motor and engine torques. When a positive acceleration is requested, both the engine and motor provide positive torque to propel the vehicle and when the requested acceleration goes negative the motor torque goes negative which shows the motor power is being sent into the battery for charging (regenerative braking) while the engine turns off. Since the original plot is somewhat unclear a portion of the result is replicated in Figure 61 for clarity. The quick transients visible at around 660 to 680sec are present because although the vehicle is stopped there is some simulated jerking occurring that is requesting a high acceleration. With further work these transients could be smoothed out and would not appear in the results.

Next, a results plot of acceleration and battery power will be shown (Figure 62) and then a portion of the results will be reshown for clarity (Figure 63). Generally, when the acceleration is positive the battery power is positive which indicates power being drawn from the battery to provide power to the motor for propulsion and when the acceleration goes negative the battery power goes negative which indicates power being sent to the battery for charging. However, there are instances when acceleration is positive or close to zero and the battery power is negative. This is because the control strategy is using engine only propulsion with extra engine power being sent through the generator and into the battery for charging.

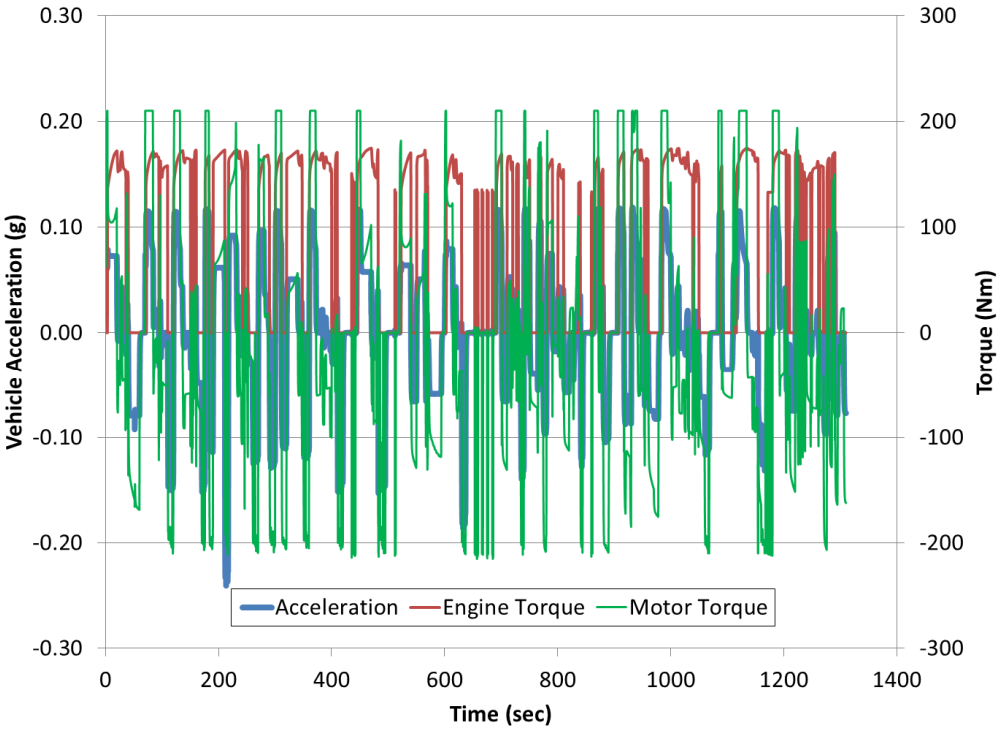

Figure 60. Vehicle Acceleration with Motor and Engine Torques.

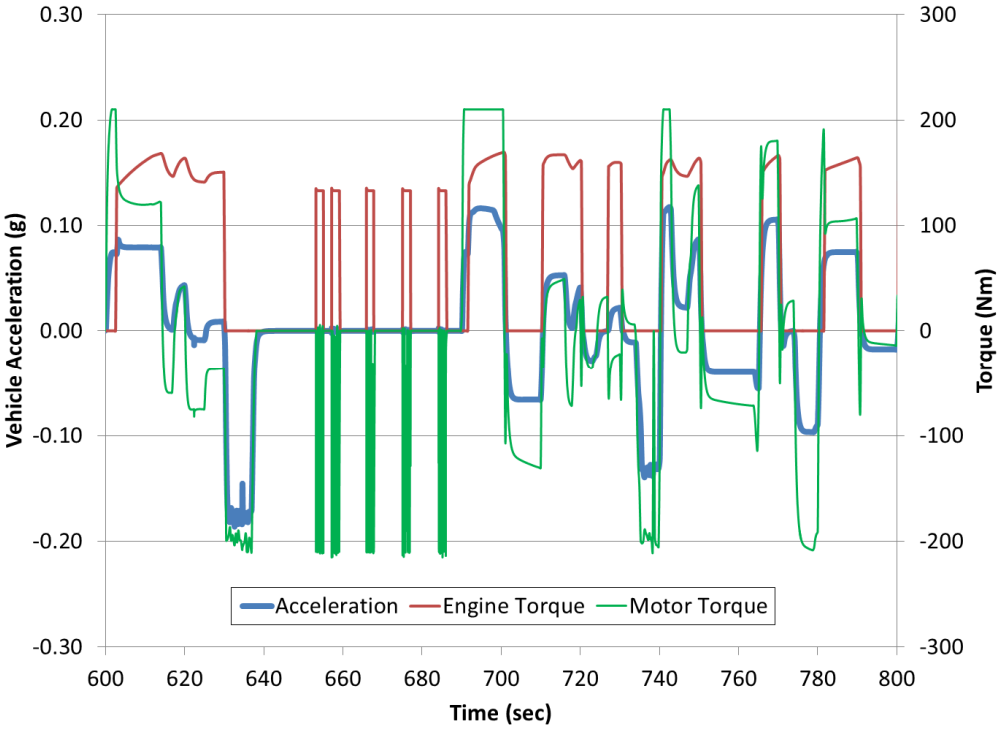

Figure 61. Portion of Vehicle Acceleration with Motor and Engine Torques.

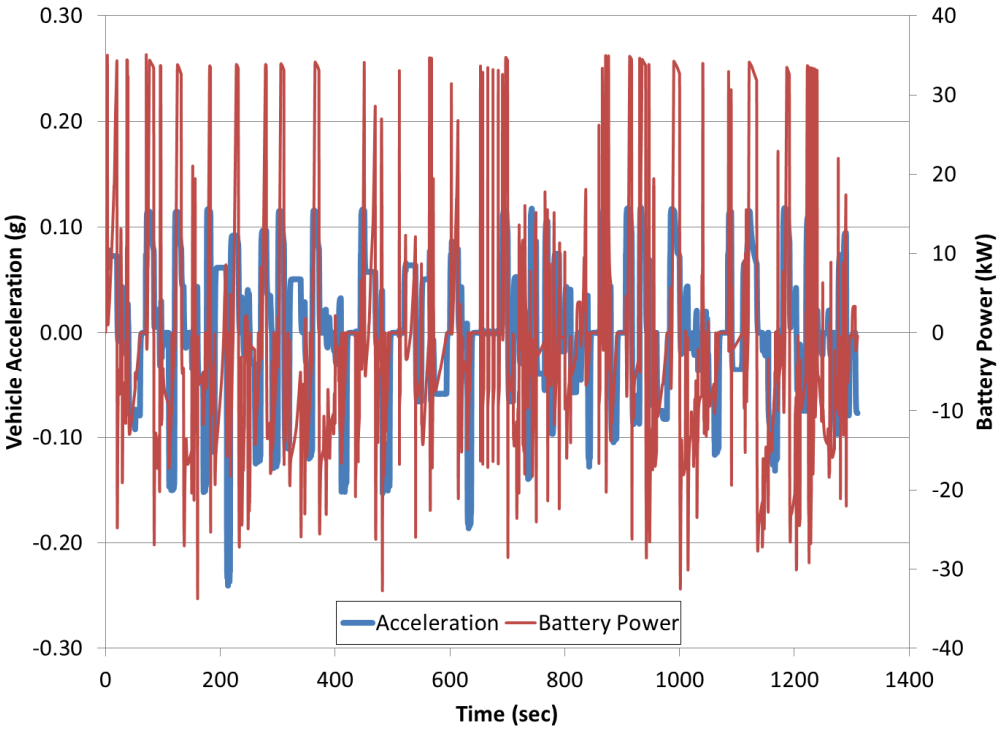

Figure 62. Vehicle Acceleration with Battery Power.

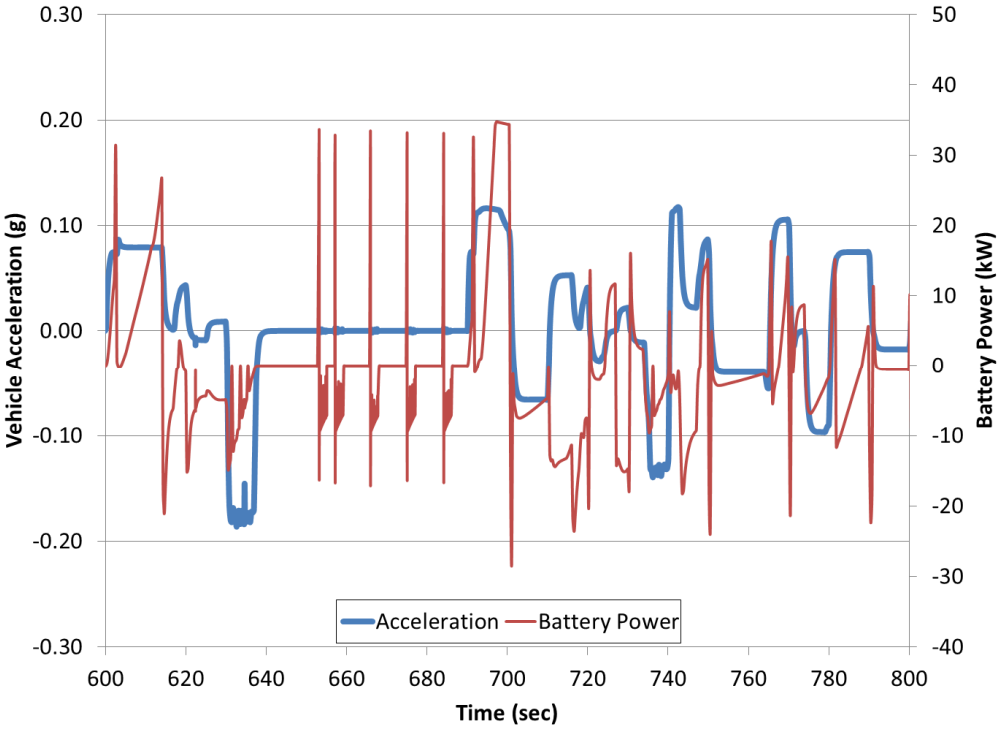

Figure 63. Portion of Vehicle Acceleration with Battery Power.

CHAPTER 7

CONCLUSIONS AND FUTURE WORK

This chapter will briefly discuss the both the conclusions drawn from this research and cover some recommendations for future work with the developed model. After analyzing the simulation results and the available dynamometer results the mode; created was determined to be a reasonable representation of the Escape. Most of the recommendations for future work concern the use of the map based objects in this model. By using more detailed, user built component models the accuracy of the model could be greatly improved.

Conclusions

For the simulation, the vehicle speed tracks the target speed set in the AL-University drive cycle very well, as shown in Figure 64 below. Due to the model's ability to closely follow the drive cycle provided while maintaining appropriate operating conditions for all major components of the vehicle, the model can be assumed to be a reasonable representation of the actual Ford Escape Hybrid. With further research and testing, the model can be improved and can achieve a simulated performance that accurately represents the actual Escape. Once this accuracy is obtained, the model and GT Suite can be used to begin experimentation with the control scheme and component parameters in order to study the effects of different control schemes and components.

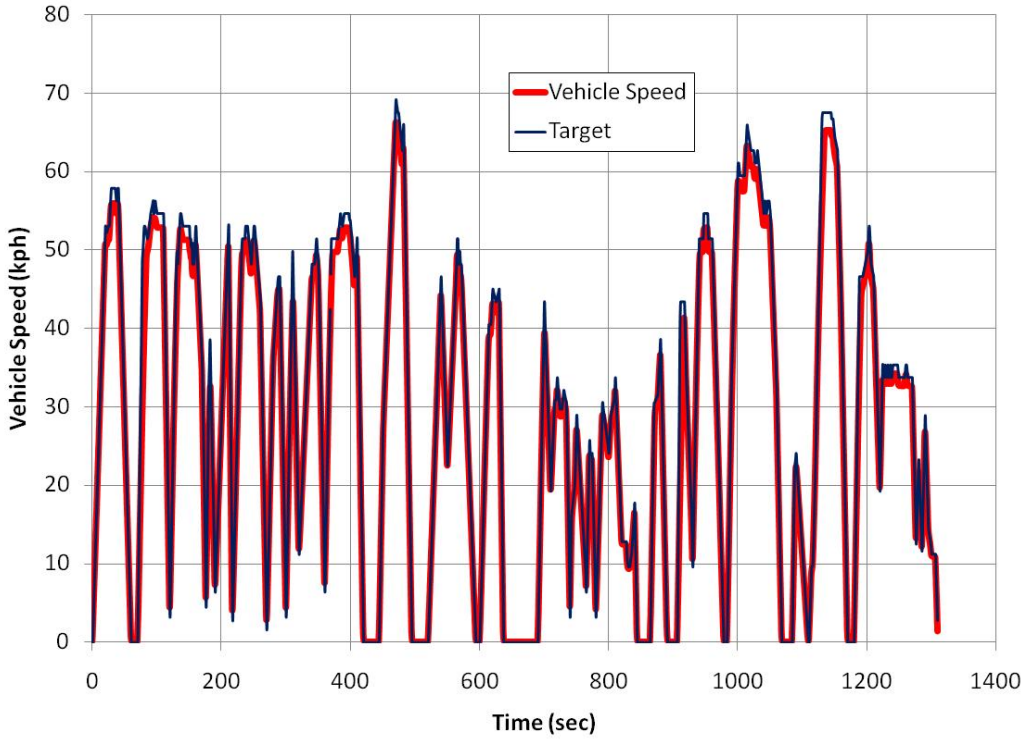

Figure 64. Simulation and Target Speed for GT Suite Escape.

Vehicle

The suspension parameters for the vehicle were not included in the vehicle body model and these parameters could have an effect on the pitching of the vehicle that could affect its acceleration and deceleration characteristics. Also the coefficient of drag was assumed to be constant at 0.4 throughout the simulation, however, this value could change depending on the ambient conditions and the condition of the vehicle's exterior.

Engine

For the engine, an engine state object was used. This object just provides a map based model for the engine and is incapable of performing any thermal analysis. Also, many of the available parameters for this object were left ignored due to a lack of data. The brake specific

fuel consumption (bsfc) data as well as the emissions data (species specific) could be used to improve upon the engine state object used for this project.

The greatest improvement in the engine model though could be realized through the construction of an engine model that utilizes the engine component elements (such as pistons, crankshafts and manifold geometry) to create a detailed engine model. If such a model were built, the performance characteristics of the engine model could be more closely matched to the actual engine since the model would not rely on as many assumptions as the engine state model does. Additionally, EGR could be incorporated into the model, transient thermal analysis could be acquired and flow characteristics through the manifolds and cylinders could be seen.

Motor and Generator

Like the engine, the motor and generator are simply map based objects ('MotorGeneratorMap') that make several assumptions about the power delivery and performance of the motors. If the motors were created using the 'Motor' object a better component model could be created and used. This would improve the model performance without going as far as an in depth build of a motor via inductance, resistance and rotating mechanical parts within GT Suite.

Battery

Further research into the battery properties could result in an improved battery component model for this vehicle model. Getting data from the battery is challenging due to the relatively high currents and voltages of the battery and their transient behavior, the best way to obtain this data would be via the vehicle CAN port. However, as previously discussed, the CAN port data is highly proprietary and thus difficult to read so approximations had to be made when creating the battery for this model. The approximations were slightly adjusted to achieve desired

battery performance, thus the parameters used are not necessarily indicative of the properties of the actual Escape battery.

Drivetrain

In the drivetrain, several model shortcomings are present although the effects of these are minimal due to the components' similarity with other similar vehicle parts. The inertias throughout the drive shafts and rotating gears were estimated since the actual parts could not be removed to experimentally determine their inertias. Therefore, estimations had to be made for all axles, differentials and gears in the Escape model that reflect the values used in a Prius model developed by GT Suite. However, the inertias were increased slightly from the Prius model due to the assumed larger size of the Escape components.

The main improvement that could be made in the drivetrain is within the eCVT. As described earlier, the eCVT operates using a planetary gear set with two inputs. While the number of teeth for the ring, planets and sun gears were known as well as the final drive gear ratio of the engine and motor, the gear masses, inertias and diameters were unknown and an estimation was used based on the values of the aforementioned parameters for the Prius model.

Control System

The control strategy used in this model was a generic system based on the discussion of the control system development given by McGee, et al. Although the paper discussed the steps in designing the control system, the final control strategy is never divulged. Thus, the furthest point in the control strategy development was used a basis for the control strategy employed by the Escape model. If more information could be attained in regard to the control system, a better control system can be used in the model and the performance characteristics would better match those of the actual Escape.

In areas where the control system given by McGee, et al had some missing portions, a judgment was made to fill in the missing portions; these portions mainly consisted of certain inputs or outputs required by GT Suite objects. Also, the gains used in the Escape controller were not given due to their sensitive nature. These values were estimated using the Prius control gains and then tuned to achieve system performance close to that of the actual Escape.

REFERENCES

Aswani, D., Cook, J., Grizzle, J., McGee, R., Opila, D. "Incorporating Drivability Metrics into Optimal Energy Management Strategies for Hybrid Vehicles." IEEE Conference on Decision and Control. 2008.

Atkins, R. "An Introduction to Engine Testing and Development." SAE International. April 8, 2009.

Bossche, P., Maggetto, G., Mierlo, J. "Models of Energy Sources for EV and HEV: Fuel Cells, Batteries, Ultracapacitors, Flywheels and Engine-Generators." January 8, 2003.

Bradley, T., Frank, A. "Design, Demonstration and Sustainability Impact Assessments for Plug-In Hybrid Electric Vehicles." *Renewable and Sustainable Energy Reviews 13*. 2009.

Chen, Z., Mi, C. "An Adaptive Online Energy Management Controller for Power-Split HEV Based on Dynamic Programming and Fuzzy Logic." IEEE. 2009.

Department of Energy Advanced Vehicle Testing Activity. "2005 Ford Escape-8237 Hybrid Battery Test Results." 2005.

Edmunds.com, Inc. *2005 Ford Escape*. Available from http://www.edmunds.com/ford/escape/2005/features-specs.html. 12 January 2010.

Environmental Protection Agency. "Inventory of U.S. Greenhouse Gas Emissions and Sinks: 1990-2007," 2009.

Environmental Protection Agency (EPA). 1996. *Vehicle Preconditioning Procedure*. Available from http://www.epa.gov/otaq/emisslab/testproc/703j.pdf. 1 March 2011.

Ford Motor Company. *Escape Hybrid Powertrain Control/Emissions Diagnosis 2005 Service Manual*. Detroit: Helm Inc., 2004.

Ford Motor Company. *2005 MY OBD System Operation Summary for Hybrid Electric Vehicles* (May 2004). Available from http://www.motorcraftservice.com/vdirs/diagnostics/pdf/OBDSM500_HEV.pdf. 12 January 2010.

Grabainowski, Edward. 2005. *How the Ford Escape Hybrid Works*. Available from http://auto.howstuffworks.com/ford-escape.htm. 9 March 2011.

Heywood, J.B. and Kromer, M.A. “Electric Powertrains: Opportunities and Challenges in the U.S. Light-Duty Vehicle Fleet.” Laboratory for Energy and the Environment. May 2007.

Hisada, Hideki, Takao Taniguchi, Kazumasa Tsukamoto, Kozo Yamaguchi and Kenji Suzuki, *AISIN AW New Full Hybrid Transmission for FWD Vehicles*. SAE Paper 2005-01-0277.

Karbowksi, D., Kwon, J., Pagerit, S., Rouseau, A., Pechmann, K. “”Fair” Comparison of Powertrain Configurations for Plug-In Hybrid Operation Using Global Optimization.” SAE International. 2009.

McGee, Ryan, Fazal Syed, Stephen Hunter and Deepa Ramaswamy. “Power Control for the Escape and Mariner Hybrids.” SAE International, 2007.

Miller, J. “Propulsion Systems for Hybrid Vehicles.” The Institution of Electrical Engineers. 2004.

MSN Autos. “Ford Escape Hybrid Compare – Engines and Performance.” Available from http://autos.msn.com/research/compare/engines.aspx?c=0&i=0&ph1=t0&ph2=t0&tb=0&dt=0&v=t99213&v=t98786&v=t98790. 1 March 2011.

Rairigh, Phil. “Ford Motor Company Hybrid Vehicles.”Michigan Clean Fleet Conference, May 2007.

Thomas, C.E. Sandy. “Transportation Options in a Carbon Constrained World: Hybrids, Plug-In Hybrids, Bio-fuels, Fuel Cell Electric Vehicles and Battery Electric Vehicles.” International Journal of Hydrogen. July 29, 2009.

APPENDIX A

This appendix contains the front panels and block diagrams of the various LabVIEW VIs utilized during this project.

A.1 LabVIEW Escape AI Project Tree

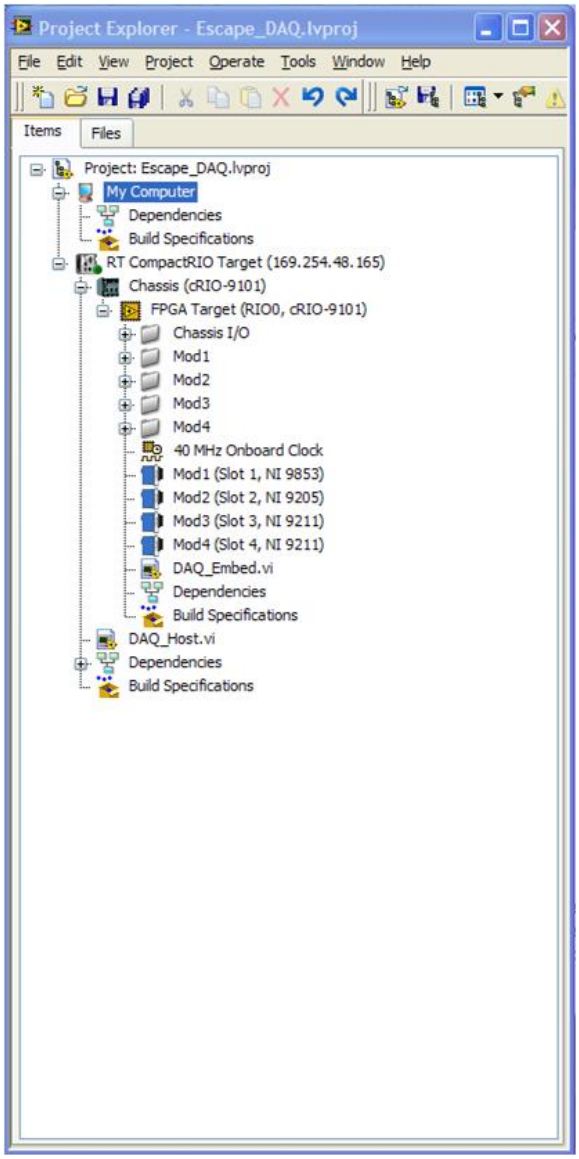

A.2 Escape AI Embedded VI Front Panel

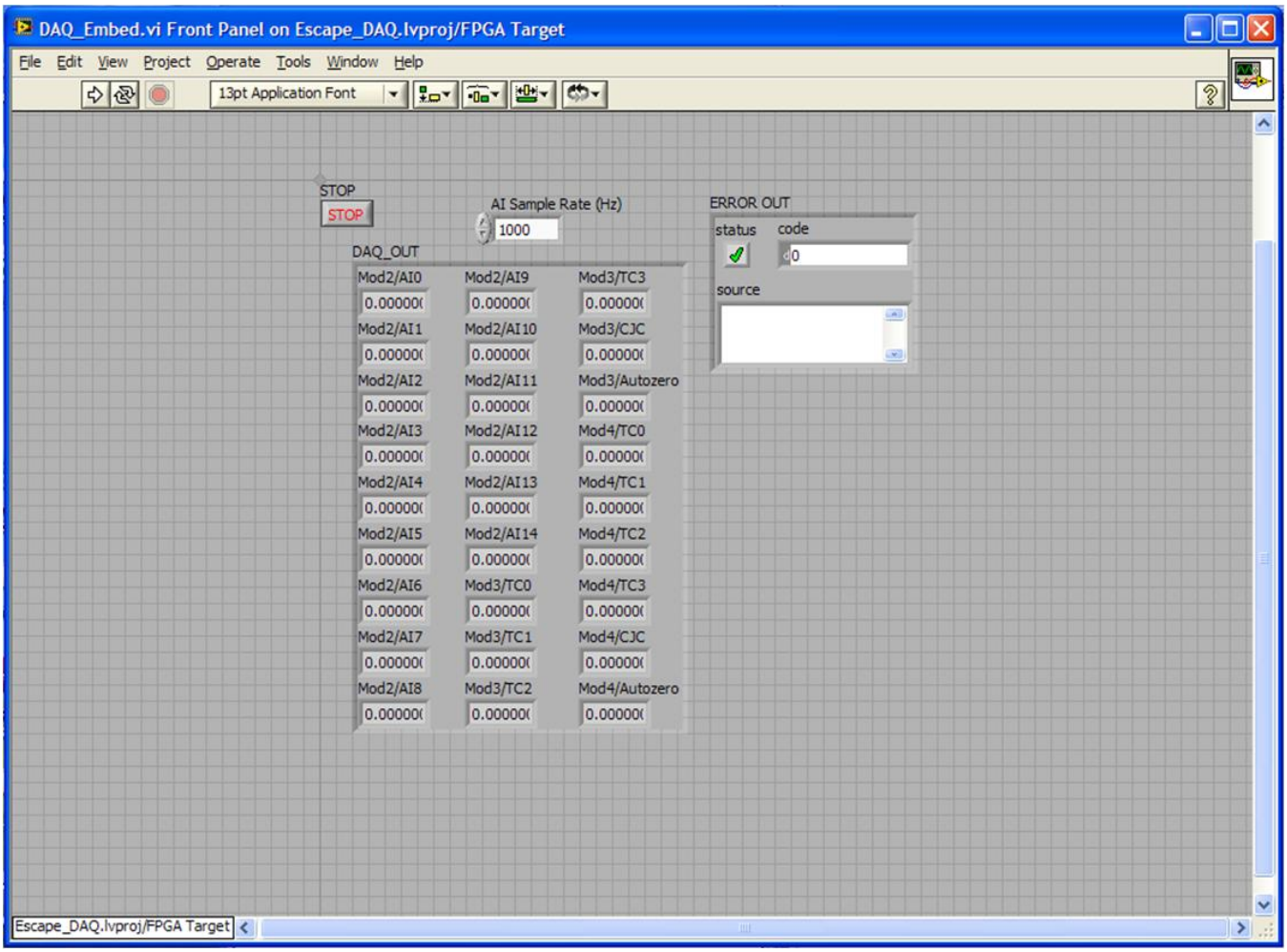

A.3 Escape AI Embedded VI Block Diagram

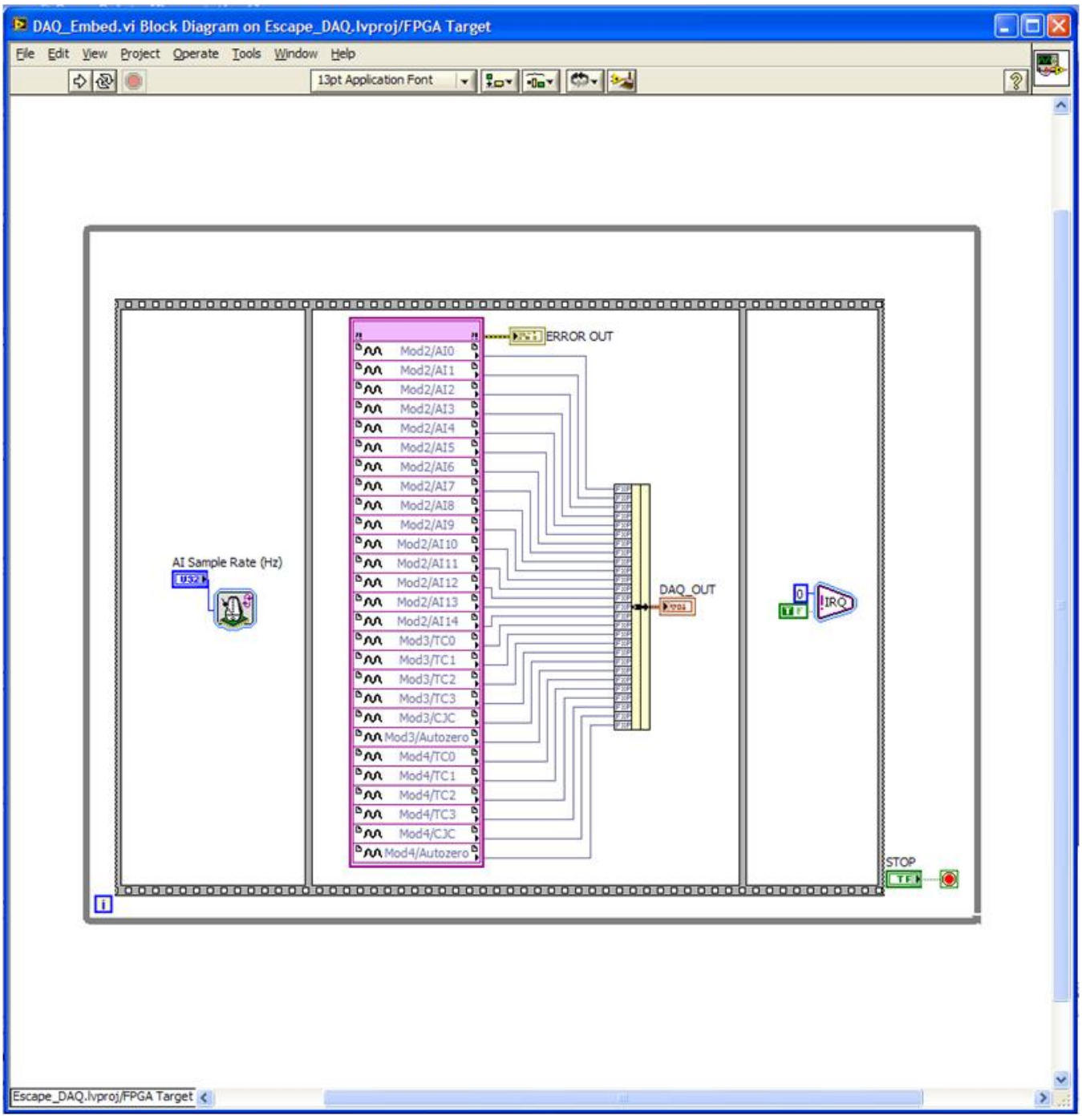

A.4 Escape AI Host VI Front Panel

A.5 Escape AI Host VI Block Diagram

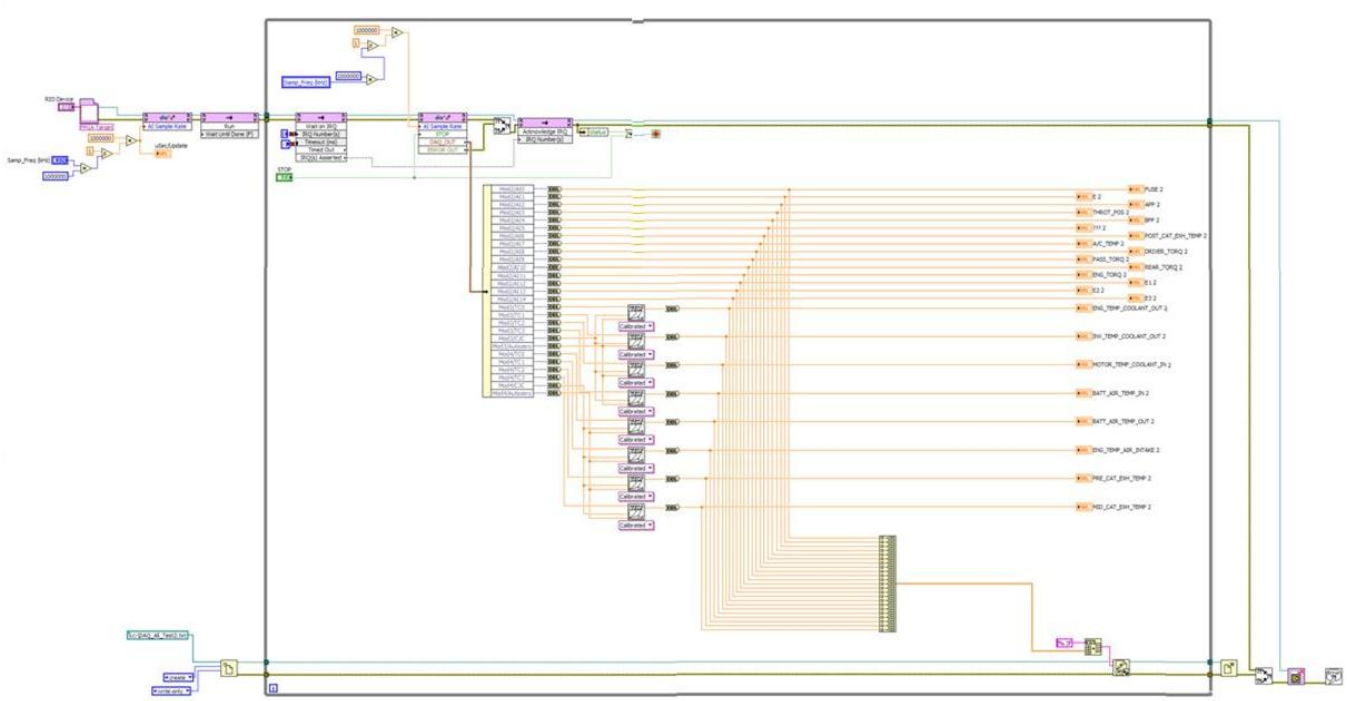

APPENDIX B

This appendix contains the MATLAB code used to process the DAQ data as well as sample plots of the DAQ data after MATLAB processing. For this sample data, no particular drive cycle was followed; functionality test data is used.

B.1 MATLAB Code

```
%Processing algortihm for 2005 Ford Escape Hybrid DAQ Signals
clear all
clc

%Import text file
data=load('DAQ_06182010.txt');
[n,m]=size(data);

%Establish time scale (1Hz sampling)
fs=10; %Hz
dt=1/fs; %sec
t=0:dt:dt*(n-1); %sec

%Apply calibrations to get desired output units
Vfuse=0.0097*data(:,1)-0.00001; %Voltage accross fuse (Volts)
Vsupp=3.1368*data(:,2)+0.2697; %Supply voltage to Modules (Volts)
APP=-0.3571*data(:,3)+1.4071; %Accelerator Pedal Position Sensor (0 -> 1.0)
TPS=0.2646*data(:,4)-0.1508; %Throttle Position Sensor (0 -> 1.0)
BPP=data(:,5); %Brake Pedal Position Sensor (0 -> 1.0)
Unknown=data(:,6); %Should read 0V, but doesn't
PoCET=172*data(:,7)-100; %Post-Cat Exhaust Temperature (degC)
ACTemp=290*data(:,8)-100; %A/C Temperature (degC)
Qfuel=0.016*data(:,13); %Fuel Flow (gpm)
Iconv=150*data(:,14); %Current in/out of DC/DC Converter (Amps)
I12V=150*data(:,15); %Current in.out of 12V Battery (Amps)
EngTemp=data(:,16); %Engine Coolant Outflow Temeprature (degC)
InvOutTemp=data(:,17); %Inverter Coolant Outflow Temperature (degC)
MotInTemp=data(:,18); %Motor Coolant Inflow Temperature (degC)
BattInTemp=data(:,19); %Battery Air Inflow Temperature (degC)
BattOutTemp=data(:,20); %Battery Ait Outfloe Temperature (degC)
```

```
EngAirInTemp=data(:,21); %Engine Intake Air Temperature (degC)
```

```
PrCET=data(:,22); %Pre-Cat Exhaust Temperature (degC)
MCET=data(:,23); %Mid-Cat Exhaust Temperature (degC)

%Since torque sensors have different calibration curves for V>0 and V<0
DrivTorq=zeros(n,1); %Front Left Torque Sensor (Nm)
PassTorq=zeros(n,1); %Front Right Torque Sensor (Nm)
RearTorq=zeros(n,1); %Rear Axle Torque Sensor (Nm)
EngTorq=zeros(n,1); %Engine Torque Sensor (Nm)
for i=1:n
   if data(:,9)>=0
      DrivTorq(i,1)=200.08*data(i,9)-0.009;
   else
      DrivTorq(i,1)=200.1*data(i,9)-0.0777;
   end
   if data(:,10)>=0
      PassTorq(i,1)=-200.77*data(i,10)-0.552;
   else
      PassTorq(i,1)=-199.63*data(i,10)-0.0597;
   end
   if data(i,11)>=0
      RearTorq(i,1)=216.74*data(i,11)+0.6386;
   else
      RearTorq(i,1)=-216.16*data(i,11)+0.7222;
   end
   if data(i,12)>=0
      EngTorq(i,1)=174.4817*data(i,12)-1.3423;
   else
      EngTorq(i,1)=-174.1932*data(i,12)-1.0304;
   end
end

%Now construct the plots that will be output
figure(1)
clf
box on
subplot(3,1,1)
plot(t,APP,'k-')
title('APP')
ylabel('Percent')
subplot(3,1,2)
plot(t,TPS,'b-')
title('TPS')
ylabel('Percent')
subplot(3,1,3)
plot(t,BPP,'r-')
title('BPP')
```

```
xlabel('Time (sec)')
ylabel('Percent')

figure(2)
clf
box on
subplot(4,1,1)
plot(t,DrivTorq,'r-')
title('Front Left (Driver) Torque')
ylabel('Torque (N-m)')
subplot(4,1,2)
plot(t,PassTorq,'b-')
title('Front Roght (Passenger) Torque')
ylabel('Torque (N-m)')
subplot(4,1,3)
plot(t,RearTorq,'g-')
title('Rear Axle Torque')
ylabel('Torque (N-m)')
subplot(4,1,4)
plot(t,EngTorq,'k-')
title('Engine Torque')
xlabel('Time (sec)')
ylabel('Torque (N-m)')

figure(3)
clf
box on
subplot(2,1,1)
plot(t,Iconv,'r-')
title('DC/DC Converter Current Flow')
ylabel('Current (Amps)')
subplot(2,1,2)
plot(t,I12V,'b-')
title('12V Battery Current Flow')
xlabel('Time (sec)')
ylabel('Current (Amps)')

figure(4)
clf
box on
plot(t,Qfuel,'k-')
xlabel('Time (sec)')
ylabel('Flow Rate (gpm)')
title('Fuel Flow')

figure(5)
```

```
clf
box on
subplot(3,1,1)
plot(t,ACTemp,'k-')
title('A/C Temperature')
ylabel('Temperature (degC)')
subplot(3,1,2)
plot(t,BattInTemp,'b-')
title('Battery Air In Temperature')
ylabel('Temperature (degC)')
subplot(3,1,3)
plot(t,BattOutTemp,'r-')
title('Battery Air Out Temperature')
xlabel('Time (sec)')
ylabel('Temperature (degC)')

figure(6)
clf
box on
subplot(2,1,1)
plot(t,InvOutTemp,'g-')
title('Inverter Coolant Outflow Temperature')
ylabel('Temperature(degC)')
subplot(2,1,2)
plot(t,MotInTemp,'m-')
title('Motor Coolant Inflow Temperature')
xlabel('Time (sec)')
ylabel('Temperature (degC)')

figure(7)
clf
box on
subplot(2,1,1)
plot(t,EngTemp,'r-')
title('Engine Coolant Outflow Temperature')
ylabel('Temperature (degC)')
subplot(2,1,2)
plot(t,EngAirInTemp,'b-')
title('Engine Intake Air Temperature')
xlabel('Time (sec)')
ylabel('Temperature (degC)')

figure(8)
clf
box on
subplot(3,1,1)
```

```
plot(t,PrCET,'b-')
title('Pre-Cat Exhaust Temperature')
ylabel('Temperature (degC)')
subplot(3,1,2)
plot(t,MCET,'g-')
title('Mid-Cat Exhaust Temperature')
ylabel('Temperature (degC)')
subplot(3,1,3)
plot(t,PoCET,'r-')
title('Post-Cat Exhaust Temperature')
xlabel('Time (sec)')
ylabel('Temperature (degC)')
```

B.2 APP, BPP and TPS Sensor Signals

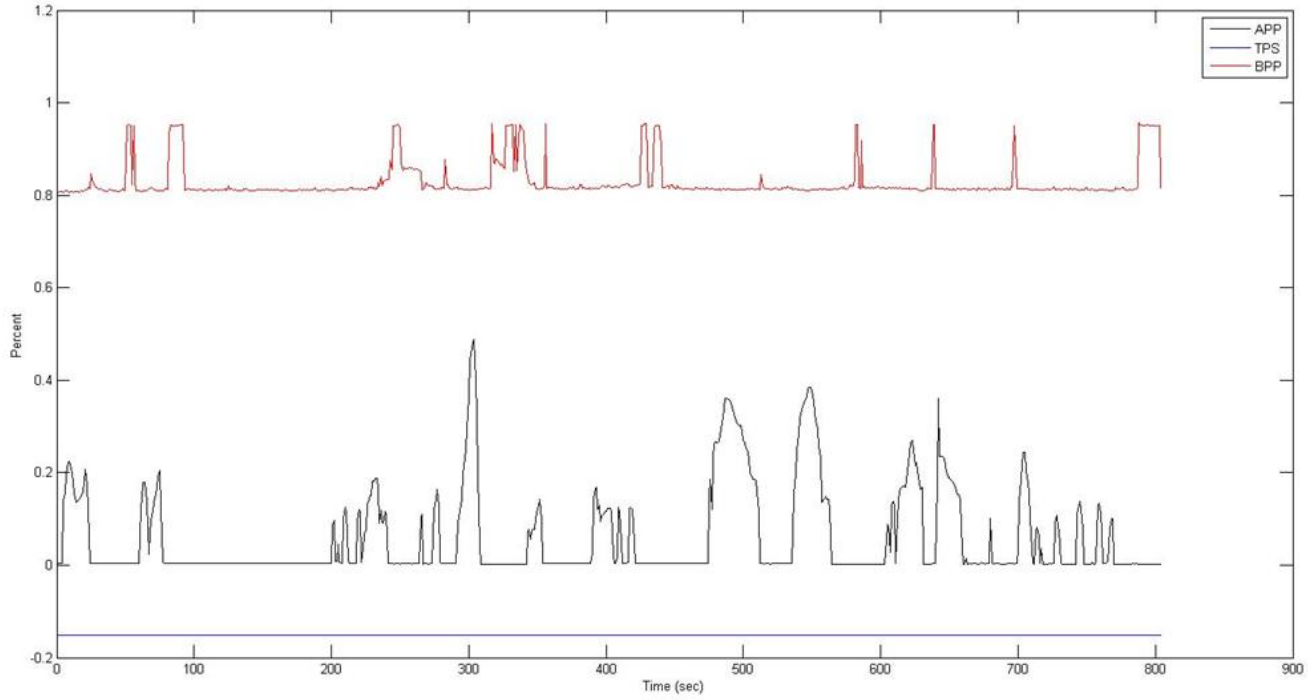

B.3 Axle Torque Signals

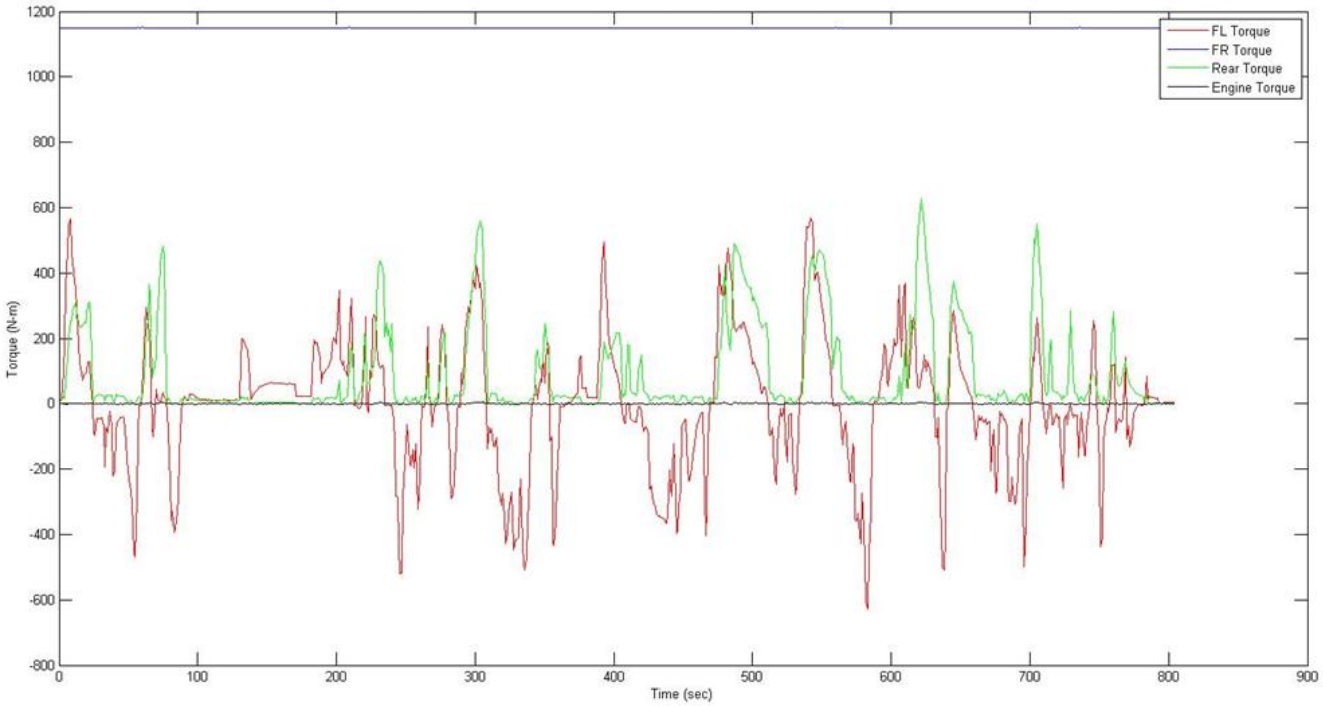

B.4 Current Flow Signals

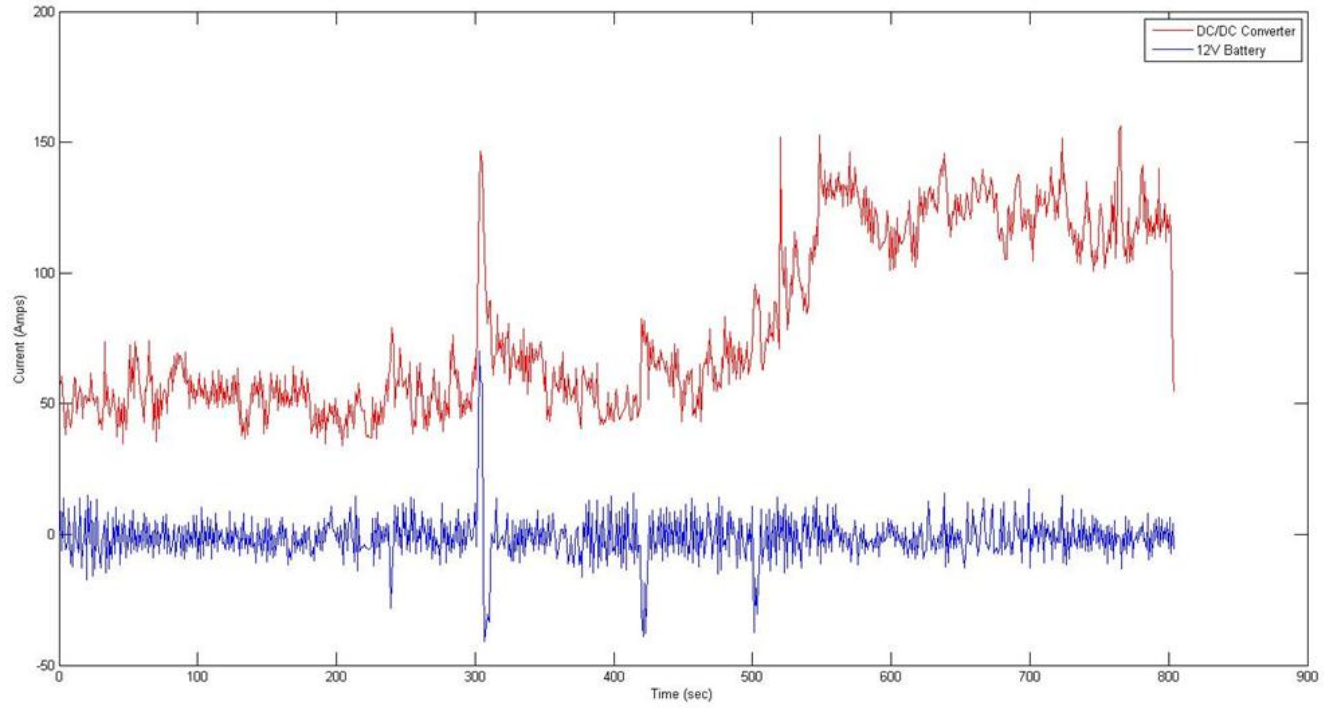

B.5 Fuel Flow Rate Signal (gpm)

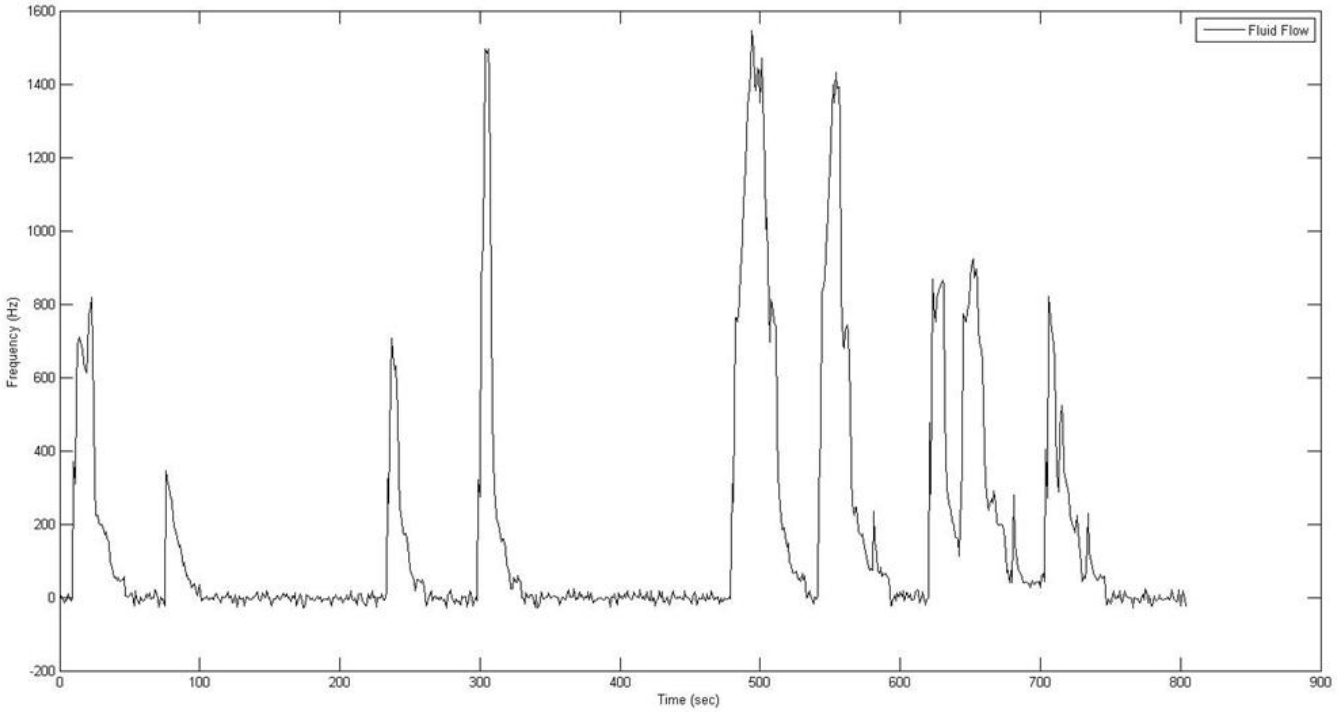

B.6 Electronics and A/C Temperature Signals

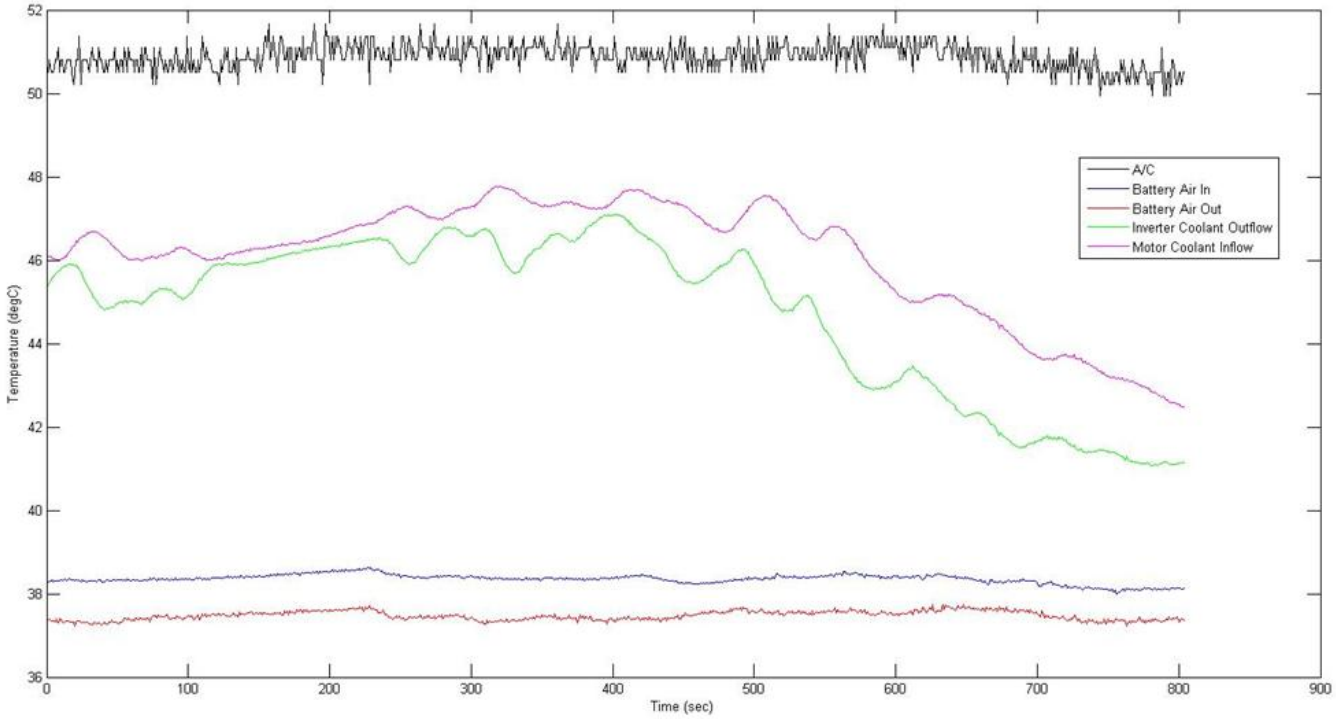

B.7 Engine Coolant Temperature Signals

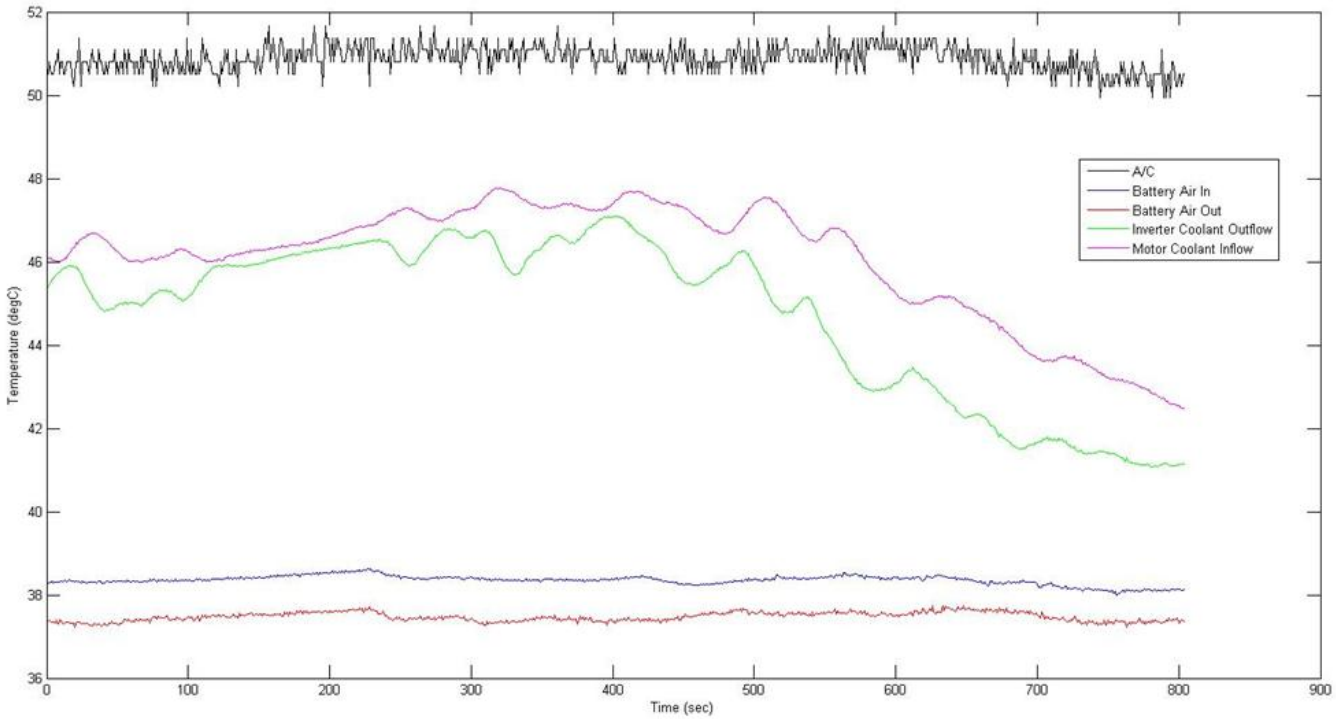

B.8 Catalytic Converter Temperatures

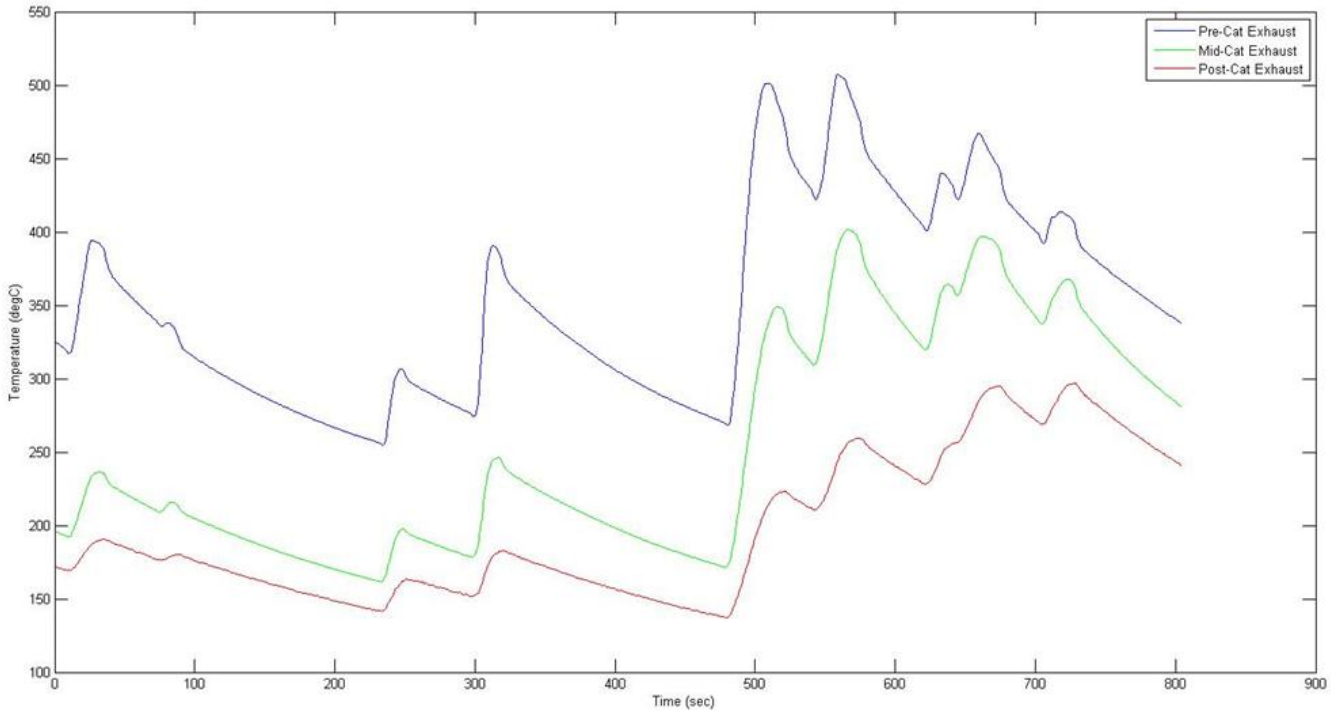

APPENDIX C

This appendix contains vehicle data for the 2005 Escape Hybrid used in this research.

C/D TEST RESULTS

ACCELERATION Seconds
Zero to 30 mph: 3.7
40 mph: 5.5
50 mph: 7.9
60 mph: 10.8
70 mph: 14.6
80 mph: 19.7
90 mph: 28.6
Street start, 5-60 mph: 11.1
Top-gear acceleration, 30-50: mph 4.6
50-70 mph: 7.2
Standing 1/4-mile: 18.2 sec @ 77 mph
Top speed (governor limited): 102 mph

BRAKING
70-0 mph @ impending lockup: 195 ft

HANDLING
Roadholding, 300-ft-dia skidpad: 0.73 g
Understeer: minimal moderate excessive

FUEL ECONOMY
EPA city driving: 33 mpg
EPA highway driving: 29 mpg
C/D-observed: 25 mpg

Curb weight: 3839 lb, Test weight; 4125lb

Power (SAE net): 155 bhp (combined motor/engine)
Power (SAE net): 133 bhp @ 6000 rpm
Torque (SAE net): 129 lb-ft @ 4500 rpm
Redline: 6000 rpm

ELECTRIC MOTOR
Type: 3-phase AC permanent-magnet synchronous electric motor powered by 250 1.3-volt nickel-metal hydride batteries
Power (SAE net): 94 bhp @ 3000-5000 rpm

DRIVETRAIN
Transmission: continuously variable automatic

Final-drive ratio: 3.04:1
4-wheel-drive system: full time with automatic rear-axle engagement and open front
and rear differentials

DIMENSIONS
Wheelbase: 103.1 in
Track, front/rear: 61.3/60.9 in
Length/width/height: 174.9/70.1/70.4 in
Ground clearance: 8.0 in
Drag area, Cd (0.40) x frontal area (28.9 sq ft):11.6 sq ft
Curb weight: 3839 lb
Weight distribution, F/R: 56.4/43.6%
Curb weight per horsepower: 24.8 lb
Fuel capacity: 15.0 gal

APPENDIX D

This appendix contains parameters from the model that are defined as functions of other variables.

D.1 Open Circuit Voltage for HV Battery

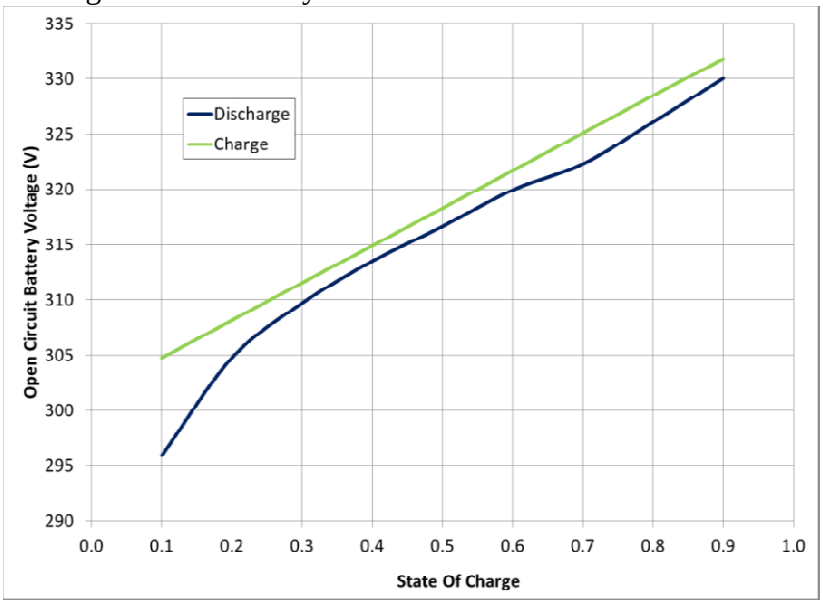

D.2 Internal Resistance for HV Battery

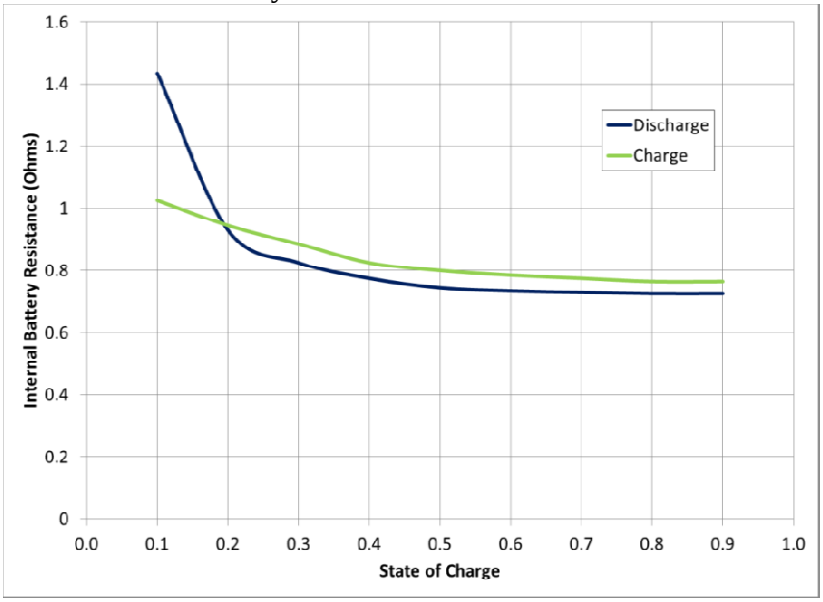

D.3 Electromechanical Conversion Efficiency for Motor

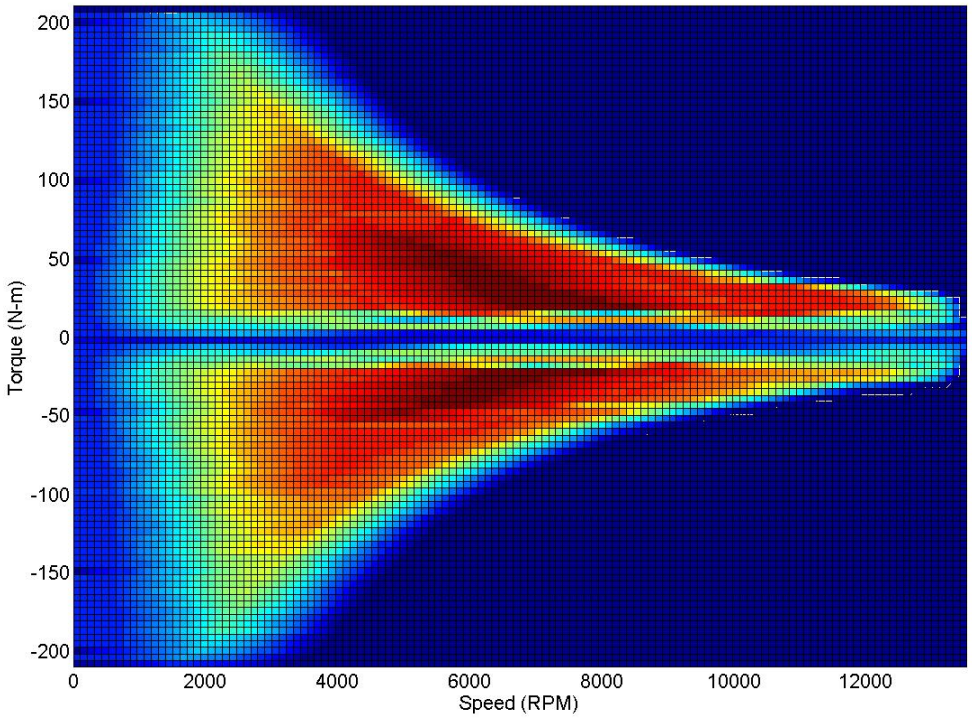

D.4 Maximum Brake Torque for Motor

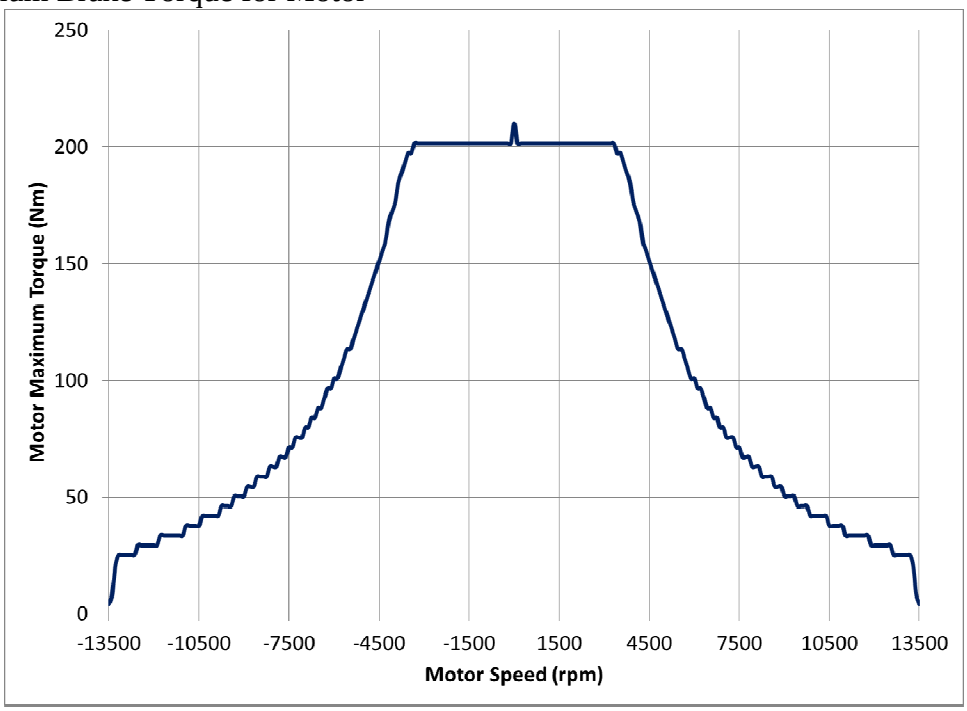

D.5 Minimum Brake Toque for Motor

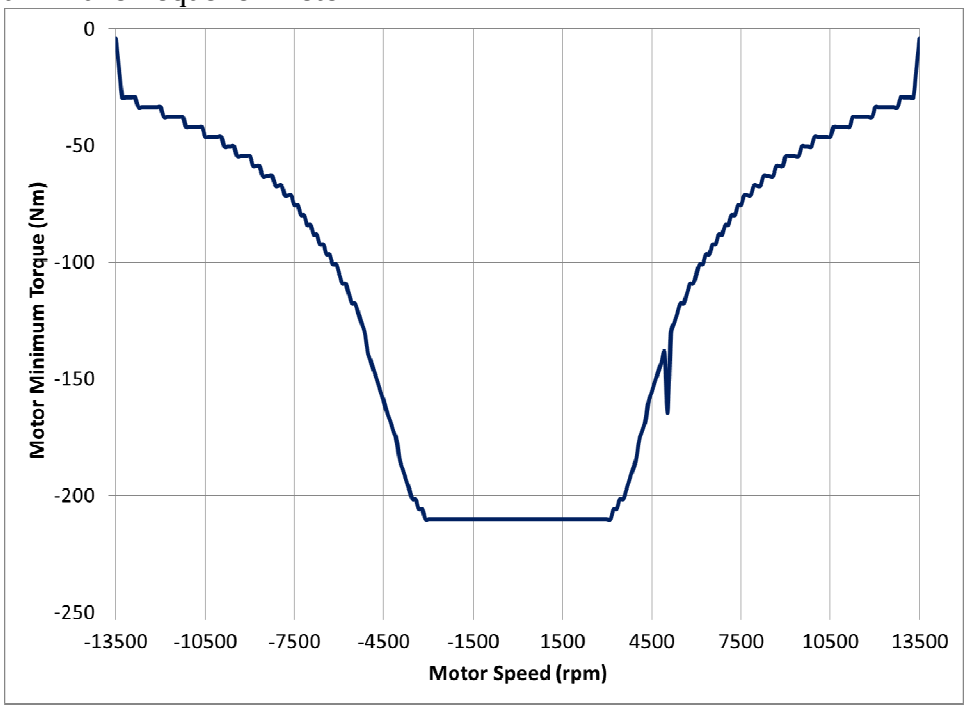

D.6 Electromechanical Conversion Efficiency for Generator, Max=0.96

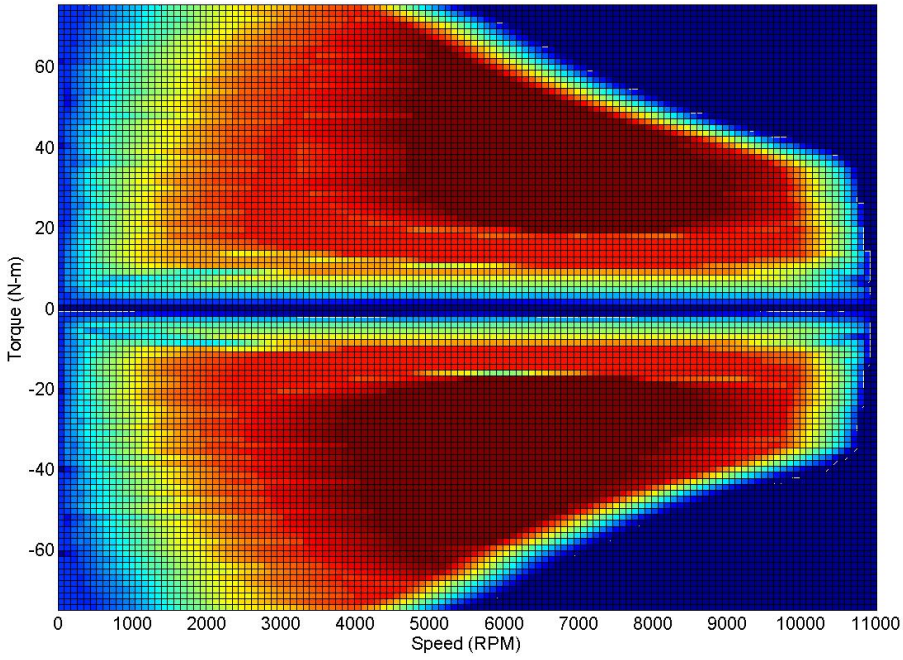

D.7 Maximum Brake Torque for Generator

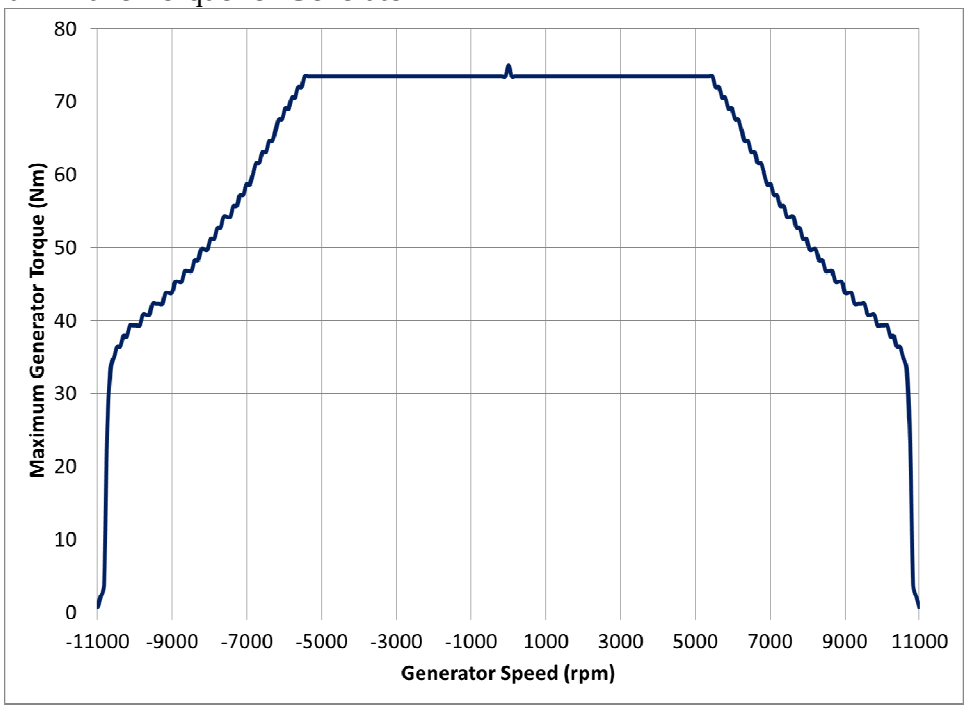

D.8 Minimum Brake Torque for Generator

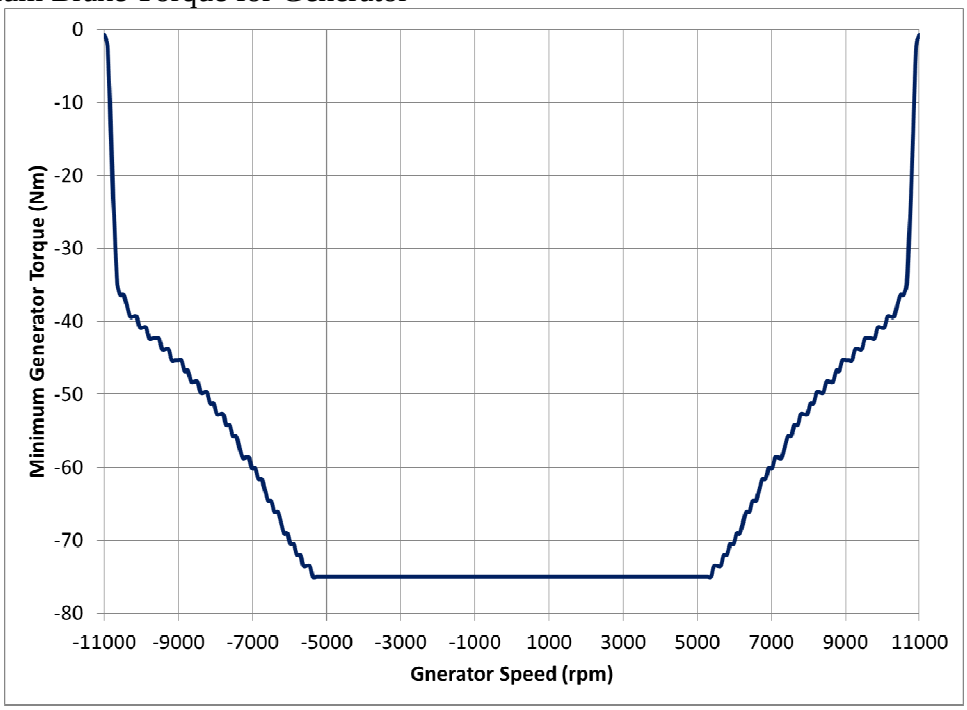

D.9 Mechanical Output Map for Engine